

IN VITRO AND *IN VIVO* EFFECTS OF CRUDE EXTRACT OF
ACANTHUS EBRACTEATUS VAHL. ON HUMAN CERVICAL
CARCINOMA : ROLE OF P53 AND VEGF

Miss Taksanee Mahasiripanth

A Dissertation Submitted in Partial Fulfillment of the Requirements
for the Degree of Doctor of Philosophy in Physiology program
(Interdisciplinary)
Graduate School
Chulalongkorn University
Academic Year 2011

บทคัดย่อและแฟ้มข้อมูลฉบับเต็มของวิทยานิพนธ์นี้ได้รับการขึ้นทะเบียนในฐานข้อมูลปัญญาจุฬาฯ (CUIR)
เป็นแฟ้มข้อมูลของนิสิตเจ้าของวิทยานิพนธ์ที่ส่งผ่านทางบัณฑิตวิทยาลัย

The abstract and full text of theses from the academic year 2011 in Chulalongkorn University Intellectual Repository (CUIR)
are the thesis authors' files submitted through the Graduate School.

CHAPTER I

INTRODUCTION

Cervical cancer is the malignant cancer which occurs within epithelial layers of cervical mucosa. In the year 2008, cervical cancer is the second most common cancer in women worldwide, with approximately 529,409 new cases and about 274,883 deaths, and about 86% all cases and death found in developing countries including Thailand [1]. In Thailand, according to WHO/ICO report in the year 2010 that the age-standardized incidence and mortality rates of cervical cancer in Thai women is second only to breast cancer and liver cancer, respectively [2]. Nowadays, It is clearly that persistent infection with high risk human papillomaviruses (HPVs) are required for the development and maintenance of cervical cancer, since its DNA is found in almost all cervical cancers (>99.7%) [3, 4]. These cancer-associated with high risk HPVs, which HPV16 and HPV 18 are found about 70% of cervical cancers. HPV16 is the most prevalence type approximately 50% of all cervical cancers worldwide [5, 6].

The major oncogenic HPV proteins E6 and E7 are involved in the immortalization of target cells by inactivation of two cellular tumor suppressor proteins, p53 and retinoblastoma (pRb), respectively [7]. The HPV E6-mediated degradation of p53 result in cell apoptosis disruption, while HPV E7-mediated pRb degradation result in up-regulate cell cycle process [5, 8]. Then the interaction leading to induce cell proliferation, immortalization and malignancy transformation of cancerous cells following HPV infection [9]. However, tumor growth is angiogenesis dependent, and without angiogenesis tumors remain small (< 1-2 mm³). Lack of oxygen and nutrients supply to cancer cells in tumor center, results in cell hypoxia and leading to apoptosis and necrosis [10]. Tumor angiogenesis and neovascularization required vascular endothelial growth factor (VEGF), a key factor in tumor angiogenesis. Under hypoxic condition, the binding of a transcription factor Hypoxia-inducible factor-1 α (HIF-1 α) to VEGF promoter is a major pathway resulting in the induction of VEGF expression [11].

The current knowledge demonstrates that VEGF action is actually mediated through several pathways. Many cell types including tumor-associated stromal cells and tumor cells produce VEGF, and then acts in both a paracrine and an autocrine fashion to stimulate VEGF receptors located on endothelial cells and on stromal cells surface that result to activate neovascularization around tumors [12-14]. The highly expression of VEGF mRNA have been found in cervical lesion from localized cervical epithelial neoplasia (CIN) to invasive and metastatic cervical carcinoma [15, 16], and also associated with the increment of microvascular density (MVD) [17, 18]. Moreover, the same evidence has also been found in squamous CIN and invasive cell carcinoma of the cervix [19-22]. It is to be certain that VEGF exhibits a potent angiogenic effect for carcinogenesis, progression and metastasis of cervical cancers [14, 23, 24].

The mechanism of VEGF regulation in HPV-associated cervical cancer has been demonstrated in many ways such as, the up-regulation of VEGF expression occurs consequently the down-regulation of p53 via ubiquitin proteasome degradation induced by high risk HPV E6 protein [25]. Moreover, in HPV16-positive cervical cancer cells, both critical HPV E6 and E7 proteins can induce VEGF expression via triggered VEGF promoter directly [26, 27] and also mediated through enhance hypoxia-inducible factor 1 α (HIF-1 α) protein expression [28]. Furthermore, HPV E7 may be involve in the up-regulation of VEGF expression via *c-myc* pathway [29]. These provide rationale for the HPV-associated tumor angiogenesis in cervical cancer.

Clearly, tumor angiogenesis is pivotal in cervical cancer disease and a rational target for therapy, that current chemotherapy treatment of cervical cancer use anti-angiogenesis agent, one of the first line drug is bevacizumab acts via binding and activation of VEGF resulting cervical tumors shrink and delay tumor progression. However, this agent still being study in a Gynecologic Oncology Group (GOG) phase III trial [30]. In other choice, HPV E6 and E7 oncoproteins may be ideal molecular targets for the treatment and prevention of cervical cancer. As a result of interfering the HPV E6/E7 activity, the stabilization and accumulation of active p53 protein induce cell cycle arrest or apoptosis and may be down-regulated VEGF expression that inhibits tumor growth consequently. Moreover, disruption of HPV E6 promoting VEGF-dependent angiogenesis can inhibit the growth and

development of cervical cancers [26-28]. Although, there are many chemotherapeutic or anti-angiogenic drugs for treatment of cervical cancer, it mostly causes of weakness in patients due to its toxicity. Therefore, traditional plants were considered as an important potential source for the treatment of cancer, that may be more safety to the normal cells.

During the last decade, there have been many reports of antitumor potential of Thai medicinal plants, *Acanthus ebracteatus* Vahl. (*Acanthaceae* family) or Ngueak pla mo (Thai name), which is the one of many folk medicinal plants used against cancer disease in Ayurveda. Since *A. ebracteatus* Vahl. and other species *Acanthus ilicifolius* Linn. have similar therapeutic effects, they are used interchangeably in Thai folkloric medicine. Pharmacological researches of this plant and its species had shown many bioactivities, including immunopotentiating effect [31], hepatoprotective and antioxidative [32], antimutagenicity and anticarcinogenic [33-35], and anti-inflammatory [36]. This plant composes of high chemical constituents of alkaloids, flavonoids [37], triterpenoid [38], quaternary amino acid [39], and polysaccharide [40]. Previous isolations of active compounds of this plant, sulphur, stigmasterol, β -sitosterol, lupeol, polysaccharide, megastigmane, aliphatic alcohol, and six benzoxazinoids glycoside had been reported [41, 42]. However, the active chemical constituents of *A. ebracteatus* Vahl. that exhibit antitumor effects have not been isolated and the exact mechanism still remained unclear.

Interestingly, the extract and isolated compounds from *A. ebracteatus* Vahl. and *Acanthus spp.* increased life span and survival rate, delayed on set of carcinogenesis, inhibited hepatocarcinogenesis, against tumor progression, decreased tumor growth in experimental animals [41, 43-45]. In addition, its extract and some bioactive compounds, β -sitosterol, stigmasterol, Lupeol, and benzoxazolines-2-one had cytotoxic effects to some kind of cancer cells [33, 46, 47]. Furthermore, Phisalaphong and co-workers have demonstrated that the aqueous and nanofiltration-desalted extract of *A. ebracteatus* Vahl. had anti-proliferative effect on human cervical carcinoma HeLa (HPV18-positive) cell lines [48].

However, the antitumor effect of *A. ebracteatus* Vahl. has not been studied in HPV16-positive cervical carcinoma cells. Moreover, there is still no experimental

data for inhibitory effect of this plants on tumor angiogenesis, especially, using cervical carcinoma implanted nude mice model together with the visual ability of intravital fluorescence microscopic technique. Therefore, the present study was the first investigation of the effects of aqueous crude extract of *A. ebracteatus* Vahl. on tumor angiogenesis and on tumor growth in human cervical carcinoma cell implanted nude mice and study the effects of aqueous crude extract *A. ebracteatus* Vahl. on cervical cancer apoptotic index, p53 and angiogenic biomarker VEGF expression.

Research questions

Can the aqueous crude extract of *A. ebracteatus* Vahl. inhibit tumor angiogenesis and tumor growth in human cervical carcinoma implanted nude mice? Whether its mechanism(s) related to tumor biomarkers, VEGF, and p53 or not?

Research objectives

1. To investigate the effects and mechanism of the aqueous crude extract *A. ebracteatus* Vahl. on angiogenesis in cervical carcinoma implanted nude mice model by using intravital fluorescence confocal laser scanning microscopy system.
2. To examine the effects of the aqueous crude extract of *A. ebracteatus* Vahl. on angiogenic biomarker VEGF.
3. To examine the effects of the aqueous crude extract of *A. ebracteatus* Vahl. on tumor growth.
4. To determine whether the aqueous crude extract of *A. ebracteatus* Vahl. inhibits tumor growth by increasing cervical cancer cell apoptosis due to the stabilization and accumulation of active p53 protein.

Hypothesis

The aqueous crude extract of *A. ebracteatus* Vahl. can inhibit tumor growth by inhibiting angiogenesis and/or directly inducing cancer cell apoptosis.

CHAPTER II

LITERATURE REVIEWS

Cervical cancer

Cervical cancer is a malignant tumor that occurs in the tissue of uterine cervix or cervical area. It may begin as asymptomatic pre-cancerous lesions and develops into invasive cancer over many years. According to World Health Organization (WHO), cervical cancer is the second most common cancer in women worldwide, with an estimated 529,409 new cases and 274,883 deaths in 2008, and approximately 86% of patients and death found in developing countries [2]. In Asia, the highest incidence of cervical cancer is in India, which an age-standardized rate (ASR) is 19.5 per 100,000 woman per year, and highest mortality rate is 17.43 per 100,000 woman per year. Furthermore, 125,952 new cases of cervical cancer are diagnosed annually, that about 1 of 4 of overall cervical cancer patients worldwide [49].

In South-Eastern Asian country, Cambodia has a highest incidence of cervical cancer (ASR=27.4 per 100,000 per year), followed by Myanmar, Thailand and Laos with ASR are 26.4, 25.5, and 22.1, respectively (Figure 2.1).

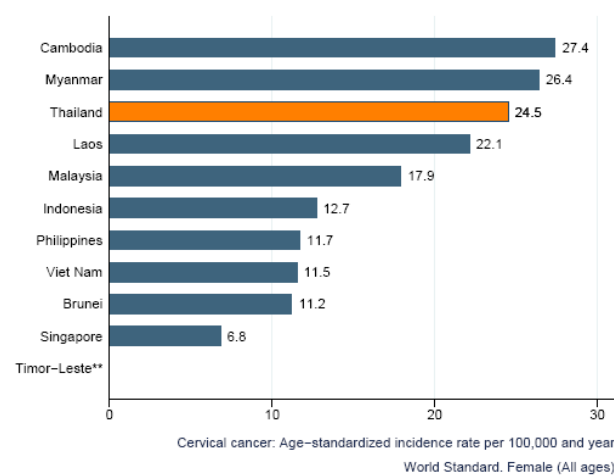


Figure 2.1 Age-standardized incidence rate (ASR) of cervical cancer in counties of South-Eastern Asia. (IARC, 2008; cited by WHO/ICO Information Centre on HPV and Cervical Cancer, 2010)[2].

In Thailand, Parkin has reported in year 2002 that cervical cancer is the most common cancer and the third cause of death among Thai women [50]. In the year 2010, WHO has reported the crude incidence rate of cervical cancer is 29.2 per 100,000 woman of all ages in Thailand, which ranked second to breast cancer (crude

incidence rate 36.7 per 100,000) compared to all over cancer types [2]. However, the cervical cancer age-standardized incidence rate is 19.5 per 100,000 per year, which is the most cancer found in woman in Thailand, followed by breast cancer and liver cancer (Table 2.1) [49].

Table 2.1 Age-standardized incidence rate (ASR) of over all cancers in Thai woman.

Cancer types	Age-standardized incidence rate (per 100,000 and year)
Cervical cancer	19.5
Breast cancer	17.2
Liver cancer	16.0
Lung cancer	10.0
Colorectal cancer	7.3
Ovarian cancer	5.2

(IARC, 2008, cited by WHO/ICO Information Centre on HPV and Cervical Cancer, 2010)[2].

Human papillomavirus and Cervical cancer

It is now clear that persistent infection with human papillomaviruses (HPVs) are required for the development and maintenance of cervical cancer, and the high-risk HPV DNA was found in almost all cervical cancers (>99.7%) [3, 4]. These HPVs- associated cervical cancer are classified as high-risk HPV types, and HPV16 and HPV 18 are responsible for about 70% of cervical cancers. HPV16 is the most prevalent high-risk HPV in the general population, and is responsible for approximately 50% of all cervical cancers [5, 6].

Human papillomaviruses (HPVs), a group of oncogenic small DNA virus belongs to the *Papillomaviridae* family [51]. HPVs particles contain of 8,000 base-pairs (bps) in length of a circular dsDNA which are enveloped with a capsid protein. The viral genome is separated into three functional regions such (i) long control

region (LCR) is a non-coding upstream regulatory region, (ii) an early region consisting of open reading frames (ORFs) E1, E2, E4 - E7, which encode for early proteins necessary for viral replication and oncogenic activity, (iii) late region, which encodes for two viral envelope proteins, major capsid protein (L1) and minor capsid protein (L2). All genes are responsible for regulation of gene expression, replication, and its packaging into virus particles [6].

HPVs perfectly adapt to the environment of the host cervical mucosa, and induce the transformation of cervical epithelial cell [52]. The viral life cycle initiates when viral particles infect into the basal cells of cervical epithelium through micro abrasions or trauma. HPV life cycle can be separated into two stages. First one is the nonproductive stage of early infection that viral genome maintain in form of episome by E1 and E2 activities. HPV DNA can be divided into two daughters by basal cell division, and one cell remains locate in basal layer or stem cell contributing a latent infection, while the other one is pushed and differentiate up to the supra-basal layer. Second stage is the productive, viruses replicate and amplifies its genome to higher copy number, expresses L1 and L2 gene for producing capsid protein in this supra epithelial layer, and for releasing as mature viral particles into the cervical area environment [53].

The current concept of mechanism of HPVs induce cervical carcinogenesis is that during the line of viral infection, the viral genome becomes integrated into the host DNA randomize [54, 55]. When viral genome integration occurs, result in disruption of the viral E2 gene that leading loss of control over expression of viral oncoproteins E6 and E7. E6 and E7 viral oncoproteins are critical molecules in the process of virus replication, which by interaction with a number of cellular proteins. Both oncoproteins interfere with functions of tumor suppressor proteins which regulate cell cycle and cell apoptosis, resulting in initiate pre-cancerous lesions and cancer [56].

Binding of E6 oncoproteins to host p53 tumor suppressor protein via the E6-Ap protein causes facilitates p53 degradation through the ubiquitin proteolytic pathway [57]. As a result of decreases the half-life of the p53 protein in infected cells, and p53-mediated cell cycle control is lost [58]. As a consequence, loss of p53

protein, these effective allow DNA-damaged cells to continue dividing without checkpoint controls, and hence, obstruction of p53 function can initiate carcinogenesis and formation of malignant tumors, the over expression of E6 and E7 proteins enable uncontrolled proliferation of infected cells through activates cellular cyclin E and A [59, 60] and then allow immortalization and malignancy transformation of cells [61]. While E7 protein binds to the cellular tumor suppressor protein retinoblastoma (pRb) and interfere pRb function by inhibition of pRb and E2F interaction, it will trigger the expression of proteins necessary for DNA replication [9, 62]. During tumor progression, the viral genomes often integrate into the host chromosome, which results in a constant level of E6/E7 proteins via stabilization of the mRNA, accumulation of oncogene mutations, further loss of cell-growth control, and ultimately cancer [63].

P53 status in cervical cancer

As described above, cervical cancer which presents of high risk HPV E6 protein induced the cellular ubiquitination-proteolytic system accelerated loss of p53 protein. Furthermore, viral genome E6 and E7 express continuously to maintain cells transformed phenotype, however, p53 gene was still functional as wide-type p53 in HPV-positive cervical cancer cell lines [64, 65]. Level of E6 has p53-dependent to be equal to p53-dependent anti-apoptotic properties [66]. Certainly, disruption of HPV E6 protein expression or blockage HPV E6 activity results in activation of cell apoptosis due to increase in p53 levels [67, 68]. Likewise, an anti-sense will down-regulate E6-AP expression, or catalytically inactive of E6-AP mutant, which could accumulate p53 in HPV-positive cell [69, 70]. Additionally, Deng and co-workers (2006) have provided evidence showing that a traditional Chinese herb medicine (TCM), Yigan Kang (YGK) could restore a normal p53 tumor suppressor protein in HeLa-HPV18-positive cervical cancer cells, this evidence has been correlated with repression of transcription of E6 oncoprotein [71]. Although, a slightly increased the apoptotic cell death found in this study, however, this herb has also showed the effect on inducing reversion of the tumorigenic phenotype, with YGK-treated HeLa cells implanted SCID mice showed much less aggressive tumor growth than untreated. Thus, the down-regulation of viral E6/E7 genes might be direct effect to inhibition of invasive cervical cancer [72]. Therefore,

drugs or compounds that effect to suppress HPV E6 oncoproteins expression or interfere E6-AP activity may possible being use for treatment in cervical cancer disease.

Tumor angiogenesis and cervical cancer development

Angiogenesis is a critical factor concerned in the development and progression of cancer that occurs almost in solid tumors, including in cervical cancer, as adaptation of cancer mass and its growth away from the exiting blood supply. The rapid proliferation and increased oxygen consumption of tumor cells lead to the formation of a hypoxic microenvironment that is believed to be the primary regulator of angiogenesis [73]. The oxygen tension of tumor tissue dropped below physiologic levels needed for oxidative metabolism [13]. An important of pro-angiogenic signaling occurs in response to hypoxic condition. This condition HIF-1 α protein accumulated when tumor growth beyond 1-2 mm³, needed more oxygen and nutrients and became hypoxic tumor cells, is strictly dependent on angiogenesis. In normoxia conditions, HIF-1 α is continuously degrade by the ubiquitin-proteasome pathway [74]. Under hypoxic conditions, HIF-1 α subunit translocated into the nucleus, where bind with HIF-1 β subunit. As consequence, an active HIF-1 complex acts as a transcription factor enable up-regulation of growth factors including VEGF. The induction of VEGF gene expression by hypoxia in tumor cells involves both an increase in the rate of gene transcription, mediated by the transcription factor HIF-1 α [75], and enhancement of the stability of VEGF mRNA [76].

Mechanisms of tumor angiogenesis

Angiogenesis is a complex process relates between cells, soluble factors, and ECM components. The structuring of a neovascular network needs various events including [77] :

1. Endothelial cells (ECs) and pericytes activation by changes of cells morphology for proliferation and secretion, local vasodilatation, increased vascular permeability, accumulation of extravascular fibrin
2. Basement membrane degradation by proteases
3. Sprouting of ECs by migration in to the interstitial space
4. ECs proliferation
5. Lumen formation
6. Generation of new basement membrane with the recruitment of pericytes
7. Fusion of the newly formed vessels

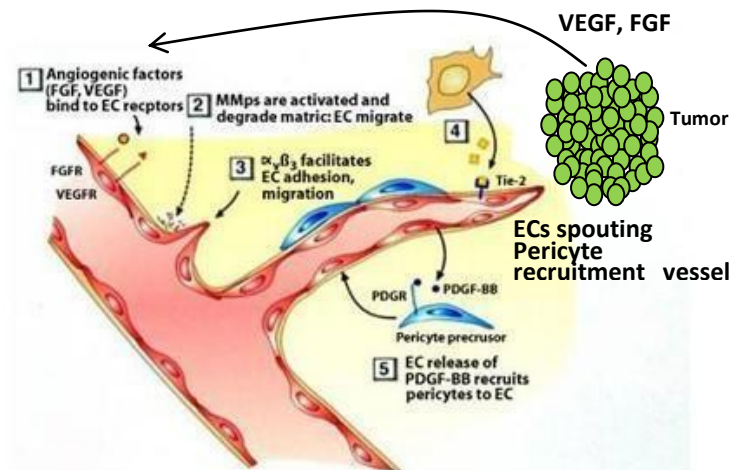


Figure 2.2 Process of tumor angiogenesis (Modified from Klagsbrun and Moses, 1999) [78].

As described above, sprouting-type angiogenesis is a key event in cervical cancer neovascularization. The regulation of angiogenesis in cervical cancer is mainly through hypoxic-mediated angiogenic pathway. However, the mechanism of angiogenesis in HPV-positive cervical cancer is related to the dysregulation of wild-type p53 tumor suppressor protein that causes of pro-angiogenic factors activation including up-regulation of VEGF expression [25]. Furthermore, the interruption of

p53 function, E6 viral protein has been shown to increase the induction of HIF-1 independently, thus increasing VEGF in the other ways [79].

Angiogenesis is an important phenotype in cervical cancer. Numerous studies have assessed angiogenesis in cervical cancer lesion as an independent prognosis marker for the disease. Almost a decade later, a lot of report that analysis of angiogenesis biomarker using immunohistochemistry was performed on cervical tumor specimens. The microvascular density was measured by immunohistochemistry staining for CD31, a non specific endothelial marker, in all stage of cervical cancer patients. Previous studies have shown that increased angiogenesis evaluated by MVD from CD31 staining was correlated with the grade of high-grade cervical intraepithelial neoplasm (CIN), a premalignant lesion of cervical cancer [20, 80]. Similarly, the highly density of micro vessel has been found in lesion of cervical epithelial neoplasia (CIN I-III) [18], early invasion (stage Ib-IIb) [17, 23], invasive and metastatic stage in cervical cancer [15, 16]. In addition, squamous CIN and invasive cell carcinoma of the cervix have also found increasing of MVD [19-22].

Clearly, angiogenesis is central to cervical cancer development, progression and prognosis, thus angiogenesis is pivotal in this disease and a rational target for therapy. Prominent roles of angiogenesis in cervical cancers are directly related to HPV induce p53 dysregulation and stabilization of HIF-1 α , both of which result in the up-regulation of VEGF.

Role of VEGF in cervical cancer development

VEGF is the main growth and survival factor for endothelial cells (ECs) which is necessary for vascular development [81, 82]. VEGF is a 40 to 45 kDa homodimeric protein which produced by a wide variety of cells and majority tumor cells. The VEGF family compose about six isoforms, and VEGF-A is the most important pro-angiogenic factor. Different isoforms of VEGF have been identified sharing ordinary receptors : VEGFR-1 or Flt-1, VEGFR-2 or KDR/Flk-1 and VEGFR-3 or Flt-4. Both VEGFR-1 and VEGFR-2 are located on ECs which function in cell proliferation, survival and migration. VEGF acts via paracrine mechanism to stimulate ECs that have abundant VEGF receptors (VEGFR), and also

acts in an autocrine fashion to stimulate VEGFR located on stromal cells surface [12-14].

VEGF or vascular permeability factor (VPF), is a heparin-like angiogenic growth factor. VEGF is a potent angiogenic factors which found in almost kinds of tumor, and play an important role in tumor angiogenesis. The main functions of VEGF include activation of ECs proliferation, increasing the vascular permeability and ECs migration toward tumor cells that result in generating neovascularization around tumors. Numerous studies have demonstrated that the expression of VEGF mRNA correlates with MVD of tumor tissue, and it is an important prognosis marker for differing human cancers, including cervical cancer [83]. The major mechanism of the regulation of VEGF expression mediated via Hypoxic response mechanism. In addition, there are many factors that involve in regulation of VEGF expression such as hormones, growth factors, oncogenic proteins, and tumor suppressor proteins [11]. According to numerous factors as mentioned, HPV oncoproteins play as causative agent of cervical cancer that may be one of the critical factors regulate the VEGF expression in cervical neoplasia. The up-regulation of VEGF and subsequent angiogenesis occurred, resulting from either blockage of p53 induction following DNA damage or increasing of p53 degradation [25]. Additionally, increasing VEGF expression had been found in experiment models of interfering of p53 function by HPV E6 oncoprotein, result in accumulation of HIF-1 α expression [79].

Moreover, many previous studies have showed that high risk HPV E5,E6, E7 oncoproteins activate VEGF promoter directly, resulting in VEGF up-regulation [26, 27, 84]. Furthermore, the up-regulation VEGF expression has also mediated through accumulation of HIF-1 α in HPV16-positive cervical cancer cells [28]. Several studies have reported the correlation between HPV viral titer and the expression of VEGF in CIN [85], that support the idea that the inactivation of p53 by E6 viral protein is involve in the regulation of VEGF expression [86]. Regarding all reports, HPV oncoproteins play an important role in the regulation of VEGF expression and angiogenesis in cervical cancer.

Acanthus ebracteatus Vahl.

A. ebracteatus Vahl. is one of the fourteen globally semi-mangrove plants, which is a member of the genus *Acanthus* in *Acanthaceae* family (Table 2.1) [87]. The vernacular names of this plant are difference among various countries such as;

English:	Sea holly
Malaysia:	Jeruju Hitam, Jeruju, Beruju, Chakar Bebak
Indonesia:	Jeruju, Daruju (Java), Juruju (Sumatra)
Philippines:	Kollil (Palauan), lagiwliw, ragoyroy (Dalangdang-Zambal)
Vietnam:	O ro
Cambodia:	Trohjekcragh pkapoe sar, Trohjeikcragh slekweng
Thailand:	Ngueak pla-mo, Ngueak plaamo dok muang, Nam-mo, Naagh Plamoh, Ja Kreng (Pattani province) [88]

Table 2.2 The family and species of the semi-mangrove plants

Family	Species
1. Acanthaceae	<i>Acanthus ebracteatus</i> Vahl.
	<i>Acanthus ilicifolius</i> Linn.
	<i>Acanthus volubilis</i>
	<i>Acanthus xiamenensis</i>
2. Euphorbiaceae	<i>Excoecaria agallocha</i>

	<i>Excoecaria indica</i>
3. Lythraceae	<i>Pemphis acidula</i>
4. Palmae	<i>Mauritia flexuosa</i> <i>Nypa fruticans</i> <i>Phoenix paludosa</i> <i>Oncosperma tigllarium</i>
5. Sterculiaceae	<i>Heritiera littoralis</i> <i>Heritiera fomes</i> <i>Herittiera globosa</i>

The synonyms of this plants are *Acanthus ilicifolius* Lour. and *Dilivaria ebracteatus* Pers. [89, 90]. This plant is commonly found in South-East Asia to northern Australia especially in east coast of Peninsular Malaysia, but less common in Indonesia. In Thailand, *A. ebracteatus* Vahl. is commonly distributed in the mangrove of brackish water canal or wetlands of seaside. This plant is well grown in tropical and subtropical area, where the water temperature is higher than 24 °C in the summer season and the annual rainfall more than 1,250 mm [87].

This plant is an erect herbaceous with woody material only seen in older branches. The stem is green to dark brown to black color and the armed with numerous spines. It can grow up to 1.5-2 meters tall, scarcely branched, with adventitious aerial roots. The leaves resemble those of holly with the leaf blade being dark green, stiff and deeply lobed oblong, 12-20 cm x 3-5 cm; spike up to 10 cm long. The apex of the lobes each has a sharp spine. Theirs flower are bracts ovate in terminal or axillary spikes of about 10 cm long with several flowers, bracteoles early caduceus, calyx lobes ovate, corolla lobe elliptical-oblong, 2.5 cm x 2 cm, white color but rarely pale blue color. *A. ebracteatus* Vahl. is gregarious and very common in tidal rivers. The fruit is a square-shape capsule which explodes when ripe and projecting the seeds measure up to 2 m from the plant, and the seeds are off-white and flat [90, 91].



Figure 2.3 *Acanthus ebracteatus* Vahl. (From <http://www.tropicalplantbook.com>)

Traditional use of *A. ebracteatus* Vahl.

Many countries in Asia, *A. ebracteatus* Vahl. has been used as folk medicine for a wide range of tropical diseases in Ayurveda. In India, whole plants are used as astringent, expectorant and stimulant, the roots are used as a cough remedy, the tender shoots and leaves are used as a snake-bite cure [92].

In Malaysia, its leaves and the boiled seeds are commonly used as an ingredient of a cough medicine and the seeds are also used for poulticing boils, or the decoction is drunk against boils [90, 93]. Two or three seeds are used to treat intestinal worms in children [89, 93]. The juice from leaves are used for preventing the hair loss. For snake-bite, the roots are used against snake venom in immediately, and the fruit pulp is used to poultice snake-bite wounds in Kalimantan. In addition, the roots are used to treat Herpes Zoster [89].

In Indonesia, the roots are used to poultice the wound that enhance the wound healing. In addition, the roots and ground ginger are taken together to salve the flatulence and treat the colic disease. A poultice may be used to relieve rheumatic pain, and in sometime the stems and leaves are used as purgative [89].

In Philippines, the leaves and roots boiled are used in the form of a decoction against asthma [89]. The roots are applied with boiled milk, is commonly used in leucorrhoea and tonic drinks.

In Vietnam, whole plants are used as diuretic agent, the root used to treat paralysis [89].

In Burma, the shoots may be used against snake venom, and the leaves are used to treat the rheumatism [89].

In China, the stem and roots are useful against hepatomegaly, hepatitis, as anticancer such as lymphoma, coughs, chronic fever, paralysis and asthma [93, 94].

In Thailand both genus of *Acanthus spp.*, *Acanthus ebracteatus* Vahl. and *Acanthus ilicifolius* Linn. have been used in the same way as traditional medicine, the plant is used as a purgative and anti-inflammatory in arthritis [36]. The whole plant is boiled in water for bath in order to heal rash and skin diseases. The fresh plant is crushed and applied as a poultice in boils or taken orally as depurative. The fruits are taken orally to ease menstrual disorder [95]. It has been also reported that its leaves dispensed with pepper (*Piper nigrum L.*) can be used as tonic pills for longevity [90].

The biochemical composition of *Acanthus ebracteatus* Vahl. and *Acanthus ilicifolius* Linn.

The biochemical constituents of *A. ebracteatus* Vahl. and its species, *A. ilicifolius* Linn. have been investigated. From the year 1955 to 2009, many reports demonstrated that *A. ebracteatus* Vahl. and *A. ilicifolius* Linn are composed of high biochemical constituents of alkaloids, flavonoids, aliphatic glycosides, lignans glycosides, megastigmane glycosides, phenylpropanoids, phenylethanol glycosides [37, 38, 42, 46, 96-99], triterpenoids [38, 41, 100], sterols [41, 46, 100, 101], quaternary amino acid [39], polysaccharides [40, 41], adenosine [96], sulphur [41], octacosyl alcohol [46], and ilicifolioside B [35]. The biochemical compounds which found in *A. ebracteatus* Vahl. and *A. ilicifolius* Linn are shown in Table 2.2.

Alkaloids Alkaloids isolated from *A. ebracteatus* Vahl. and *A. ilicifolius* Linn. can be classified into three types, pyridines, benzoxazolinones, and benzoxazin-3-ones [87]. Now a day, two pyridine, three benzoxazolinone, and eight benzoxazin-3-one alkaloids have been found in *A. ebracteatus* Vahl. and *A. ilicifolius* Linn. as shown in Table 2.2.

Flavonoids Ten flavonoids have been reported from *A. ebracteatus* Vahl. and *A. ilicifolius* Linn., one flavone, five flavones-*O*-glycoside, and three flavones-*C*-glycoside as shown in Table 2.2.

Aliphatic glycosides Five aliphatic glycosides, ebracteatoside B, ilicifolioside B, ilicifolioside C are aliphatic triglycoside, while ebracteatoside C and ebracteatoside D are aliphatic diglycosides have been isolated from *A. ebracteatus* Vahl. and *A. ilicifolius* Linn. as shown in Table 2.2 [35, 42, 102].

Lignan glycosides Eleven lignin glycosides have been isolated from *A. ebracteatus* Vahl. and *A. ilicifolius* Linn., and can be categorized into four types, cyclolignans, 2,4-diaryl tetrahydrofuranoid lignans, 2,5-diaryl tetrahydrofuranoid lignans and bisepoxylignan glycosides as shown in Table 2.2 [37, 38, 42, 96, 103].

Megastimane glycosides Seven megastimane glycosides have been reported from *A. ebracteatus* Vahl. and *A. ilicifolius* Linn. as shown in Table 2.2 [35, 42, 104].

Phenolic glycosides Seven phenolic glycosides have been isolated from *A. ebracteatus* Vahl. and *A. ilicifolius* Linn. as shown in Table 2.2 [42, 102, 104].

Phenylethanol glycosides Twelve phenylethanol glycosides have been reported from *A. ebracteatus* Vahl. and *A. ilicifolius* Linn. as shown in Table 2.2 [42, 96, 102, 105].

Triterpenoid Six triterpenoid glycosides, one triterpenoidal saponin [38], and five pentacyclic triterpenes, β -amyrin, α -amyrin, oleanolic acid, ursolic acid have been isolated from *A. ilicifolius* Linn., while lupeol have been reported from both *A. ilicifolius* Linn. and *A. ebracteatus* Vahl. as shown in Table 2.2 [41, 100].

Sterols Seven sterols, cholesterol, camptosterol, 28-Isocuposterol, stigmaterol- β -D-glucopyranoside, and stigmast-7-en-3 β -ol have been reported from *A. ilicifolius* Linn. [46, 100, 101], while stigmaterol and β -sitosterol have been isolated from *A. ilicifolius* Linn. and *A. ebracteatus* Vahl. as shown in Table 2.2 [41, 100, 101].

Polysaccharides Bioactive polysaccharides, neutral and acidic polysaccharides fractions have been reported in the extract from the stem of *A. ebracteatus* Vahl. [40, 41] (Table 2.2).

Miscellaneous Sulphur and quaternary amino acid have been found from *A. ebracteatus* Vahl. [39, 41], while octacosyl alcohol, adenosine, and iliciliosides B have been reported from *A. ilicifolius* Linn [46, 96, 102]) (Table 2.2).

Table 2.3 The biochemical composition of *Acanthus ebracteatus* Vahl. and *Acanthus ilicifolius* Linn.

Chemical constituents	Category	Bioactive compounds
Alkaloids	Pyridines	Trigonellin ^b [37]
		Acanthicifoline ^b (5-methoxy-1-methyl-2,4-dihydro-1H-2,7-naphthyridin-3-one) [37]
	Benzoxazolinones	2-Benzoxazolinone (BOA) ^b [46, 97, 99, 106]
		5,5'bis-benzoxazoline-2,2'-dione ^b [107]
		Benzoxazolinone glucoside ^b [108]
	benzoxazin-3-ones	Blepharin (HBOA-Glc) ^c (2R)-2-O- β -D-glucopyranosyl-2H-1,benzoxazin-3(4H)-one [42, 46, 99]

		(2 <i>R</i>)-2- <i>O</i> -β-D-glucopyranosyl-4-hydroxy-2 <i>H</i> -1,4-benzoxazin-3(4 <i>H</i>)-one (DIBOA-Glc) ^c [42, 46]
		(2 <i>R</i>)-2- <i>O</i> -β-D-glucopyranosyl-7-hydroxy-2 <i>H</i> -1,4-benzoxazin-3(4 <i>H</i>)-one (DHBOA-Glc) ^b [42, 46, 109]
		7-chloro-(2 <i>R</i>)-2- <i>O</i> -β-D-glucopyranosyl-2 <i>H</i> -1,4-benzoxazin-3(4 <i>H</i>)-one ^b [42, 46, 109]
		7-chloro-(2 <i>R</i>)-2- <i>O</i> -β-D-glucopyranosyl-4-hydroxy-2 <i>H</i> -1,4-benzoxazin-3(4 <i>H</i>)-one (7-Cl-DIBOA-Glc) ^c [42, 104]
		(2 <i>R</i>)-2- <i>O</i> -β-D-glucopyranosyl-5-hydroxy-2 <i>H</i> -1,4-benzoxazin-3(4 <i>H</i>)-one ^b [46, 104]
		2,6-dimethoxy- <i>p</i> -hydroquinone 1- <i>O</i> -β-glucopyranoside ^b [104]
Flavonoids	Flavone	Syringic acid β-glucopyranosyl ester ^b [104]
	Flavone- <i>O</i> -glycosides	Quercetin ^b [38]
		Quercetin 3- <i>O</i> -β-D-glucopyranoside ^b [37]

Table 2.3 The biochemical composition of *Acanthus ebracteatus* Vahl. and *Acanthus ilicifolius* Linn. (continued)

Chemical constituents	Category	Bioactive compounds
Flavonoids	Flavone- <i>O</i> -glycosides	Apigenin-7- <i>O</i> -β-D-glucuronide ^c [42, 110]
		Methylapigenin-7- <i>O</i> -β-D-glucuronate ^b [110]
		Luteolin-7- <i>O</i> -β-D-glucuronide ^a [42]
		Apigenin-7- <i>O</i> -glucuronide ^b [110]
	Flavone- <i>C</i> -glycosides	Acacetin 7- <i>O</i> -rutinoside ^b [35]
		Schaftoside ^a [42]
		Vecenin-2 (VCN-2) ^a [42] (Apigenin 6,8-di- <i>C</i> -glucoside)
		Vitexin ^b [35]

Aliphatic glycosides	Aliphatic diglycoside	Ebracteatosides C ^a (6R)-7-octene-1,6-diol 6- <i>O</i> -β-D-glucopyranosyl-(1→2)- <i>O</i> -[β-D-glucopyranoside [42]
Aliphatic glycosides	Aliphatic diglycoside	Ebracteatosides D ^a (6R)-7-octene-1,6-diol 6- <i>O</i> -β-D-xylopyranosyl-(1→6)- <i>O</i> -[β-D-glucopyranoside [42]
	Aliphatic triglycosides	Ebracteatosides B ^a (3R)-1-octene-3-ol-3- <i>O</i> -β-D-xylopyranosyl-(1''→6')- <i>O</i> -[β-D-glucopyranosyl-(1''→2'')]- <i>O</i> -β-D-glucopyranoside [42]
		Ilicifolioside B ^b [102, 111]
		Ilicifolioside C ^b [102, 111]

Note The chemical constituents were isolated from *A. ebracteatus* Vahl. (a), *A. Ilicifolius* Linn. (b), or both species (c).

Table 2.3 The biochemical composition of *Acanthus ebracteatus* Vahl. and *Acanthus ilicifolius* Linn. (continued)

Chemical constituents	Category	Bioactive compounds
Lignans glycosides	Cyclolignan glycosides	(+)-lyoniresinol 3 α -O- β -D-glucopyranoside ^c [37, 38, 42]
		(-)-lyoniresinol 3 α -O- β -D-glucopyranoside ^c [37, 38, 42]
		Acanfolioside ^b
		((+)-lyoniresinol 3 α -[2-(3,5-dimethoxy-4-hydroxy)-benzoyl]-O- β -glucopyranoside) [96]
		(+)-lyoniresinol 3 α -O- α -D-galactopyranosyl-(1 \rightarrow 6)-O- β -D-glucopyranoside ^b [112]
	(+)-lyoniresinol 2 α -O- α -D-galactopyranosyl-3 α -O- β -D-glucopyranoside ^b [112]	
	2,4-diaryl tetrahydrofuranoid lignans	Alangilignoside C ^b [96]
		(8R,7'S,8'R)-5,5'-dimethoxylariciresinol 4'-O- β -D-glucopyranoside ^c [38, 42]
		Dihydroxymethyl-bis(3,5-dimethoxy-4-hydroxyphenyl) tetrahydrofuran-9(or9')-O- β -glucopyranoside ^b [96]
	Bisepoxylignan glucosides	(+)-syringaresinol-O- β -D-glucopyranoside ^b [96]
		(+)-syringaresinol-O- β -D-apiofuranosyl-(1 \rightarrow 2)-O- β -D-glucopyranoside ^a [42]
		Magnolenin C ^a [42]

Note The chemical constituents were isolated from *A. ebracteatus* Vahl. (a), *A. ilicifolius* Linn. (b), or both species (c).

Table 2.3 The biochemical composition of *Acanthus ebracteatus* Vahl. and *Acanthus ilicifolius* Linn. (continued)

Chemical constituents	Category	Bioactive compounds
Megastigmane glycosides		(6R,7E,9S)-9-hydroxy-megastigman-4,7-dien-3-one-9-O-β-D-glucopyranoside ^b [35]
		(6S,7E,9S)-6,9-dihydroxy-megastigman-4,7-dien-3-one-9-O-β-D-glucopyranoside ^b [35]
		(6R,7E,9R)-9-hydroxy-megastigman-4,7-dien-3-one-9-O-β-D-glucopyranoside ^b [35]
	Sesquiterpenoids (Megastigmane glycoside derivative)	Plucheoside B ^c [42, 96]
		Alangionoside C ^a [42]
		Premnaionoside ^a [42]
		Ebracteoside A ^c [42, 96]
Phenolic glycosides (Phenylpropanoid glycosides)		2,6-dimethoxy-p-hydroquinone 1-O-β-D-glucopyranoside ^b [96]
		Syringic acid O-β-D-glucopyranosyl ester ^b [96]
		Zizybeoside I ^a
		(Benzyl alcohol 7-O-β-D-glucopyranosyl-(1→2)-O-β-D-glucopyranoside) [42]
		Isoverbascoside ^a [42]
		Verbascoside ^c [38, 42]
		(Z)-4-coumaric acid 4-O-β-D-glucopyranoside ^b [99, 102, [102]
(Z)-4-coumaric acid 4-O-β-D-apiofuranosyl-(100→20)-O-β-D-glucopyranoside ^b [102]		

Note The chemical constituents were isolated from *A. ebracteatus* Vahl. (a), *A. ilicifolius* Linn. (b), or both species (c).

Table 2.3 The biochemical composition of *Acanthus ebracteatus* Vahl. and *Acanthus ilicifolius* Linn. (continued)

Chemical constituents	Category	Bioactive compounds
Phenylethanol glycosides		Acteoside ^c [42, 102, 105]
		Isoacteoside ^c [42]
		Phenylethyl- <i>O</i> - β -D-glucopyranosyl-(1 \rightarrow 2)- β -D-glucopyranoside ^c [42]
		Cistanoside F ^b [99, 102]
		Isocistanoside F ^b [99, 102]
		Cistanoside E ^b [42]
		Campneoside I ^b [42, 102, 105]
		Campneoside II ^b (β -hydroxyacetoside) [42, 96]
Phenylethanol glycosides		Illicifoliosides A ^b [42, 102, 105]
		Illicifoliosides D ^b [42, 102, 105]
		Leucosceptoside A ^c [42, 102, 105]
		Martynoside (MAR) ^c [42, 102, 105]
Triterpenoids	Triterpenoids	Saponin ^b [α -L-arabinofuranosyl-(1 \rightarrow 4)- β -D-glucuronopyranosyl(1 \rightarrow 3)]-3 β -hydroxylup-20(29)-ene [38]
	Pentacyclic triterpenes	Ursolic acid ^b [100]
		Oleanolic acid ^b [100]
		β -Amyrin ^b [100]
		α -Amyrin ^b [100]
		Lupeol ^c [41, 100]

Note The chemical constituents were isolated from *A. ebracteatus* Vahl. (a), *A. ilicifolius* Linn. (b), or both species (c).

Table 2.3 The biochemical composition of *Acanthus ebracteatus* Vahl. and *Acanthus ilicifolius* Linn. (continued)

Chemical constituents	Category	Bioactive compounds
Sterols		Cholesterol ^b [100, 101]
		Campesterol ^b [100, 101]
		Stigmaterol ^c [41, 100, 101]
		β -Sitosterol ^c [41, 100, 101]
		28-Isocuposterol ^b [41, 100, 101]
		Stigmasteryl- β -D-glucopyranoside ^b [46]
		Stigmast-7-en-3 β -ol ^b [97]
Polysaccharides		Pectin polysaccharides ^a [40, 41]
Miscellaneous		Sulphur ^a [41]
		quaternary amino acid ^a [39]
		Octacosyl alcohol ^b [46]
		Adenosine ^b [96]
		Ilicifoliosides B ^b [102]

Note The chemical constituents were isolated from *A. ebracteatus* Vahl. (a), *A. ilicifolius* Linn. (b), or both species (c).

Biological activities of *A. ebracteatus* Vahl. and *A. ilicifolius* Linn.

Bioactivity studies of the extracts from *Acanthus spp.*, *A. ebracteatus* Vahl. and *A. ilicifolius* Linn. have been reported many biological activities, including larvicidal activity [113], antiviral [33], antibacterial and antimicrobial [114, 115], improve wound closure [116], immunopotentiating effect [31], anticarcinogenic [34, 45, 117], antioxidative and hepatoprotective [32], antimutagenicity [117], analgesic and anti-inflammatory [118], anti-tumor promoting activity [34, 41].

Table 2.4 Biological activities of bioactive constituents of *A. ebracteatus* Vahl. and *A. ilicifolius* Linn.

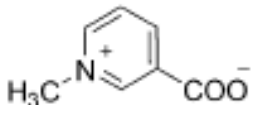
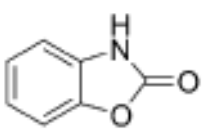
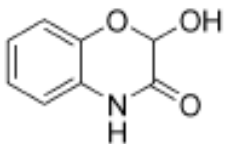
Categories	Bioactive constituents	Biological activities
Alkaloids	 <p>Trigonelline (TRG)</p> <p><i>A. ilicifolius</i></p>	Anti-oxidative activity [119] Anti-carcinogenic [119-122] Anti-migraine [119] Sedative [123] Anti-pyretic [124] Anti-septic [119] Hypocholesterolemic [119, 125] Hypoglycemic activities [119, 126] Diuretics and antitussive [127] Anti-diarrhea [124]
	 <p>2-Benzoxazolinone (BOA)</p> <p><i>A. ilicifolius</i></p>	Mycelial growth inhibitor [128] Anti-inflammatory [129] Anti-microbial [130] Selective retardation of cell cycle at G2/M checkpoint in meristematic cells [131]
	 <p>2,4-dihydroxy-1,4-benzoxazin-3-one (DIBOA)</p> <p><i>A. ebracteatus</i> <i>A. ilicifolius</i></p>	Mycelial growth inhibitor, Insecticide, anti-germination, antifeedant [128] Allelopathy [130, 132] Prostatic cells growth inhibitor [133] Auxin inhibitor, mutagenicity [134]

Table 2.4 Biological activities of bioactive constituents of *A. ebracteatus* Vahl. and *A. ilicifolius* Linn. (continued)

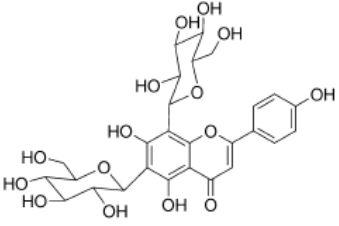
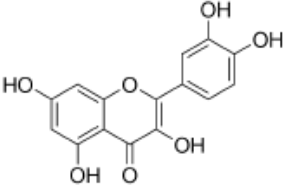
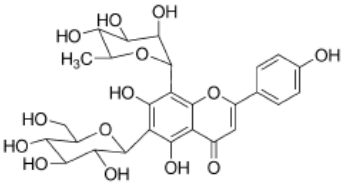
Categories	Bioactive constituents	Biological activities
Flavonoids	 <p>Vicenin-2 (VCN-2) <i>A.ebracteatus</i></p>	<p>Oviposition stimulant [135]</p> <p>Anti-proliferative, anti-angiogenic and pro-apoptotic effects in carcinoma of prostate (CaP) [136]</p>
	 <p>Quercetin <i>A. ilicifolius</i></p>	<p>Inhibition of tyrosine kinase activity [137]</p> <p>Anti-oxidative activity [138, 139]</p> <p>Anti-angiogenic activity [140]</p> <p>Cell cycle regulation in human gastric cancer cells [141]</p> <p>Induction of apoptosis in human leukemia HL-60 cell [142]</p>
	 <p>Schaftoside <i>A.ebracteatus</i></p>	<p>Antifeedant [135]</p>

Table 2.4 Biological activities of bioactive constituents of *A. ebracteatus* Vahl. and *A. ilicifolius* Linn. (continued)

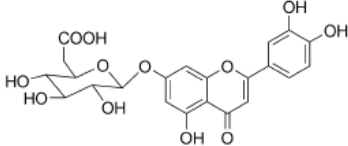
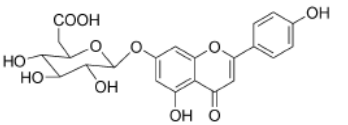
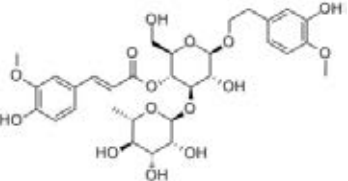
Categories	Bioactive constituents	Biological activities
Flavonoids	 <p>Luteolin <i>A.ebracteatus</i></p>	Antigonadotropic [143, 144] Lens aldose reductase inhibitor [145]
Flavonoids	 <p>Apigenin-7-O-β-D-glucuronide <i>A.ebracteatus</i> <i>A. ilicifolius</i></p>	Anti-inflammatory [146] Anti-oxidative activity [147] Anti-HIV [148] Anti-ulceric [149]
Phenylethanol glycosides	 <p>Martynoside (MAR) <i>A.ebracteatus</i> <i>A. ilicifolius</i></p>	Anti-oxidative activity [150-153] Anti-proliferative [154, 155] Cytotoxicity [156] Anti-metastatic [156]

Table 2.4 Biological activities of bioactive constituents of *A. ebracteatus* Vahl. and *A. ilicifolius* Linn. (continued)

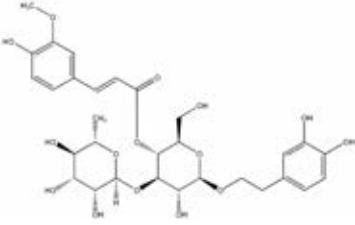
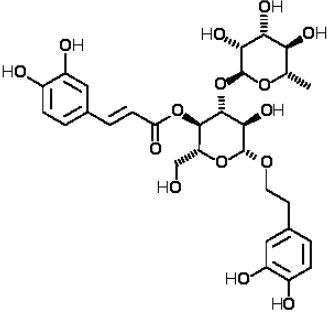
Categories	Bioactive constituents	Biological activities
Phenylethanol glycosides	 <p data-bbox="596 748 847 909">Leucosceptoside A <i>A. ebracteatus</i> <i>A. ilicifolius</i></p>	<p data-bbox="932 450 1310 517">Anti-oxidative activity [150, 151, 154]</p> <p data-bbox="932 551 1235 584">Anti-proliferative [155]</p> <p data-bbox="932 618 1209 651">PKCα-inhibitor [157]</p> <p data-bbox="932 685 1177 719">Antibacterial [158]</p> <p data-bbox="932 752 1155 786">Analgesic [159]</p>
	 <p data-bbox="624 1397 820 1682">Acteoside (Verbascoside) <i>A. ebracteatus</i> <i>A. ilicifolius</i></p>	<p data-bbox="932 943 1299 1010">Anti-oxidative activity [150, 151, 160-165]</p> <p data-bbox="932 1043 1310 1111">Anti-proliferative [155, 166, 167], [168]</p> <p data-bbox="932 1144 1241 1178">Cytotoxicity [160, 169]</p> <p data-bbox="932 1211 1273 1245">PKCα-inhibitor [157, 170]</p> <p data-bbox="932 1279 1310 1346">Down-regulation of ICAM-1 [171]</p> <p data-bbox="932 1379 1278 1413">Teromerase inhibitor [172]</p> <p data-bbox="932 1447 1257 1480">Anti-metastatic [42, 169]</p> <p data-bbox="932 1514 1246 1547">Anti-bacterial [173-175]</p> <p data-bbox="932 1581 1193 1615">Anti-viral [176-178]</p> <p data-bbox="932 1648 1315 1682">Anti-inflammatory [179, 180]</p> <p data-bbox="932 1715 1331 1805">Blocking inducible nitric oxide synthase (iNOS), COX-2, and AP-1 activation [181, 182]</p> <p data-bbox="932 1839 1262 1872">Immunomodulating [175]</p> <p data-bbox="932 1906 1289 1939">Hepatoprotective [183-185]</p>

Table 2.4 Biological activities of bioactive constituents of *A. ebracteatus* Vahl. and *A. ilicifolius* Linn. (continued)

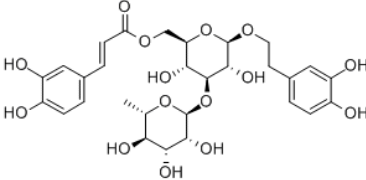
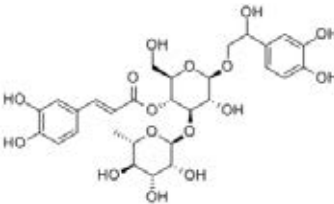
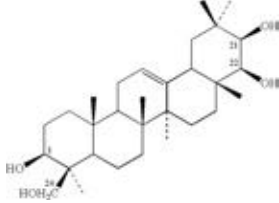
Categories	Bioactive constituents	Biological activities
Phenylethanol glycosides	 <p>Isoacteoside (Isoverbascoside)</p> <p><i>A.ebracteatus</i> <i>A. ilicifolius</i></p>	<p>Anti-oxidative activity [151, 152, 161, 184, 186]</p> <p>Anti-proliferative [155]</p> <p>Anti-neoplastic [187]</p> <p>Antiviral [176]</p> <p>Hepatoprotective [161, 184]</p> <p>Immunosuppressive [188]</p> <p>Analgesic [159]</p>
Phenylethanol glycosides	 <p>β-hydroxyacteoside (Campneoside II)</p> <p><i>A.ebracteatus</i> <i>A. ilicifolius</i></p>	<p>Anti-oxidative activity [179, 189]</p> <p>5-HETE formation inhibitor [174]</p> <p>Antibacterial [190]</p>
Triterpenoids	 <p>Saponin</p> <p><i>A. ilicifolius</i></p>	<p>Anti-angiogenic [191-193]</p> <p>Anti-tumor, anti-proliferative, induces cell apoptosis [192]</p> <p>Anti-protozoa [193]</p>

Table 2.4 Biological activities of bioactive constituents of *A. ebracteatus* Vahl. and *A. ilicifolius* Linn. (continued)

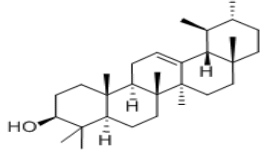
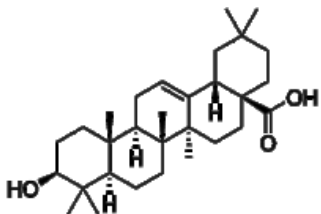
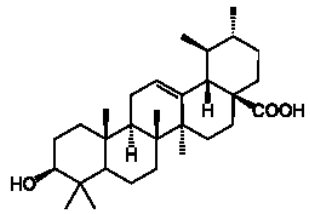
Categories	Bioactive constituents	Biological activities
Triterpenoids	 α -Amyrin <i>A. ilicifolius</i>	Anti-inflammatory [194-196] Gastroprotective [197] Cytotoxicity [198]
	 Oleanolic acid (OA) <i>A. ilicifolius</i>	Anti-tumor property [199, 200] Anti-angiogenic [201] Cytotoxicity [202, 203] Anti-inflammatory [194, 204-206] Anti-oxidative activity [207] Hepatoprotective [205, 208] Gastroprotective [209] Antifungal [210]
	 Ursolic acid (UA) <i>A. ilicifolius</i>	Anti-tumor property [199, 210] Anti-angiogenic [201] Inhibition of mouse skin tumorigenesis [210] Cytotoxicity [202, 210] Anti-inflammatory [194, 210, 211] Anti-oxidative activity [195, 212] Hepatoprotective [210] Antihistamine [210] Antimicrobial [210]

Table 2.4 Biological activities of bioactive constituents of *A. ebracteatus* Vahl. and *A. ilicifolius* Linn. (continued)

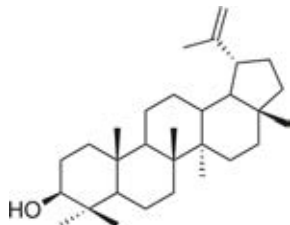
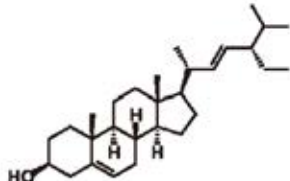
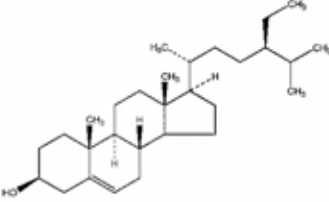
Categories	Bioactive constituents	Biological activities
Triterpenoids	 <p>Lupeol</p> <p><i>A. ilicifolius</i></p>	<p>Anti-tumor [213, 214]</p> <p>Inhibit tumor growth in prostate cancer [167]</p> <p>Anti-angiogenic [215], [216]</p> <p>Induction of cells apoptosis : via Fas/FasL in prostate cancer cells and human pancreatic cells [167, 213, 217]</p> <p>Anti-proliferative via alteration of P53, NF-kB, Akt, AP1 [217]</p> <p>Suppression of tumor growth and metastasis in HNSCC mice model [218]</p> <p>Anti-carcinogenesis of mouse skin induce by DMBA and benzoyl peroxide [167, 219]</p> <p>Anti-oxidative activity [220]</p> <p>Anti-protozoa [214]</p> <p>Anti-inflammatory [194-196, 221]</p> <p>Anti-microbial [214]</p>
Sterols	 <p>Stigmasterol</p> <p><i>A. ebracteatus</i></p> <p><i>A. ilicifolius</i></p>	<p>Anti-oxidative activity [207]</p> <p>Antiviral [222, 223]</p> <p>Antibacterial [224]</p>

Table 2.4 Biological activities of bioactive constituents of *A. ebracteatus* Vahl. and *A. ilicifolius* Linn. (continued)

Categories	Bioactive constituents	Biological activities
Sterols	 <p style="text-align: center;">β-sitosterol</p> <p style="text-align: center;"><i>A. ebracteatus</i> <i>A. ilicifolius</i></p>	<p>Promotion of cancer cell apoptosis via alteration p53/p21, activation of Caspase-3 and induction of Bax/Bcl-2 ratio via activate Fas signaling [225-227]</p> <p>Anti-proliferative [227]</p> <p>Pro-angiogenic activity [228, 229]</p>
Polysaccharides	Polysaccharides	<p>Immunopotentiating [40, 230-232]</p> <p>Anti-tumor [231, 233]</p> <p>Anti-angiogenic [234, 235]</p> <p>Anti-oxidative activity [231, 236]</p>

The anti-tumor potential of *A. ebracteatus* Vahl.

Since *A. ebracteatus* Vahl. and *A. ilicifolius* Linn. have similar therapeutic effects, they are used interchangeably in Thai folkloric medicine [237]. The last decade, the extract from *Acanthus sp.* has been tested for anti-tumor and anti-cancer potentials *in vitro* and *in vivo*. Animal studies have demonstrated that a crude aqueous extract from the roots of *A. ilicifolius* Linn. could increase up to 70 per cent the survival rate of Friend Leukemia Virus-induced leukemic Swiss mice without producing toxicity [44, 238]. In addition, it has been demonstrated that a crude extract of *A. ebracteatus* Vahl. showed no mutagenic effect, but rather possessed antimutagenic activity in a *Salmonella*/microsome mutagenicity test. Moreover, Tiwawech and co-workers (1993) have demonstrated that crude extract of *A. ebracteatus* Vahl. is a secure compound to use, which exerted the inhibitory effects on diethylnitrosamine (DEN)-induced hepatocarcinogenesis in Wistar rats [45]. Interestingly, the greatest inhibition was found when given *A. ebracteatus* Vahl. at

low dose (0.06 g/ kg BW per day) when treatment after DEN injection group. This suggests that this plant may have an inverse dose response effect, and the ordinary therapeutic dose of the extract use in human (0.06 g/ kg BW per day) will be the most suitable and effective dose level, however it must be in ongoing trials. Since the inhibitory effect of crude extract was greatest when treated after DEN induction, so this plant might be involved at the promotion and progression phases of hepatocarcinogenesis rather than at initiation phase. Taken together evidence indicated that crude extract of *A. ebracteatus* Vahl. had anticarcinogenic activity against the occurrence of liver cancer.

In 1998, Siripong and co-workers have studied on antitumor potential of active constituents from *A. ebracteatus* Vahl. roots. The result showed that crude extract and five isolated compounds from this plant did not have cytotoxic activity against P388 lymphocytic leukemia (*in vitro*, $IC_{50} > 30 \mu\text{g/ml}$ by MTT assay) [41]. However, a weak antitumor activity of aqueous extract (100 mg/kg BW of *A. ebracteatus* Vahl. intraperitoneum route for 5 days) against Sarcoma 180 ascites cell (1×10^6 cell/rats ip) transplanted in ICR rats was observed. This suggested that this plants may not have a direct effect on cancer cell, and *in vivo* antitumor activity which was claimed for the treatment of cancer in Thai traditional medicine may come from indirect pathway.

In addition, Babu and co-workers have studied antitumor and anticarcinogenic activity of *Acanthus* spp. (*A. ilicifolius* Linn.), the alcoholic extract of *A. ilicifolius* Linn. exhibited non-toxic to Dalton's lymphoma ascites tumor cells (DLA) and Ehrlich ascites tumor cells (EAC), but toxic towards lung fibroblast (L-929) cells (IC_{50} 18 $\mu\text{g/ml}$) in 72 hours treatment [34]. Moreover, the extract (250, 500 mg/ kg BW) was found to be effective against tumor progression and carcinogenesis of skin papilloma formation in mice. Furthermore, oral administration of the extract (500 mg/ kg BW) reduced the tumor volume and increased the life span by 75% in ascites tumor (EAC cells) harboring animals. This suggested that the effect of this plant may be specific to cancer cell types.

Recently, Phisalaphong and co-workers have used aqueous extract of *A. ebracteatus* Vahl. and the desalted product from nanofiltration (NF) to determine the

cytotoxicity effect to two types of cancer cell, human epidemoid carcinoma (KB) and human cervical carcinoma (HeLa) cell lines [48]. The initial aqueous extract showed cytotoxicity against both KB ($IC_{50} \sim 4,000 \mu\text{g/ml}$) and HeLa ($IC_{50} \sim 3,800 \mu\text{g/ml}$) cell lines while the desalted product showed better cytotoxicity against both KB and HeLa cell lines with IC_{50} values of 3,200 and 3,500 $\mu\text{g/ml}$, respectively. Although, the desalted extract showed the better cytotoxic than the initial extract, but it was not significantly.

Furthermore, several studies indicated that some bioactive compounds which are found in *A. ebracteatus* Vahl. had an antitumor activity to some kind of cancer cells. For example, β -sitosterol had antitumor effect on CA755 (carcinoma 755), L1210 (L1210 lymphoid leukemia), WA (walkwer 256 carcinosarcoma), but no effect on B16 (B16 melanocarcinoma), LE (Lewis lung carcinoma), SA (Sarcoma180), KB (Human nasopharyngeal carcinoma) [47]. In addition, Stigmasterol was not affect on P388 (lymphatic leukemia), CA, L1210, SA, and WA cancer cell lines. Beside, Lupeol had an antitumor effect on WA, but no effect on LE, PS, SA and KB cancer cell lines. Moreover, it has been reported that Lupeol in dose 0.025% w/v had anti-proliferative effect on Hep-G2 (human hepatocellular carcinoma), A-431 (human epidermoid cells), H-411E (rat liver hepatoma cells) with 79%, 70% and 44%, respectively. Moreover, benzoxazolines-2-one has been found in extracts from the roots of *A. ilicifolious* Linn. [46] and ribose derivatives of this compounds are known to be active as anticancer and antiviral agents [33]. Taken together, it supports that *A. ebrateatus* Vahl. has different effects on specific cancer cells type.

Toxicity of *A. ebracteatus* Vahl.

A few of *in vivo* studies of *A. ebracteatus* Vahl. toxicity reported that it caused kidney damage during the long-term and high-dose treatments in rats. This toxic effect might be related to a high salt level of the aqueous extract due to the growth location of *A. ebracteatus* Vahl. in brackish water. In 1987, Yanapirut and co-workers have demonstrated that *A. ilicifolius* Linn. (1-10 g/kg BW by orally for 2 weeks) was non-toxic to Swiss mice, but when using high doses (10-100 times of

the therapeutic drug in human used for 8 weeks) for a long period of time might cause abnormalities of the urinary system, such as nephritis [44]. Furthermore, the chronic toxicity of *A. ebracteatus* Vahl. have been studied in rats by Siripong and co-workers in 2001 [239]. Wistar rats were chronic oral administrated with the aqueous extract for 12 months at the doses of 0.06, 0.6 and 3.0 g/ kg BW/ day, which equivalent of the crude drug 0.27, 2.7 and 13.5 g/kg or 1, 10 and 50 times of the therapeutic drug in human used, respectively. The result showed that *A. ebracteatus* Vahl. extract did not affect to the body weight gains, the overall behavior, hematological, blood urea nitrogen (BUN) and albumin also slightly increase in high dose treatment. Histopathological findings showed also mild degree of some changes of livers and kidneys in all experimental groups, without dose-related, exceptionally significant increase in nephropathy was observed in female rats receiving extract at the doses of 2.7 and 13.5 g/ kg. So that, an aqueous extract of *A. ebracteatus* Vahl. may be safe for human use but prolong use and overdoses should be avoid to prevent nephrotoxic effect of the drug.

CHAPTER III

MATERIALS AND METHODS

Experimental design

To study the effects of aqueous crude extract of *A. ebracteatus* Vahl. on tumor angiogenesis and tumor growth in human cervical carcinoma both *in vitro* and *in vivo* model. This study was divided into 2 parts as follows:

Part I: *In vitro* study: To test anti-proliferative effect of aqueous crude extract of *A. ebracteatus* Vahl. on different types of cancer cells.

Part II: *In vivo* study: To test the anti-angiogenic effect of aqueous crude extract of *A. ebracteatus* Vahl. in human cervical carcinoma cells-implanted nude mice model.

Experimental scheme of Part I protocol : *In vitro* study of anti-proliferative effect of aqueous crude extract of *A. ebracteatus* Vahl.

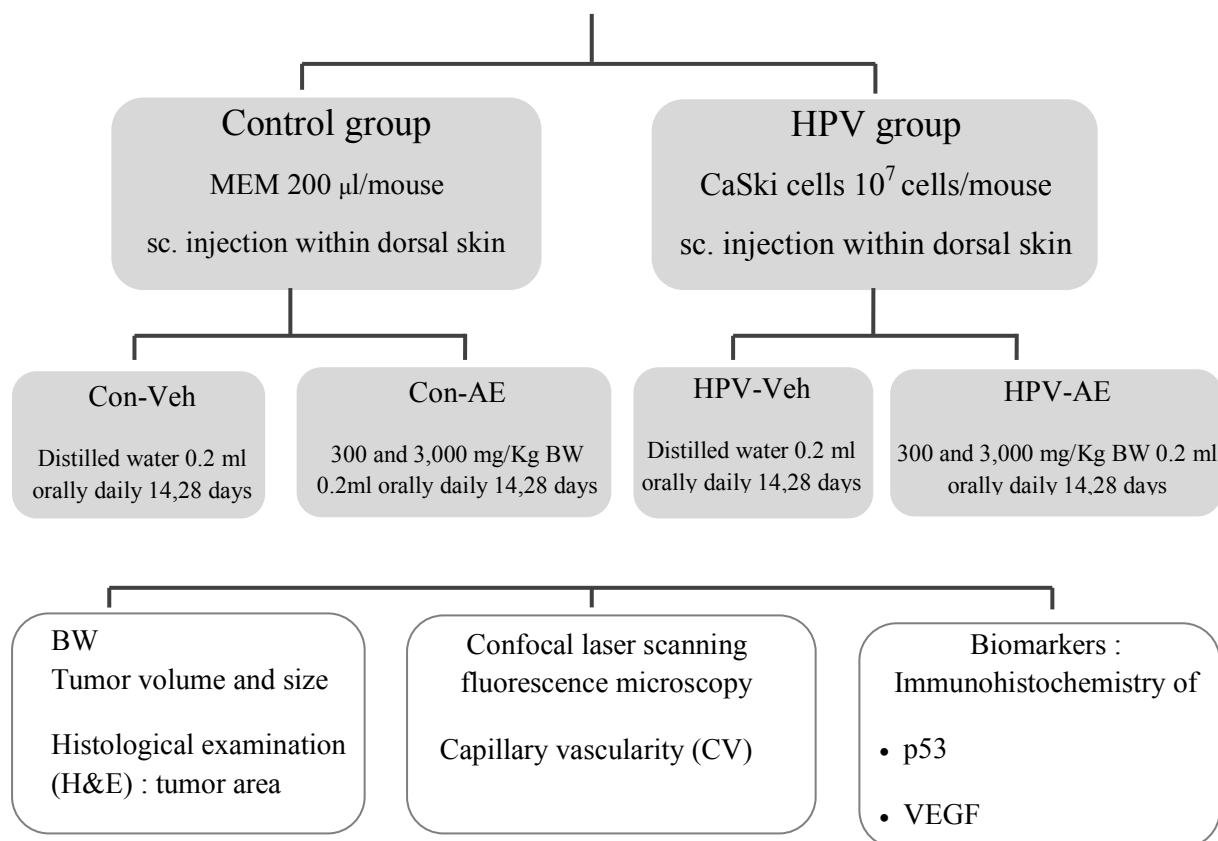
- CaSki : Human cervical carcinoma cell lines (HPV16-positive)
- HeLa : Human cervical carcinoma cell lines (HPV18-positive)
- HepG2 : Human hepatocellular carcinoma cell lines
- HDFs : Human dermal fibroblast cells

Experimental scheme of Part II : *In vivo* study

BALB/C- nude mice

Female 5-6 weeks,

BW 20-25 g



Research methodology

Preparation of aqueous crude extract of *A. ebracteatus* Vahl (AE).

A. ebracteatus Vahl. raw material were collected in Thailand, and aqueous crude extract of *A. ebracteatus* Vahl. was prepared and supplied by Natural Product Research Group, Research and Development Institute, The Government Pharmaceutical Organization (GPO), Thailand.

In brief, fresh leaves and stems of *A. ebracteatus* Vahl. were chopped into small pieces and air-dried. Then, 15 kg ground dried matters were boiled with distilled water (1 kilogram per 20 Liters of water) for 3 hours, twice a times. Then water extract was collected and filtered. The filtrate was dried by spray drying and 1,800 gm of light creamy-white powder was obtained. The powder extract was then kept in foil sachet (20 grams per pack) with desiccant [40]. The powder extract was suspended with distilled water or cell culture medium for bioactivities investigation.



Figure 3.1 The powder of aqueous crude extract of *A. ebracteatus* Vahl. and its solution when dissolved with distilled water.

Cell line cultivation

Three types of human cancer cell lines and one of normal cell line were used in this study. Human cervical carcinoma which contains the integrated HPV-DNA, CaSki (HPV-16 positive) and HeLa (HPV-18 positive) cells, Hepatocellular carcinoma cells, HepG2 were obtained from the American Type Culture Collection (ATCC, Manassas, VA, USA) and Human dermal fibroblast cells, HDFs was purchased from Cell Applications Inc, USA. All cancer cells were grown in Minimum Essential Medium (MEM) (GIBCO BRL, Gaithersburg, MD)

supplemented with 10% heat-inactivated fetal bovine serum (FBS) (Invitrogen, CA, USA), antibiotic mixture of penicillin (50 unit/ml) and streptomycin (50 µg/ml) (Bio Basic Inc., Canada) and 2 mM L-glutamine.

HDFs cells were maintained in Fibroblast Growth Medium (FGM; Cell Applications Inc, USA) supplemented with low serum growth supplement (1%FBS), EGF (5µg/ml), bFGF/Heparin/BSA (1.5µg/ml:5mg/ml:100µg/ml), Hydrocortisone (1mg/ml), and Gentamicin/Amphotericin B. All cells were cultured in a 37°C, 5%CO₂ humidified incubator and changed fresh medium every other day and were sub-cultured when reach 80% confluent to maintain cell growth in log stage. Cells were trypsinized by 0.025% trypsin-EDTA (Invitrogen, USA) before used. The human cervical carcinoma cell lines, CaSki cells which contain several hundred gene copies of integrated HPV-16 DNA were used in this study. CaSki were obtained from the American Type Culture Collection (ATCC) (CRL-1550 Lot No: 3794357). The cell was grown in Minimum Essential Medium (MEM) (GIBCO BRL, USA) supplemented with 10% heat-inactivated fetal bovine serum (FBS) (Invitrogen, USA), antibiotic mixture of penicillin (50 unit/ml) and streptomycin (50 µg/ml) (Bio Basic Inc., Canada) and 2 mM L-glutamine. The cell was cultured in a 37°C, 5%CO₂ humidified incubator and changed fresh medium every other days. The cell was sub-cultured when reached to 80% confluent to maintain cell growth in log stage. The cell was trypsinized into single cell before being used.

Experimental animal preparation

Inbred female BALB/c-nude mice (body weight 20-25 g) were obtained from the National Laboratory Animal Center, Salaya Campus, Mahidol University, Nakornpathom, Thailand. All animal experiments were conducted according to the “Ethical Guidelines for the Uses of animals” by The National Research Council of Thailand (1999) and approved by the Institutional Animal Care and Use Committee of Chulalongkorn University, Thailand. The mice were housed in a specific pathogen germ-free environment where temperature was 25 ± 3 °C, 60-70% air

humidify and 12h light-dark cycle. During the experiment, the mice were fed with standard laboratory chow and sterile water *ad libitum*.

The mice were divided into 2 groups and 12 sub-groups as follow:

- 1) Control mice without cancer cell injection were divided into 6 sub-groups:
 - 1.1 control mice received distilled water for 14 days (Con-Veh_14d; n=4),
 - 1.2 control mice received distilled water for 28 days (Con-Veh_28d; n=4),
 - 1.3 control mice received AE 300 mg/kg BW for 14 days (Con-300AE_14d, n=5),
 - 1.4 control mice received AE 300 mg/kg BW for 28 days (Con-300AE_28d, n=5),
 - 1.5 control mice received AE 3,000 mg/kg BW for 14 days (Con-3,000AE_14d, n=4),
 - 1.6 control mice received AE 3,000 mg/kg BW for 28 days (Con-3,000AE_28d, n=4).
- 2) HPV mice, which were injected with Caski cells and divided into 6 sub-groups:
 - 2.1 HPV mice received distilled water for 14 days (HPV-Veh_14d; n=5),
 - 2.2 HPV mice received distilled water for 28 days (HPV-Veh_28d; n=4),
 - 2.3 HPV mice received AE 300 mg/kg BW for 14 days (HPV-300AE_14d, n=3),
 - 2.4 HPV mice received AE 300 mg/kg BW for 28 days (HPV-300AE_28d, n=4),
 - 2.5 HPV mice received AE 3,000 mg/kg BW for 14 days (HPV-3,000AE_14d, n=5),
 - 2.6 HPV mice received AE 3,000 mg/kg BW for 28 days (HPV-3,000AE_28d, n=4).

The AE supplementation was started 1 week after inoculation of CaSki cancer cells and treatment durations were 14 and 28 days.

Experiment protocol

Part I : *In vitro* study of anti-proliferative effect of aqueous crude extract of *A. ebracteatus* Vahl. in human cervical carcinoma cell culture by MTT assay

Preparation of aqueous crude extract of *A. ebracteatus* Vahl. (AE) for in vitro assay

The powder of *A. ebracteatus* Vahl. aqueous crude extract was suspended in complete culture medium in difference concentration (10^{-3} – 10^4 µg/ml) and then were filtered through sterile cellulose acetate syringe filter with pore size 0.2 µm (Acrodisc, Thomas Scientific, USA) and kept at 2-8°C cover with light protection before being use. This AE solution must be prepared fresh before every experiment under aseptic technique in all process.

Determination of short-term (3 hours) cytotoxicity of the AE aqueous crude extracts by trypan blue exclusion method

Short-term cytotoxicity were carried out using CaSki, HeLa, HepG2, and HDFs cells, 1×10^6 cells in AE (10^{-1} – 10^4 µg/ml) dissolved with 1 ml 10%FBS MEM and then seed into 12-wells plate. Cells were incubated at 37 °C in a humidified incubator, 5% CO₂ for 3 hours. The viable cells were counted in a haemocytometer using the trypan blue exclusion method as described by Babu and colleague in 1995 and 2002 [32, 34, 240].

Determination of 24, 48 and 72 h-time anti-proliferative activity of AE aqueous crude extract by 3-(4,5-Dimethylthiazol-2-yl)-2,5-diphenyl tetrazolium bromide (MTT) Assay.

Preparation of the cell lines for MTT assay

The anti-proliferative effect of AE was determined in CaSki, HeLa, HepG2 and HDFs cells by using 3-(4,5 dimethylthiazol-2-yl)-2,5-diphenyl-tetrazolium bromide assay (MTT) (Sigma Chemical Co., St. Louis, MO). According to the MTT data was different depending on the cells and culture conditions used. Thus, the cell number must be optimized, cell density was determined during log growth stage by performing a cell titration experiment to develop linear relationship between

absorbance and cell concentration. Generally, in 96-wells *in vitro* assay that solid tumors have been usually used with the density varies from 10^3 - 10^5 cells/well [34, 241, 242]. So that, CaSki, HeLa, HepG2 and HDFs cells in a number of 1×10^4 cells/well (96-wells plate) were used in this experiment.

The MTT assay is a colorimetric assay for cellular proliferation based on the reduction of MTT agent (Sigma Chemical) by mitochondria of living cells. For all the experiments, the cell was divided into control group (untreated) and treatment group, which was exposed to various concentrations of AE crude extract 10^{-3} - 10^4 $\mu\text{g/ml}$ for 24, 48 and 72 hours of incubation durations.

MTT assay protocol

Briefly, when cells were detached by using 0.025% trypsin-EDTA into single cells, cells were then seed into 96-wells plate (1×10^4 cells per well in 100 μl of complete culture medium). The cells were allowed to grow for 24 hours at 37°C in a humidified incubator with 5% CO_2 atmosphere. On the following day, cells were divided into control group (untreated) and treated groups that were treated with different concentrations of the *A. ebracteatus* Vahl. aqueous crude extract. The medium was then removed and refilled with complete medium containing of AE (10^{-3} - 10^4 $\mu\text{g/ml}$ with total volume 100 $\mu\text{l/well}$), but for control group only medium was used.

At the end of 21-, 48- and 72-hour incubation, the medium was aspirated and 100 μl of 0.5 mg/ml MTT in serum free medium was added into each well. The plate was then incubated for 4 hours at 37°C in a humidified incubator with 5% CO_2 . After incubation, the MTT formazan which was MTT metabolic product produced by viable cells, appeared as dark-purple crystals in the bottom of the wells. The MTT solution was removed from each well carefully to prevent disruption of the cell monolayer and then was refilled with 150 μl of 99.9% dimethylsulphoxide (DMSO) (Sigma Chemical Co., St. Louis, MO). To thoroughly dissolve the formazan crystal, each plate was placed on shaking table for 5 minutes at room temperature for a minimum of 1 hour. Purple color solution was visible at this stage and then Optical Density (OD) of each plate was read by an enzyme-linked immunosorbent assay

(ELISA) plate reader (BIO-RAD Laboratories Inc., USA) at 540-nm wavelength. The MTT test was repeated at least 3 independent experiments.

The inhibitory effect of AE on cell proliferation was calculated by proportion of living cells at the same time interval by using the equation as follow;

$$\text{Cell viability (\%)} = \frac{\text{Means of ODs}}{\text{Means of ODc}} \times 100$$

$$\text{and Cell growth inhibition (\%)} = \frac{\text{Mean of ODc} - \text{Means of ODs}}{\text{Means of ODc}} \times 100$$

Where, means of ODs was an average optical density value of each AE-treated sample from triplicate replication, and means of ODc was an average optical density value of untreated control well without treatment from triplicate replication.

Analyzing of the half maximal inhibitory concentration (IC₅₀)

Dose-response curves were obtained for each cell types by plotting the percentage of growth inhibition (y-axis) versus the AE concentrations (µg/ml) (x-axis). And the 4-parameter logistic (4PL) non-linear regression equation was used to calculate the half maximal inhibitory concentrations (IC₅₀ values) of AE at 48-hour incubation using Microcal origin software program (version 5.0, Microcal software, Inc, MA, USA). The IC₅₀ value was expressed as means ± SEM of three independent experiments carried out in triplicate [243]. The IC₅₀ value was calculated from 4PL equation as follows:

$$F(X) = \frac{A_1 - A_2}{1 + (X/X_0)^P} + A_2$$

Where, X was the concentration of AE crude extract (µg/ml), F(X) was the percentage of cell growth inhibition (%), A₁ was initial or minimum value of % cell growth inhibition, A₂ was final or maximum value of % cell growth inhibition, P or

power was value of the Hill slope (+/-1), and X_0 was the midpoint of the curve (IC_{50}) (Figure 3.2).

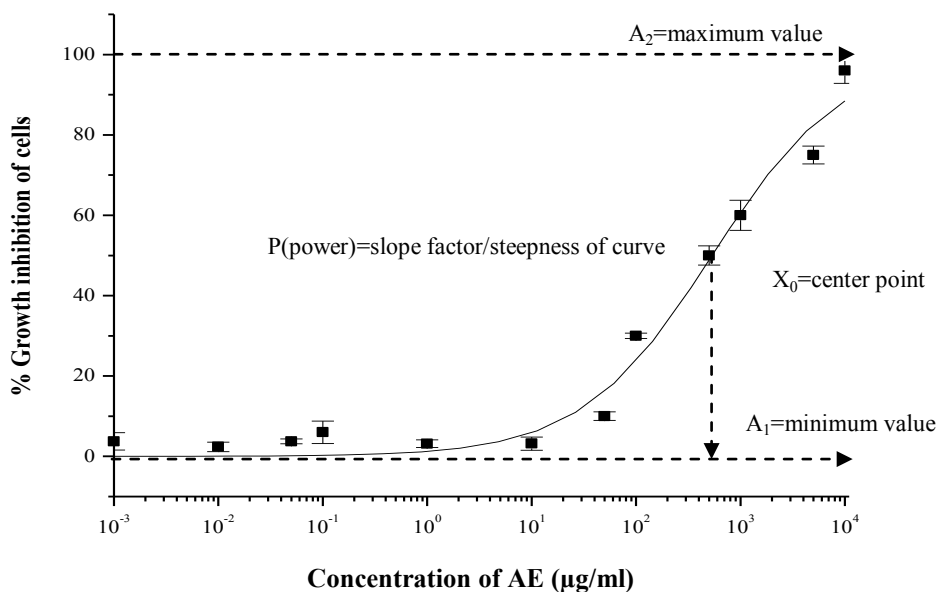


Figure 3.2 The 4-Parameter logistic nonlinear regression model

Part II : *In vivo* study the effect of AE on anti-angiogenic activity

This study determined the anti-angiogenic activity of aqueous crude extract of *A. ebracteatus* Vahl. in HPV16- associated cervical carcinoma nude mice model by using the confocal laser scanning microscopy for tumor microcirculatory study, and also investigated the associated biomarkers, p53 and VEGF. All animals were divided randomly into 2 groups; control and HPV group, which were injected with or without a human cervical cancer cells containing integrated HPV16 DNA (CaSki). As mentioned earlier, both groups were given vehicle or AE at the dosage of 300 and 3,000 mg/kg BW orally once a day for 14 and 28 days. The treatment was started when CaSki cancer cells growth reached to $\sim 0.2 \text{ mm}^3$ or tumor bud could be seen. The microvasculature was determined by labeling with fluorescence

tracer, and observed under confocal laser scanning microscope on day 14 and 28 after treatment.

Establishment of HPV 16-associated cervical cancer mice model

The HPV16-associated cervical cancer mice were prepared according to the procedure reported previously by Lertworapreecha and co-workers in 2009 [244]. For the HPV group, CaSki cells (1×10^7 cells/200 μ l (viability > 95 %)) were injected into subcutaneous layer at dorsal skin of mice. Control mice were given only MEM medium equal volume as HPV mice groups. Then, all mice were housed one animal per cage until end of experiment. All procedures were performed under aseptic conditions. In order to confirm the tumorigenesis induced by CaSki cancer cells, when the experiment was finished then tumor tissue sample from mice dorsal skin were excised and preserved with neutral buffer formalin (4% formalin, 0.4% NaH_2PO_4 , 0.65% Na_2HPO_4) immediately for histological examination. In order to study histopathological changes, formalin-fixed, paraffin-embedded tissue sample was cut in 5 μ m on a microtome with a disposable blade. The sliced tissue was fixed on to slide and stained with Hematoxylin and Eosin (H&E) staining by using automatic tissue staining (LEICA, Autostaining XL, Germany). Hematoxylin and eosin staining was investigated by the pathologist (SYL) in the (Pathological Division, Department of Obstetrics and Gynecology, Faculty of Medicine, Chulalongkorn University).

Tumor microvasculature study

The tumor microvascular imaging by the confocal laser scanning microscopy system

The tumor microvasculature was performed on days 14 and 28 after vehicle or AE crude extract treatment cancer cells inoculation, and visualized by using confocal laser scanning microscopic system (Nikon ECLIPSE E800 C1, Nikon, Japan). Firstly, the mice were anesthetized with an intraperitoneal injection of sodium pentobarbital (50 mg/ 100 g BW), and followed by catheterization of jugular vein. The polyethylene tubing 10 μ m of diameters (PE10) (Becton, Dickinson, NJ, USA) was inserted into a jugular vein of unconscious mice for an application of

fluorescence tracers (5% fluorescein isothiocyanate-labeled dextran (FITC-dextran), MW=200,000, 0.5%) (Sigma Chemical, USA).

Then mice dorsal skin was cut to open, and incised around tumor mass or the site of medium injection for the tumor microvasculature observation. This surgical procedure must be done carefully to avoid being cut off the blood vessels which were supply the tumor mass. After that, the skin with tumor mass was turned inside out and fixed with modeling wax on a plate (Figure 3.3).

For visualization of the microvascular lumen, a bolus of 0.1 ml of 5% FITC-dextran was injected into the jugular vein 5 minutes prior to the imaging. In each mouse, we observed and scanned the microvascular network on the skin surface around tumor mass by moving the microscopic stage. The tumor microvasculature observation was done by starting at 9 o'clock and moved in a clockwise direction around the tumor mass, and from outside to the center of tumor mass, that each mouse was always done by the same step. During the experiment, the fluorescent images were captured, and recorded as Windows Bitmap digital files. The laser scanning images were used for the evaluation of tumor angiogenesis, which was represented by analysis of the capillary vascularity (CV) within the tumor-bearing area by using the images analysis software, Image-Pro plus 6.0 software program (Media Cybernetics, Inc, USA).

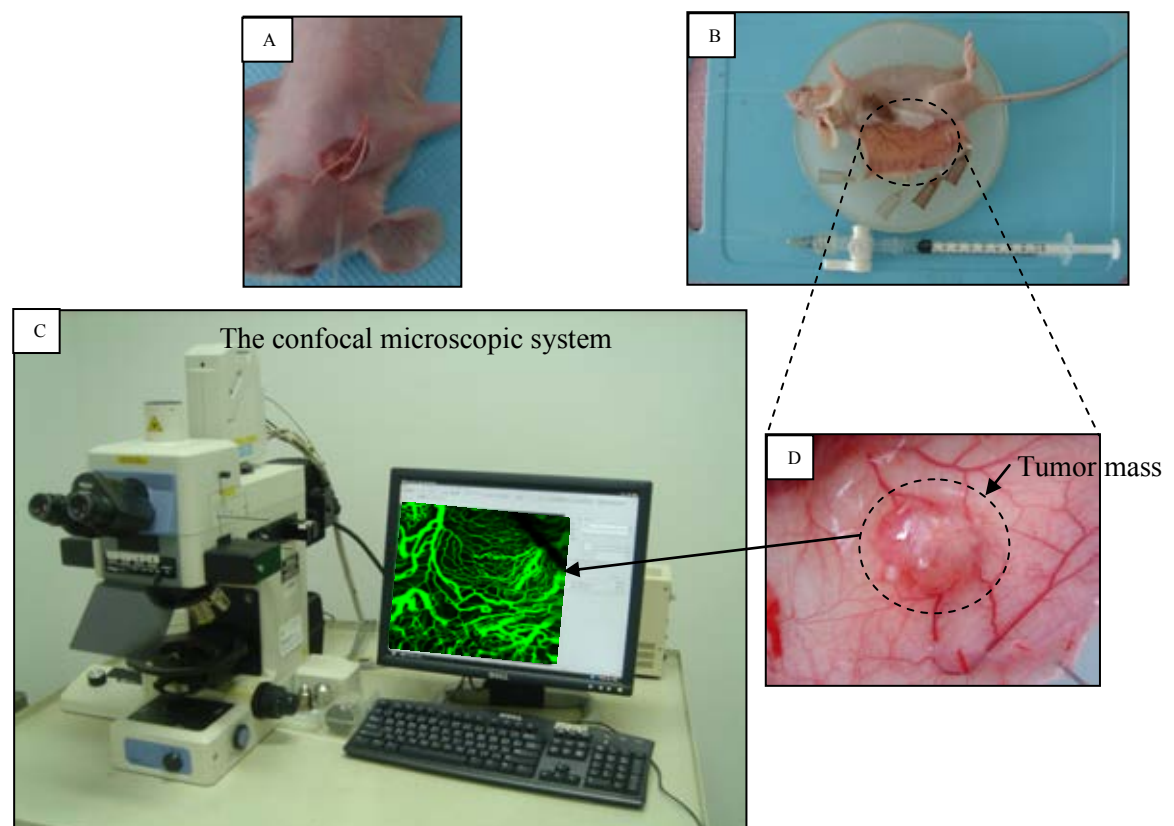


Figure 3.3 Photographs of experimental steps in tumor angiogenesis study in HPV16- associated cervical cancer nude mice model by using the confocal laser scanning microscopy system comprising the following steps: the catheterization of jugular vein with PE10 tubing (A), excision of dorsal skin around tumor mass and skin fixation for visualization under confocal microscope (B), the confocal laser microscope scanning the fluorescent image of tumor microvessels (C), the observation area of tumor microvascular network of skin surface around tumor mass (D).

Measurement of microvascular parameters : Capillary vascularity (CV)

In each mouse, the microvascular network on the surface around tumor mass were observed, scanned and recorded for 10 images, and 3 windows of the regions of interest (ROI) were drawn on each fluorescent image (frame). Three regions of interest (ROIs) from recorded fluorescent images were selected for capillary vascularity analysis (Figure 3.4), using Image-Pro plus software program [42].

In brief, each ROI was selected to cover only clear capillary network with diameter less than 15 μm [23]. Each selected ROI, both minimum and maximum level of pixel in the capillary network were determined, and the numbers of pixels located within all capillaries in each ROI were automatically calculated by using the “Histogram” functional tool of Image-Pro plus software program as shown in Figure 3.4. The proportion of the number of pixels within the capillaries to total number of pixels within the selected ROI (~ 10,000 pixels) was expressed as the percentage of capillary vascularity (CV%) for each ROI. The percentage of CV was computed by using the formula as follows :

$$\text{CV (\%)} = \frac{(\sum \text{Number of pixels within the capillaries})}{(\text{Total number of pixels within the select area})} \times 100$$



Figure 3.4 Confocal laser microscopic image of tumor microvascular and ROIs selected for measurement of capillary vascularity (CV) in each mouse. The “Histogram” functional tool of Image-Pro plus software program, which used to calculated the percentage of capillary vascularity. Tumor microvessels were visualized using FITC-dextran fluorescence, low magnification $\times 10$, Bar = 50 μm .

The CV was obtained about 25-30 ROIs in each mouse. Accordingly, averaged CV over three ROIs was performed, and the mean CV level in each group was obtained. The mean capillary vascularity level was used as an index of tumor angiogenesis.

Measurement of tumor growth : tumor size, tumor weight and histopathological examination for tumor area

When tumor microvasculature study finished, mice were sacrificed and tumor mass were carefully excised immediately. Tumor size was measured by using Vernier caliper (VWR, St. Louis, USA) then tumor mass was fixed with neutral buffer formalin. Tumor volume was calculated by the following the ellipsoid volume formula:

$$\text{Tumor Volume (mm}^3\text{)} = \pi/6 (\text{length}) \times (\text{width}) \times (\text{height}) \quad [44]$$

Immunohistochemistry for P53 and VEGF expression

The expression of p53 and VEGF proteins was assessed in paraffin-embedded sections of dorsal skin tumor lesion of mice which were collected at the end of experiment (day 14th and 28th after treatment).

The immunohistochemical analyses was conducted via the avidin-biotin-peroxidase complex method as described elsewhere [245]. The primary antibody was used for VEGF proteins are rabbit polyclonal anti-body (VEGF-A20, Santa Cruz Biotechnology, CA, USA) and p53 protein rabbit polyclonal anti-body (NB600-575, Novusbio, USA). Anti-dThdPase (Rosche Institute, Kanagawa, Japan) monoclonal antibody was used in each staining.

Protocol of P53 Immunohistochemical staining

Formalin-fixed of tissue samples were performed, paraffin-embedded were serially sectioned at 4 μm , and mounted onto the 3-aminopropyltriethoxysilane coat slides. After heated at 60 °C for 1 hour, sections were deparafinized and rehydrated. The slides were an incubated with an antigen Retrieval Solution pH 6.0 (DAKO S1699) at 95-99 °C in water bath for 40 minutes. Then, the slides were incubated with 3% hydrogen peroxide solution in distilled water 200 μL for 5 minutes to block endogenous peroxidase activity. Nonspecific background were blocked by application of 3% Normal horse serum 200 L on section slides. Application of antibodies, anti-P53 Rabbit polyclonal (1:50) 200 μL were applied on tissue sections, followed by incubated at room temperature for 60 minutes. After washed by PBS (pH7.4), visualization reagent (Envision) 200 μL were applied on tissue sections and incubated at room temperature for 30 minutes. Color was developed by using DAB (3,3'Diaminobenzidine tetrahydrochloride), and the slides were counter-stained with Hematoxylin and mounted with resinene. Negative control slides were established by replacing the primary antibody with PBS and normal rabbit serum. Known immunostaining-positive slide were used as positive controls.

Assessment of tumor p53 protein expression

Tumor area were identified under a low-magnification microscope (Nikon ECLIPSE 50i, Nikon, Japan) and the highest positively stained cells of p53 were performed using high-magnification microscope. The digital camera (Nikon DS-Fi1-L2, Nikon, Japan) and image software (NIS-Elements Basic Research (BR), Nikon INSTRUMENTS, Co., Japan) was used to monitor and capture images which were recorded as TIF format. The quantitative analysis for p53 was performed by using Image-Pro Plus software program.

Nuclear staining either as fine or coarse granular dots was considered positivity for p53. P53 expression in tumor area were assessed as percentage of positive cells. The positive association with p53 was obtained through the count of one thousand cells in 10 high power field (HPF) in each animals, using the most representative areas inside tumor area lesion. Two pathologists without prior clinical or pathological information scored expression at 100x and 200x magnification under light microscopy.

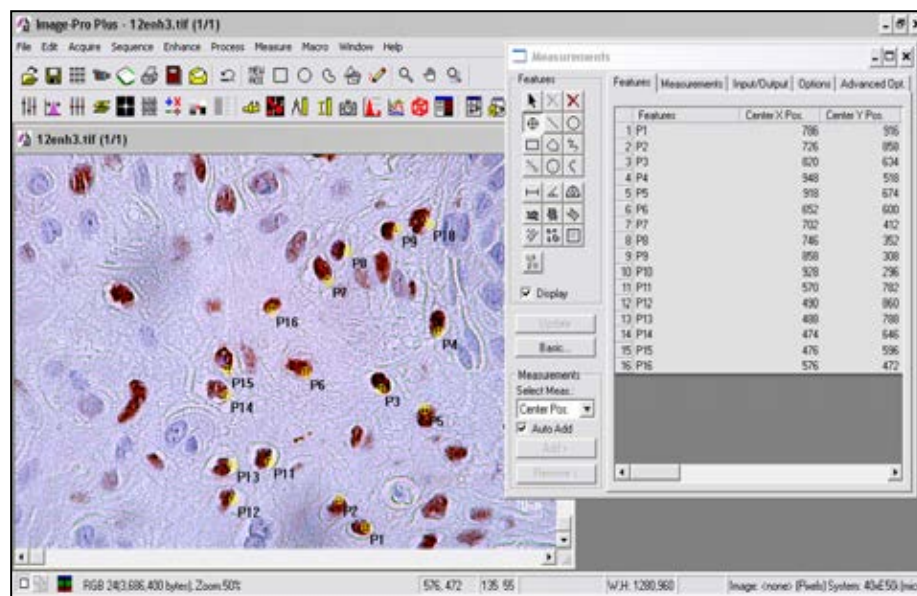


Figure 3.5 Nuclear brown color staining of anti-P53 Rabbit polyclonal in tumor tissue from CaSki cells-implanted nude mice treated with AE crude extract. Evaluation of p53 expression by count the number of p53-positive cell in 10HPF using Image-Pro plus software program, high magnification (x400).

Protocol of VEGF Immunohistochemical staining

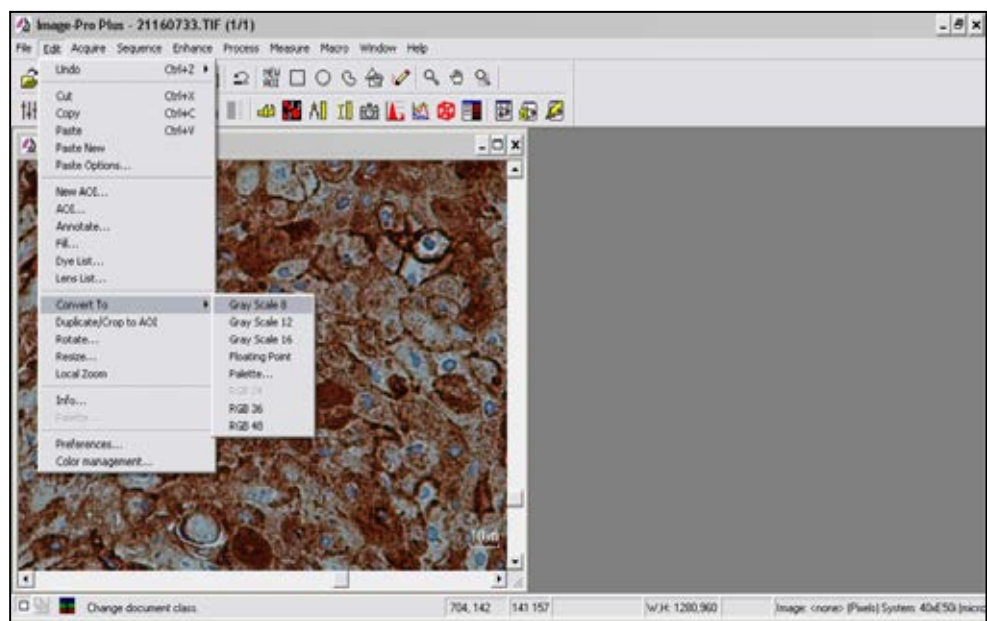
Immunostaining was performed using paraffin-embedded 4- μ m-thick tumor area sections. Sections were de-paraffinized, hydrated, blocked for endogenous peroxidase using 3% H₂O₂/H₂O, and subsequently incubated with antigen Retrieval Solution EDTA buffer (BD Pharmingen, San Diego, CA) in 95-99°C water-bath at pH 8 for 40 minutes.

Nonspecific background was blocked by application of 3% normal horse serum 200 μ L. Application of antibodies, anti-VEGF (1:100) 200 μ L were applied on tissue sections, followed by incubated at 4 °C overnight. After washed by PBS (pH7.4), 200 μ L visualization reagents, a biotin-labeled secondary antibody (biotinylated anti-rabbit immunoglobulins, Envision) were applied on tissue sections and incubated at room temperature for 30 minutes. Color was developed by using DAB (3,3' Diaminobenzidine tetrahydrochloride), and the slides were counter-stained with Hematoxylin and mounted with resinene. Negative control slides were established by replacing the primary antibody with PBS and normal rabbit serum. Known immunostaining-positive slide were used as positive controls.

Assessment of tumor VEGF protein expression

VEGF positive cell showed brown-yellow particles in cytoplasm, which were monitored and captured by digital camera (Nikon DS-Fi1-L2, Nikon, Japan) and image software (NIS-Elements Basic Research (BR)). The quantitative analysis for VEGF expression of each mouse was performed by using Image-Pro Plus 6.1 Software, and the percentage of VEGF expression was represented by proportion of VEGF staining area per total ROI area [245]. The software calculated the area of VEGF staining through 10HPF for each mouse (as shown in Figure 3.6). The RGB images were converted into binary images and discriminated between VEGF staining pixels and VEGF-negative cells staining pixels based on grayscale intensity. The percentage of VEGF expression was defined as the number of cytoplasmic VEGF-positive pixels divided by the total number of pixels within each HPF image. Accordingly, averaging VEGF expression over 10HPF images was performed, and the mean VEGF expression level in each group was used as a biomarker of tumor angiogenesis.

(A)



(B)

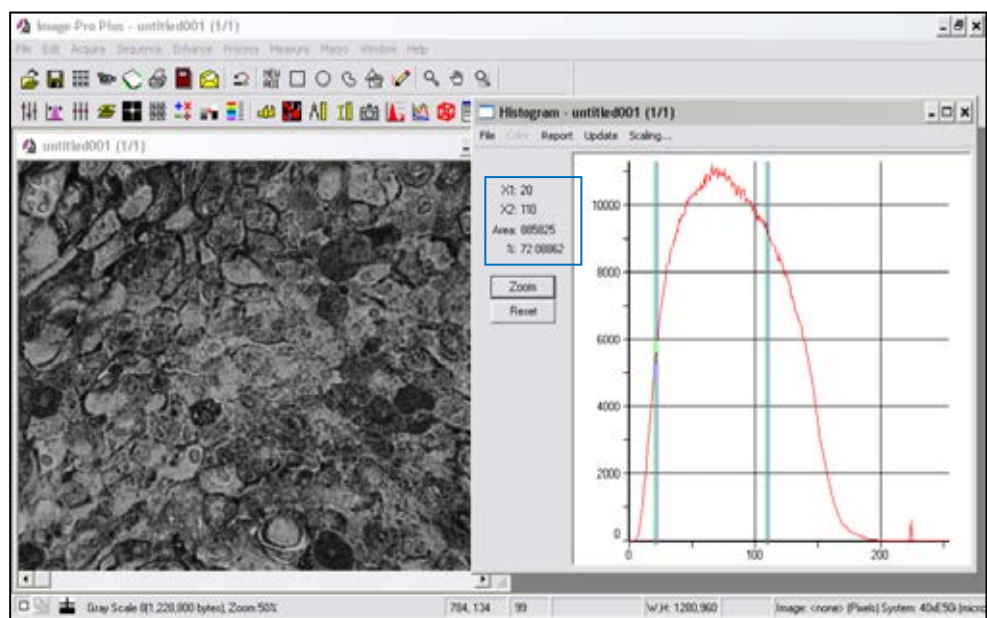


Figure 3.6 Representative VEGF immunoreactivity **(A)**, VEGF-positive brown staining in cellular cytoplasm. Quantitative of VEGF expression in converted grayscale image by using the “Histogram” functional tool of Image-Pro plus software program **(B)**, high magnification (x400).

Statistical analysis

All statistical calculations were performed using SPSS software program (version 16.0; SPSS Inc., Chicago, IL USA). All data were expressed as means and standard errors of mean (SEM). The statistical method was used including the student t-test, the one way analysis of variance (one-way ANOVA) followed by Turkey and LSD test, and pearson correlation test. The probability values less than 0.05 ($P < 0.05$) was considered to be statistically significant.

Ethical consideration

The experimental protocol will be approved by Ethics Committee, Faculty of Medicine, Chulalongkorn University. The animal study will be conducted according to the guideline for experimental animals suggested by the National Research Council of Thailand (1999).

CHAPTER IV

RESULTS

The content of this chapter consists of two major parts, including *in vitro* and *in vitro* study, which are the experimental results of anti-proliferative, anti-tumor and anti-angiogenic activities of *A. ebracteatus* Vahl. aqueous crude extract in human cervical carcinoma. In addition, the results also demonstrate the relevant mechanisms, the expressions of apoptotic and angiogenic biomarkers, P53 and VEGF, respectively.

Part I *In vitro* study of anti-proliferative effects of *A. ebracteatus* Vahl. aqueous crude extract in cancer cell lines.

The aqueous crude extract of *A. ebracteatus* Vahl. was dissolved in cell culture medium before used for cytotoxicity and anti-proliferative activity testing in three cancer cells, CaSki, HeLa, HepG2, and one normal cell, HDFs cells by using the Trypan blue exclusion method and MTT assay.

Short-term (3-hr) cytotoxicity of *A. ebracteatus* Vahl. aqueous crude extract in cancer cell lines and normal cells by Trypan blue exclusion method

The short-term cytotoxicity study of *A. ebracteatus* Vahl. aqueous crude extract on CaSki, HeLa, HepG2, and HDFs cells were performed by Trypan blue exclusion method. Trypan blue staining is used to evaluate the number of viable

cells presented in cell suspension. Base on the principle that living cells possess intact cell membrane that excluded trypan blue dye, whereas dead cells were labeled with the dye allowing to be counted. Microscopic study showed dead cell stained blue after treatment AE in various concentration 10^{-2} - 10^4 $\mu\text{g/ml}$ for 3 hours, and the percentage of number of the living and dead cell were counted (**Table 4.1**). The results demonstrated that the percentage of viable cell was higher than 90% in all treated groups (**Figure 4.1**). The results indicated that the aqueous extract was nontoxic towards HDFs, CaSki, HeLa, and HepG2 cells when treatment in short times for 3 hours.

Table 4.1 *In vitro* Short-term (3-hr) cytotoxicity of *A. ebracteatus* Vahl aqueous crude extract.

AE concentration ($\mu\text{g/ml}$)	Percentage of cell death (%)			
	CaSki cells	HeLa cells	HepG2 cells	HDFs cells
0.1	5.21 \pm 1.18	4.83 \pm 0.27	5.05 \pm 0.40	4.87 \pm 0.48
1	5.41 \pm 1.40	4.35 \pm 0.33	4.06 \pm 0.50	4.58 \pm 0.63
10	5.63 \pm 0.34	5.22 \pm 1.35	4.16 \pm 0.34	4.87 \pm 0.42
100	4.46 \pm 0.47	4.48 \pm 0.58	4.52 \pm 0.66	4.85 \pm 0.22
1,000	5.01 \pm 1.96	4.01 \pm 0.53	3.88 \pm 1.82	5.15 \pm 0.35
5,000	4.62 \pm 0.72	4.44 \pm 0.69	4.92 \pm 0.78	5.44 \pm 0.38
10,000	4.37 \pm 0.57	4.03 \pm 0.41	5.00 \pm 0.35	4.58 \pm 0.38
Control (MEM)	5.13 \pm 0.92	3.91 \pm 0.57	4.18 \pm 0.24	4.50 \pm 0.28

Note : Data are expressed as mean \pm SEM.

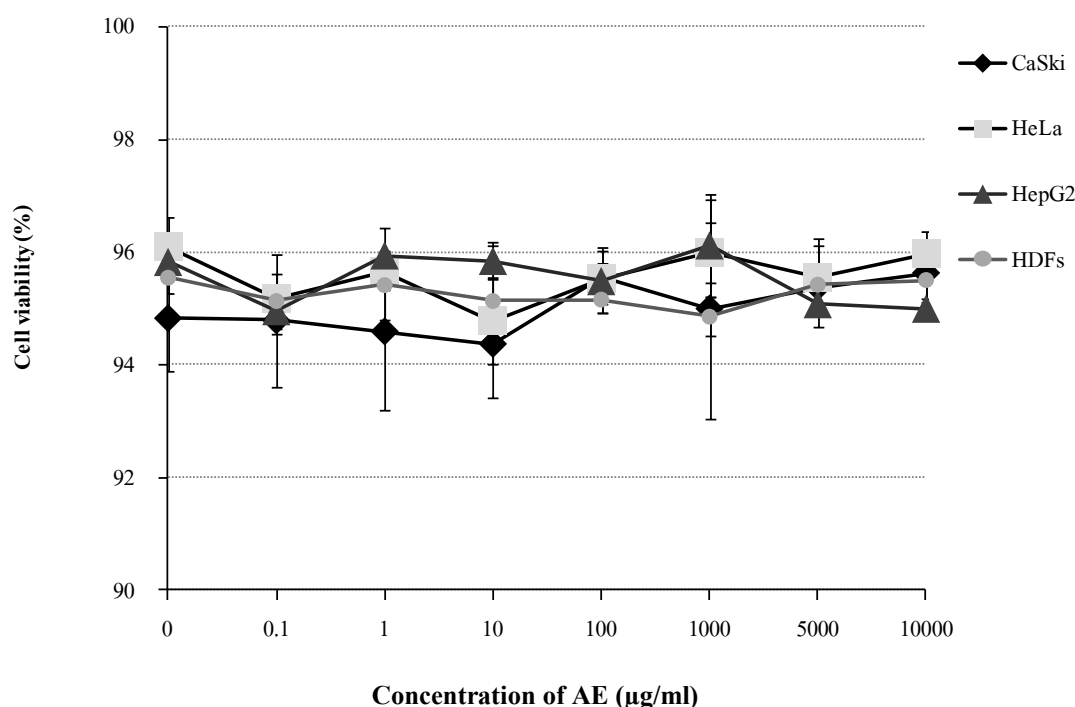


Figure 4.1 The cytotoxicity of *A. ebracteatus* Vahl. aqueous crude extract on CaSki, HeLa, HepG2, and HDFs cells for 3 hours incubation. Data are expressed as means \pm SEM of three independent experiments carried out in triplicate.

The anti-proliferative property of *A. ebracteatus* Vahl. aqueous crude extract in cancer cell lines and normal cells by MTT assay.

The anti-proliferation activity of *A. ebracteatus* Vahl. was tested by using MTT assay. Based on the principle that viable cells depend on an intact mitochondrial respiratory chain and intact mitochondrial membrane. The MTT agent is a yellow tetrazolium salt that is cleaved into a water-soluble purple formazan by succinate dehydrogenase system which belong to the mitochondrial respiratory chain and is only in viable cells. After solubilization of the formazan, the amount of dye was quantified with microplate reader at 540 nm. Therefore, toxicity of *A. ebracteatus* Vahl. aqueous crude extract on normal and cancer cells can be identified using mitochondrial dehydrogenases from viable cells.

Time-response of anti-proliferative properties of *A. ebracteatus* Vahl. aqueous crude extract

The time-response curves of AE were obtained by plotting the percentage of cell viability versus concentrations of AE in three different times of incubation 24, 48 and 72 hours (**Figure 4.2 – 4.5**). The MTT assay data used for calculated anti-proliferation activity of AE which were expressed as means of percent cell viability (**Table 4.2**).

Treatment with *A. ebracteatus* Vahl. aqueous crude extract did not show different inhibitory effects on HDFs, HeLa, HepG2 cells growth when incubated in different times 24, 48, and 72 hours (**Figure 4.2, 4.4, 4.5**). The time-response found only in Caski cells when treatment with AE aqueous crude extract at concentration of 5,000 μ g/ml. The results showed percentage of CaSki viable cells in 24 hours incubation was less than 48 and 72 hours incubation time ($P < 0.05$) (**Figure 4.2**).

Table 4.2 Percentage of cell viability of HDFs, CaSki, HeLa, and HepG2 cells when treatment with *A. ebracteatus* Vahl. aqueous crude extract in various concentration ($10^{-3} - 10^4$ $\mu\text{g/ml}$) for 24, 48, and 72 hours incubation.

Cell types	Time of incubation (hours)	Cell viability (%) / AE concentration ($\mu\text{g/ml}$)										
		0.001	0.01	0.05	0.1	1	10	50	100	1,000	5,000	10,000
HDFs	24	94.22±5.28	97.06±4.84	95.61±6.67	98.86±3.48	99.34±2.27	95.88±7.49	92.81±8.98	98.57±4.57	90.37±6.67	83.57±4.60	36.55±8.43
	48	99.92±3.11	99.69±4.85	93.09±9.46	94.66±8.60	98.86±5.60	97.94±3.85	95.23±4.41	99.55±1.11	93.63±2.94	83.30±2.31	48.24±3.70
	72	95.79±1.71	97.08±2.56	94.83±1.40	95.06±0.80	99.54±2.99	104.42±1.31	97.62±2.75	94.84±1.13	83.22±8.67	78.77±12.36	41.79±17.19
CaSki	24	99.87±2.13	99.62±3.66	97.33±4.29	96.92±3.46	101.76±5.75	98.79±4.23	100.92±3.30	104.85±8.35	93.74±2.96	86.08±7.58	69.78±14.82
	48	96.27±2.17	97.64±1.18	96.27±0.59	94.01±2.81	96.85±0.96	96.50±1.62	97.15±1.07	98.05±0.68	95.21±3.75	46.95±2.21	35.00±3.163
	72	98.72±3.43	100.63±0.40	97.63±2.84	94.99±4.62	92.74±3.10	99.81±5.43	97.66±9.65	96.90±4.77	103.31±5.97	84.20±8.30	49.26±15.28
HeLa	24	99.40±5.355	100.10±3.53	103.30±7.66	105.96±10.18	98.47±5.99	95.54±3.06	96.68±7.40	95.80±4.48	85.12±5.88	80.79±11.17	13.51±7.38
	48	96.23±2.58	96.99±3.67	96.85±3.30	99.72±2.60	98.29±1.94	99.09±1.07	97.62±3.30	98.00±3.33	91.03±4.71	67.30±8.27	11.29±5.92
	72	98.53±2.74	95.51±4.00	99.55±4.58	97.26±4.36	94.18±4.95	95.62±4.56	97.46±2.40	94.49±4.50	87.44±4.34	70.99±12.12	17.66±6.80

Note : Data are expressed as mean \pm SEM.

Table 4.2 Percentage of cell viability of HDFs, CaSki, HeLa, and HepG2 cells when treatment with *A. ebracteatus* Vahl. aqueous crude extract in various concentration ($10^{-3} - 10^4$ $\mu\text{g/ml}$) for 24, 48, and 72 hours incubation (**continued**).

Cell types	Time of incubation (hours)	Cell viability (%) / AE concentration ($\mu\text{g/ml}$)										
		0.001	0.01	0.05	0.1	1	10	50	100	1,000	5,000	10,000
HepG2	24	96.41 \pm 3.94	94.90 \pm 0.45	97.56 \pm 3.13	96.97 \pm 3.78	96.79 \pm 4.24	98.63 \pm 3.34	98.71 \pm 2.74	95.19 \pm 5.10	83.34 \pm 7.75	59.25 \pm 22.31	34.60 \pm 9.46
	48	97.22 \pm 1.80	99.27 \pm 0.23	97.70 \pm 2.07	97.85 \pm 0.70	94.23 \pm 3.59	99.00 \pm 0.66	97.10 \pm 0.83	97.49 \pm 2.20	90.76 \pm 4.56	59.39 \pm 24.33	33.48 \pm 14.17
	72	106.50 \pm 4.12	101.84 \pm 1.46	102.86 \pm 4.37	106.26 \pm 2.23	101.11 \pm 4.63	111.13 \pm 8.73	111.89 \pm 11.05	102.49 \pm 10.04	97.91 \pm 15.54	60.78 \pm 28.90	28.41 \pm 10.95

Note : Data are expressed as mean \pm SEM

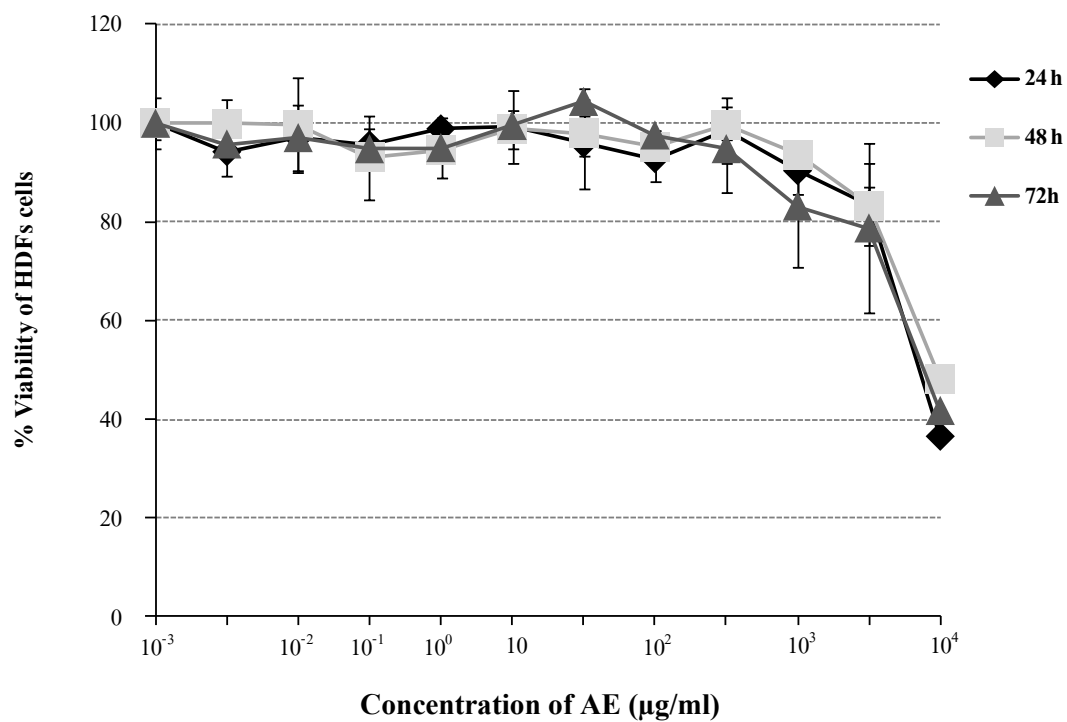


Figure 4.2 The anti-proliferative effects of *A. ebracteatus* Vahl. aqueous crude extract on human dermal fibroblast (HDFs) cells, incubation time for 24, 48, and 72 hours (mean \pm SEM).

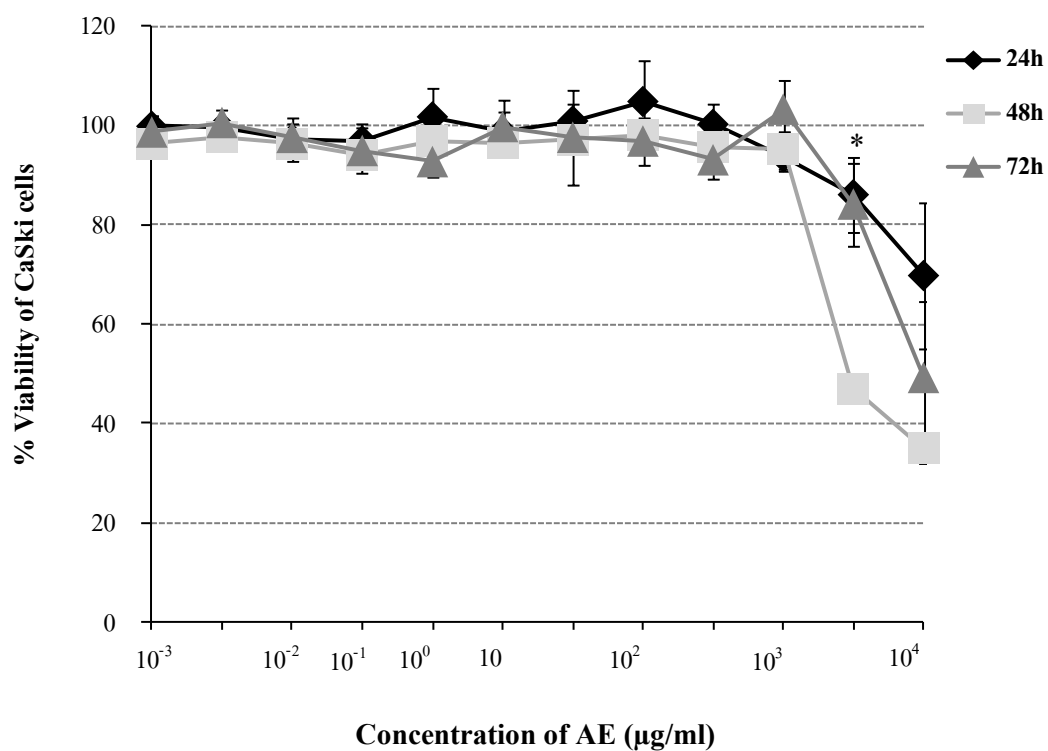


Figure 4.3 The anti-proliferative effects of *A. ebracteatus* Vahl. aqueous crude extract on human cervical carcinoma (CaSki) cells, incubation time for 24, 48, and 72 hours (mean \pm SEM).

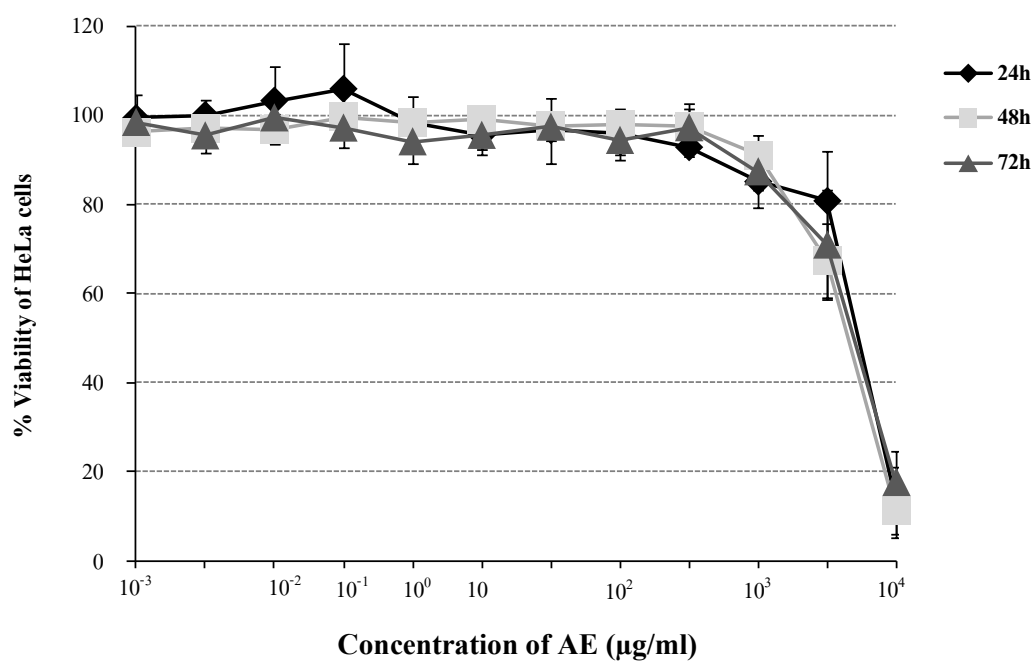


Figure 4.4 The anti-proliferative effects of *A. ebracteatus* Vahl. aqueous crude extract on human cervical carcinoma (HeLa) cells, incubation time for 24, 48, and 72 hours (mean \pm SEM).

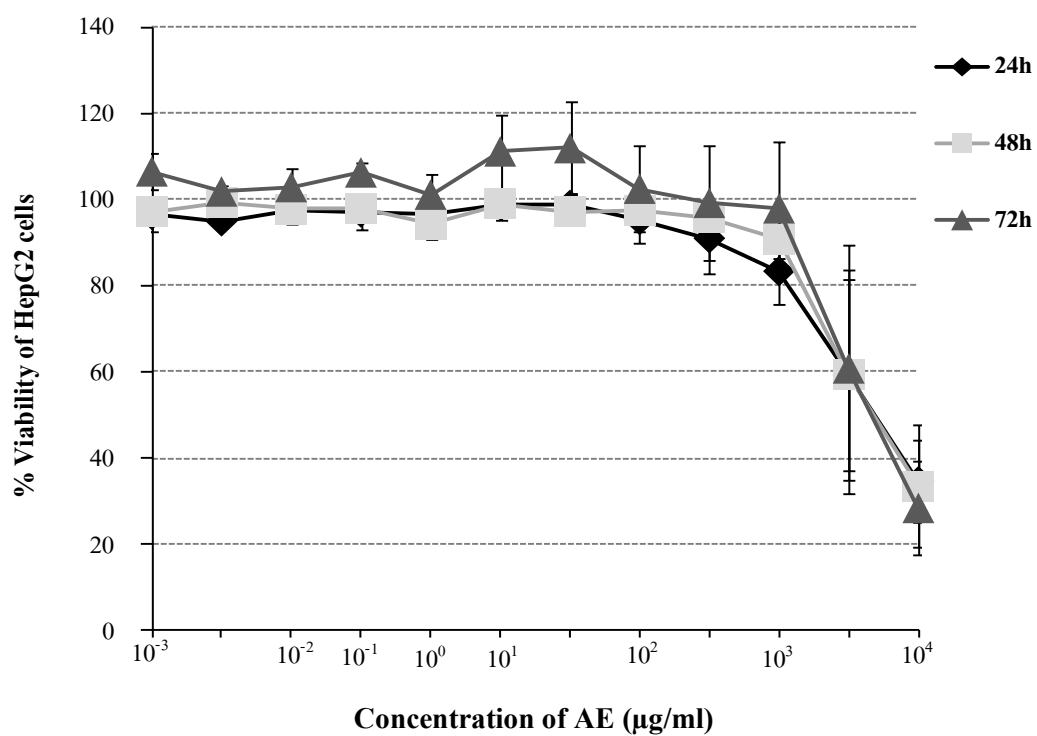


Figure 4.5 The anti-proliferative effects of *A. ebracteatus* Vahl. on human hepatocellular carcinoma (HepG2) cells, incubation time for 24, 48, and 72 hours (mean \pm SEM).

Dose-response of anti-proliferative properties of *A. ebracteatus* Vahl. aqueous crude extract

Since, the anti-proliferative activity AE aqueous crude extract did not depend on the duration of treatment. Therefore, the incubation duration for 48 hours of AE was chosen to determine the half maximal inhibitory concentration (IC_{50}). The MTT assay data used for calculated growth inhibition activity of AE which expressed as means of percent growth inhibition (**Table 4.3**).

The dose-response curves of *A. ebracteatus* Vahl. crude aqueous extract were obtained by plotting the percentage of cell growth inhibition versus concentrations of AE. Figure 4.6 – 4.9 showed the dose-response curves of MTT cell proliferation assay results of HDFs, CaSki, HeLa, and HepG2 cell lines, respectively. The IC_{50} values were obtained from three independent experiments carried out in triplicate and calculated by the non-linear regression equation (fitting by 4-parameter logistic model) using Microcal Origin (version 5.0) software program. The means of IC_{50} values of each cell were shown in Table 4.4.

AE exhibited a dose dependent growth inhibition of HDFs, CaSki, HeLa, and HepG2 cells. The IC_{50} values of AE against three cancer cells, CaSki, HeLa, and HepG2 cells was $4,984.90 \pm 498.72 \mu\text{g/ml}$, $6,072.50 \pm 573.29 \mu\text{g/ml}$, and $6,419.50 \pm 2,282.62 \mu\text{g/ml}$, respectively (**Figure 4.7 - 4.9**). While, AE inhibited HDFs cells growth with the IC_{50} values of $7,382.40 \pm 221.05 \mu\text{g/ml}$. From table 4.4, the mean of IC_{50} values of AE on CaSki cells growth was significantly lower than in normal cells, HDFs ($P < 0.01$). However, there were no significant differences of the mean of IC_{50} values between the two types of cancer cells, HeLa and HepG2 compared to HDFs cells ($P = 0.100$ and $P = 0.696$, respectively). This results indicated that *A. ebracteatus* Vahl. aqueous crude extract had an inhibitory effect to CaSki cancer cells growth more than normal cells.

Table 4.3 Percentage of growth inhibitory effects of *A. ebracteatus* Vahl. aqueous crude extract on HDFs, CaSki, HeLa, and HepG2 cells when treatment with various concentration ($10^{-3} - 10^4$ $\mu\text{g/ml}$) for 48 hours incubation.

Cell types	Growth inhibition (%) / AE concentration ($\mu\text{g/ml}$)										
	0.001	0.01	0.05	0.1	1	10	50	100	1,000	5,000	10,000
HDFs	0.08 \pm 3.11	0.31 \pm 4.85	6.91 \pm 9.46	5.34 \pm 8.60	1.14 \pm 5.60	2.06 \pm 3.85	4.77 \pm 4.41	0.45 \pm 1.11	6.37 \pm 2.94	16.70 \pm 2.31	67.89 \pm 8.88
CaSki	3.73 \pm 2.16	2.36 \pm 1.18	3.73 \pm 0.59	5.99 \pm 2.81	3.15 \pm 0.96	3.50 \pm 1.62	2.85 \pm 1.07	1.95 \pm 0.68	4.79 \pm 3.75	58.03 \pm 2.75	65.00 \pm 3.16
HeLa	3.77 \pm 2.58	3.01 \pm 2.38	3.15 \pm 2.40	0.28 \pm 0.18	1.71 \pm 0.98	0.91 \pm 0.26	2.38 \pm 1.60	2.00 \pm 1.18	8.97 \pm 4.71	32.70 \pm 8.27	88.71 \pm 5.92
HepG2	2.78 \pm 1.80	0.73 \pm 0.23	2.30 \pm 2.07	2.15 \pm 0.70	5.77 \pm 3.59	1.00 \pm 0.66	2.90 \pm 0.83	2.51 \pm 2.20	9.24 \pm 4.56	40.61 \pm 24.33	66.52 \pm 14.17

Note : Data are expressed as mean \pm SEM.

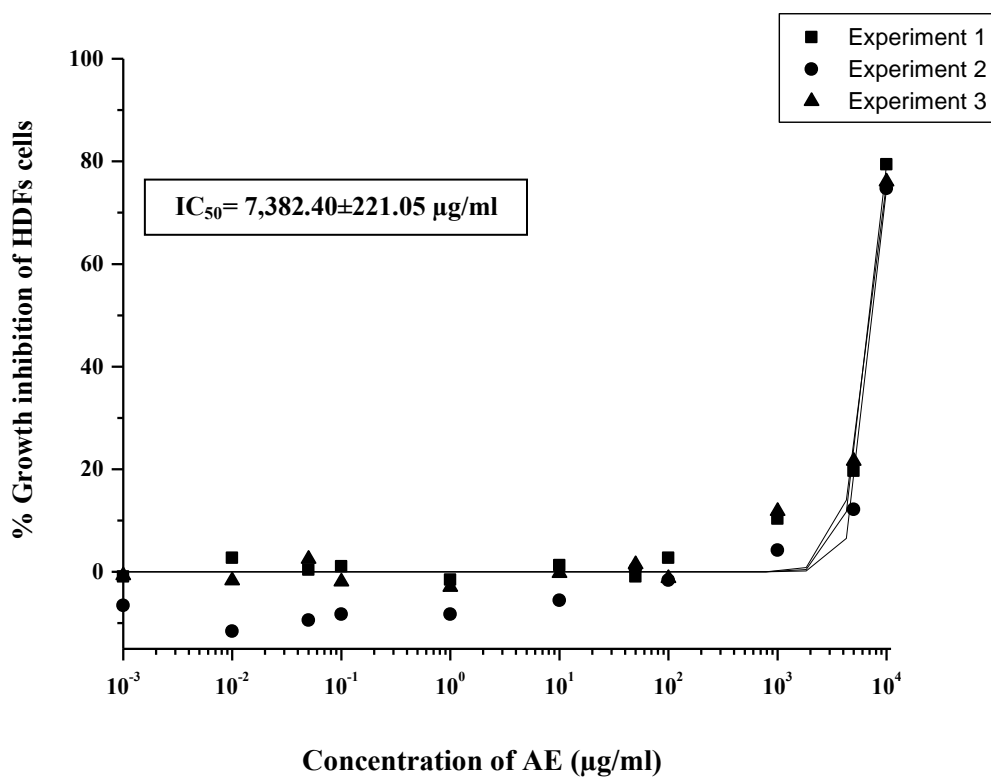


Figure 4.6 The dose response curve and IC_{50} value of *A. ebracteatus* Vahl. aqueous crude extract (48 hours of incubation time) on HDFs cells were obtained by blotting the percent inhibition versus concentration. The IC_{50} was calculated from non-linear regression equation (fitting by 4-parameter logistic model) using Microcal origin (version 5.0) software program, and expressed as means \pm SEM of three independent experiments carried out in triplicate. The IC_{50} value was required to increased cell growth inhibition from 0% to 50%.

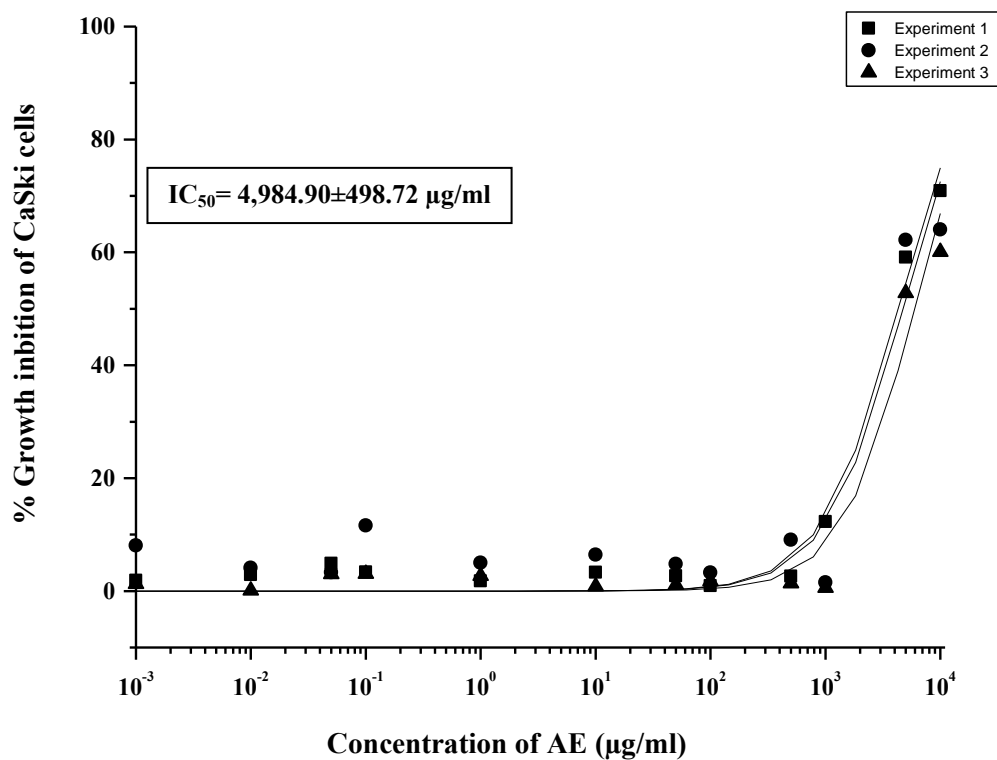


Figure 4.7 The dose response curve and IC_{50} value of *A. ebracteatus* Vahl. aqueous crude extract (48 hours of incubation time) on CaSki cells were obtained by blotting the percent inhibition versus concentration. The IC_{50} was calculated from non-linear regression equation (fitting by 4-parameter logistic model) using Microcal origin (version 5.0) software program, and expressed as means \pm SEM of three independent experiments carried out in triplicate. The IC_{50} value was required to increased cell growth inhibition from 0% to 50%.

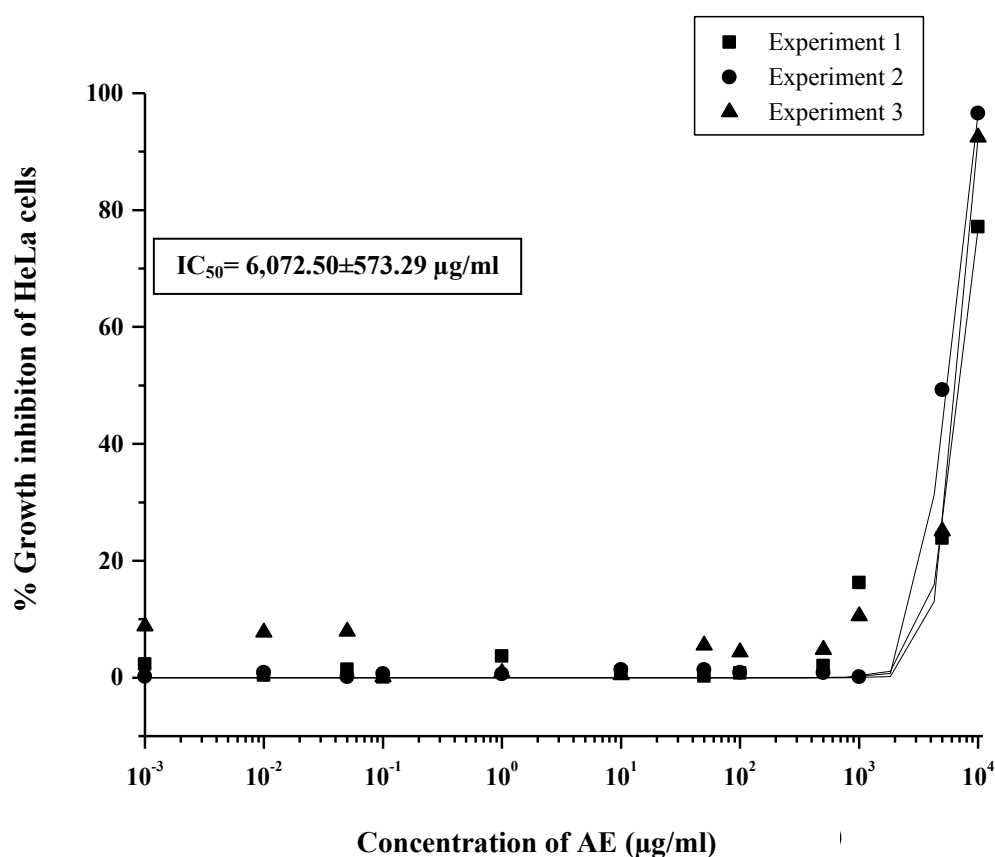


Figure 4.8 The dose response curve and IC₅₀ value of *A. ebracteatus* Vahl. aqueous crude extract (48 hours of incubation time) on HeLa cells were obtained by blotting the percent inhibition versus concentration. The IC₅₀ was calculated from non-linear regression equation (fitting by 4-parameter logistic model) using Microcal origin (version 5.0) software program, and expressed as means ± SEM of three independent experiments carried out in triplicate. The IC₅₀ value was required to increased cell growth inhibition from 0% to 50%.

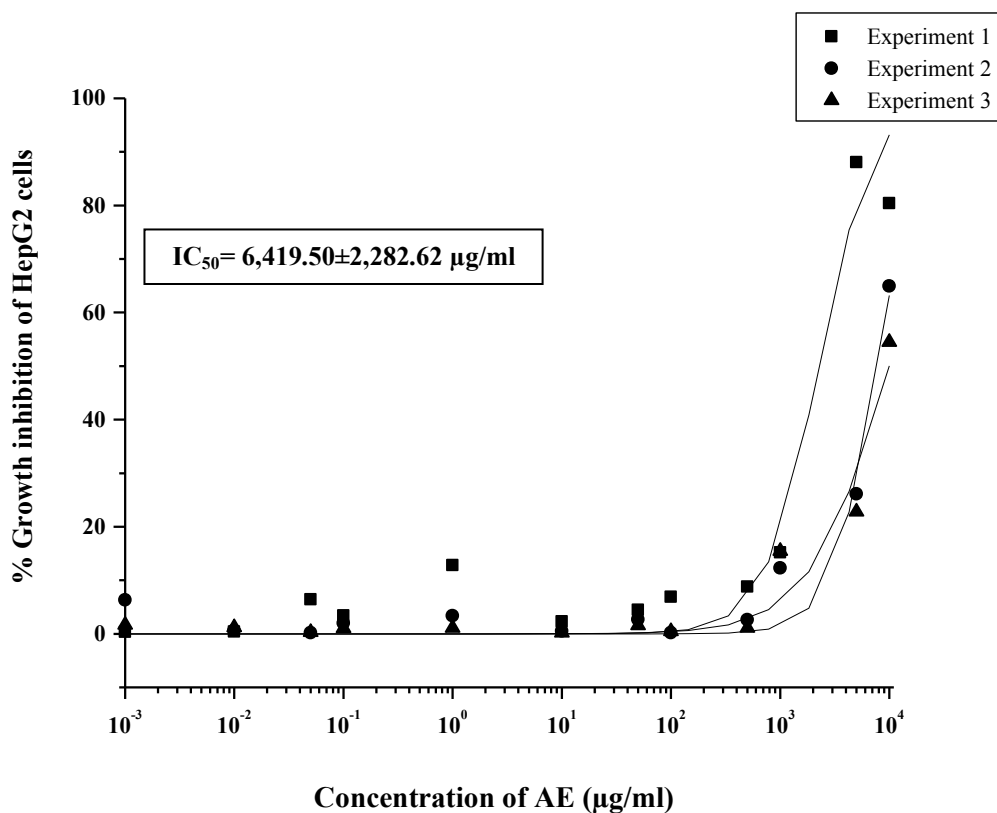


Figure 4.9 The dose response curve and IC₅₀ value of *A. ebracteatus* Vahl. aqueous crude extract (48 hours of incubation time) on HepG2 cells were obtained by blotting the percent inhibition versus concentration. The IC₅₀ was calculated from non-linear regression equation (fitting by 4-parameter logistic model) using Microcal origin (version 5.0) software program, and expressed as means ± SEM of three independent experiments carried out in triplicate. The IC₅₀ value was required to increased cell growth inhibition from 0% to 50%.

Table 4.4 Means of the half maximal inhibitory concentration (IC₅₀) of *A. ebracteatus* Vahl. aqueous crude extract against three cancer cells (CaSki, HeLa, HepG2) and one type of normal cell (HDFs) with incubation time 48 h.

Cells	IC ₅₀ (µg/ ml) of 3 experiments	Means of IC ₅₀ (µg/ ml)
HDFs	7,121.10 ± 296.88	7,382.40 ± 221.05
	7,822.03 ± 599.39	
	7,203.23 ± 351.64	
CaSki	4,290.11 ± 333.06	4,984.90 ± 498.72*
	4,712.45 ± 852.03	
	5,952.04 ± 595.81	
HeLa	7,009.56 ± 434.40	6,072.50 ± 573.29 ^{NS}
	5,031.74 ± 33.90	
	6,176.10 ± 421.22	
HepG2	2,263.06 ± 391.99	6,419.50 ± 2,282.62 ^{NS}
	7,708.35 ± 534.24	
	9,988.64 ± 1,286.13	

Notes: Data are expressed as mean ± SEM of IC₅₀ from three independent experiments carried out in triplicate and calculated from the non-linear regression equation (fitting by 4-parameter logistic model) using Microcal Origin (version 5.0) software program.

**P*<0.01 significant difference compared to HDFs cells,

^{NS} non-significant difference compared to HDFs and CaSki cells.

Part II In vivo study of anti-tumor and anti-angiogenic effects of aqueous crude extract of *A. ebracteatus* Vahl. in cervical carcinoma mice model.

This part demonstrated the anti-angiogenic and anti-tumor activities of aqueous crude extract of *A. ebracteatus* Vahl. in human cervical cancer cells contained human papillomavirus 16 DNA (HPV-16 DNA) - implanted nude mice model.

The tumor model of cervical carcinoma with HPV-16 positive

The human cervical carcinoma, CaSki cells (1×10^7 cells) were injected subcutaneously in the middle dorsum of each animal to produce the cervical tumor model. At day 1st - 3rd after cancer cells injection, the small nodule with tissue swelling and red skin at injected site was seen. One week later, the tumor mass could be observed (**Figure 4.10**). The cervical tumor was enlarged continuously until end of experiment, at day 21st and 35th after inoculation. Then the tumor nodule excisional was performed, and the stained slides with hematoxylin and eosin showed histological finding of large deposit of malignant tumor in the deep part of mouse skin, between bundles of skeletal muscle (**Figure 4.11C-H**). Morphology of cancer cells confirmed the characteristics of squamous cell carcinomas (SCC) presenting irregular round nuclei, small nucleoli, pale pink cytoplasm.

Table 4.5 demonstrated that on day 21st of tumor development, body weights of almost experimental groups, Con-Veh, Con-3,000AE, HPV-Veh, HPV-300AE, and HPV-3,000AE, were no significant difference ($P>0.05$). Nevertheless, the body weight of mice in Con-300AE group was significant less than HPV-Veh group, that was observed in day 21st during tumor progression ($P<0.05$). However, the percentage of body weight change was not significant difference between all groups ($P>0.05$).

Table 4.5 Values of mean body weight (g) for each group at different time point with and without treatment of *A. ebracteatus* Vahl aqueous crude extract.

Groups	Body weight (g)			% BW change
	At day 1 st	At day 21 th	At day 35 th	
Con-Veh	21.31±0.31 (n=8)	22.90±0.77 (n=4)	23.64±0.57 (n=4)	0.34±0.14
Con-300AE	21.21±0.32 (n=10)	20.60±0.58* (n=5)	22.46±0.67 (n=5)	0.12±0.62
Con-3,000AE	21.44±0.38 (n=8)	21.41±0.40 (n=4)	23.60±0.52 (n=4)	0.23±0.16
HPV-Veh	21.11±0.26 (n=9)	23.57±0.32 (n=5)	24.33±0.88 (n=4)	0.38±0.21
HPV-300AE	20.86±0.34 (n=7)	22.08±0.62 (n=3)	23.88±0.28 (n=4)	0.40±0.15
HPV-3,000AE	22.11±0.48 (n=9)	22.30±0.15 (n=5)	24.26±0.60 (n=4)	0.30±0.16

Notes: Data are expressed as mean ± SEM, * $P < 0.005$ significant difference compared to HPV-Veh group.

(A) At day of CaSki cells injection



(B) 3 days after CaSki cells inoculation



(C) 7 days after CaSki cells inoculation (D) 21 days after CaSki cells inoculation



(E) 35 days after CaSki cells inoculation



Figure 4.10 Photography of experimental mice after injected with CaSki cells (1×10^7 cells/200 μ l) into subcutaneously at dorsum skin (A), swelling (B) tumor bud were seen (C), and enlarged continuously at 21 days (D) and 35 days (E) after CaSki cells inoculation.

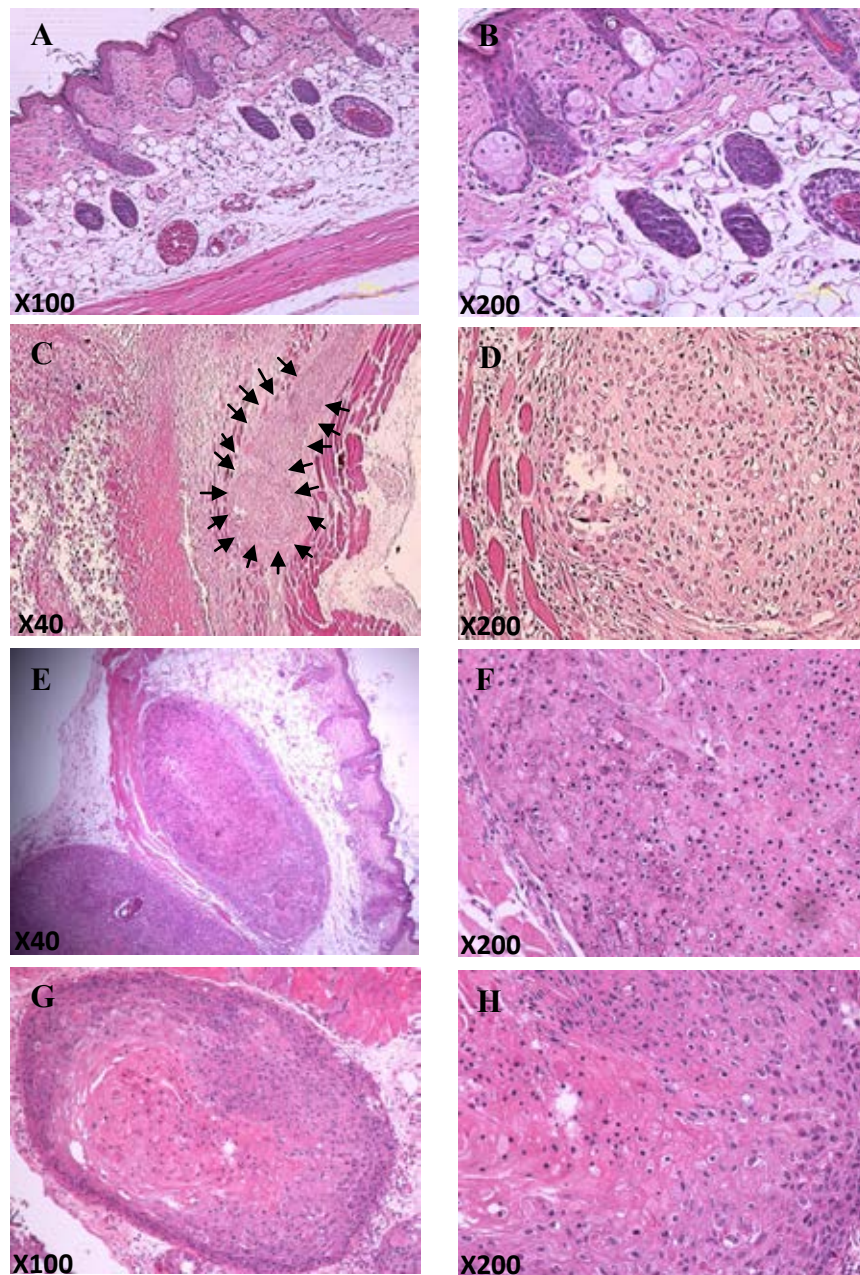


Figure 4.11 Histological finding of normal skin from control mice (**A**) and subcutaneous tumor nodules taken from CaSki cells-implanted nude mice showed marked deposit malignant tumor in deep part of skin after inoculation for 7 days (**C**), 21 days (**E**), and 35 days (**G**). Morphological study of epithelium cells of normal skin (**B**) and squamous cells carcinoma (**D, F, H**). **Notes:** The histological study by H&E, at magnification x40, x100, x200.

Effects of aqueous crude extract of *A. ebracteatus* Vahl. on Tumor Growth: Tumor volume

Table 4.6 showed the mean values of tumor volume of each group. The tumor progression were observed in all HPV groups by the increasing in tumor volume of day 28th compared to day 14th after AE or vehicle treatment ($P<0.001$). Treatment with low dose of AE (HPV-300AE) for 14 and 28 days found the increasing in tumor volume that was not significant difference from vehicle treatment. This data indicated that low dose treatment of *A. ebracteatus* Vahl. aqueous crude extract could not inhibit tumor growth. However, when treatment with high dose of AE (HPV-3,000AE), tumor volume was significant less than HPV-Veh group ($P<0.001$) (**Figure 4.12**). This inhibitory activity of high dose treatment of AE was observed when treatment for 28 days, but not in 14 days of treatment period.

The results indicated that high dose treatment of *A. ebracteatus* Vahl. aqueous crude extract for 28 days could inhibit or delay cervical carcinoma growth.

Table 4.6 Tumor volume of tumor nodule excised from each HPV- groups.

Groups	Tumor Volume (mm ³)/	
	days after treatment	
	At day 14	At day 28
HPV-Veh	103.79 ± 11.69 (n=4)	235.98 ± 7.57 [†] (n=5)
HPV-300AE	94.89 ± 9.50 ^{NS} (n=3)	245.36 ± 36.26 ^{†,NS} (n=4)
HPV-3,000AE	62.37 ± 16.56 [*] (n=5)	5.77 ± 7.55 ^{†,*,‡} (n=4)

Notes: Data are expressed as mean ± SEM,

[†] $P<0.001$ significant difference within group compare to day 14th of treatment,

^{*} $P<0.001$ significant difference compared to age matched HPV-Veh group,

[‡] $P<0.001$ significant difference compared to age matched HPV-300AE group,

^{NS} non-significant difference compared to age matched HPV-Veh group.

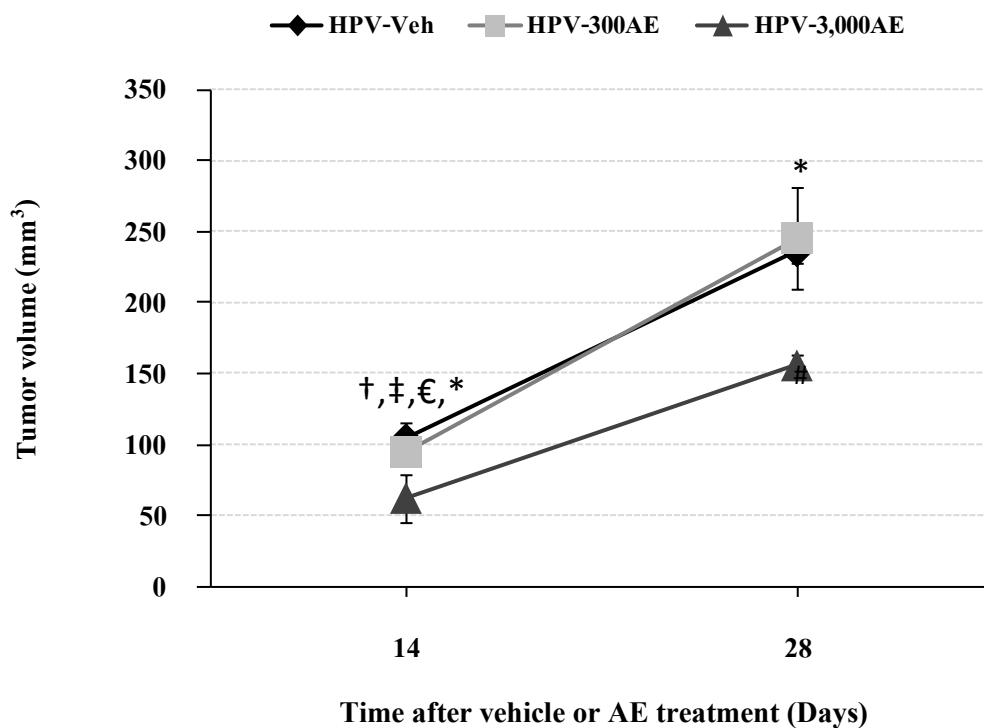


Figure 4.12 The tumor volume (mm³) of 14 days and 28 days after vehicle (distilled water), AE (300 and 3,000 mg/kg BW) treatment in HPV groups.

Notes: Data are expressed as mean \pm SEM,

† $P < 0.001$ significant difference within HPV-Veh group,

‡ $P < 0.001$ significant difference within HPV-300AE group,

€ $P < 0.001$ significant difference within HPV-3,000AE group,

* $P < 0.001$ significant difference compared to age matched HPV-Veh group,

$P < 0.001$ significant difference compared to age matched HPV-300AE group.

Tumor Angiogenesis in CaSki-implanted nude mice

After Caski cells inoculation for one week, tumor bud was seen at dorsal skin and enlarged continuously, as shown in Figure 4.10. The fluorescent images from laser confocal microscope demonstrated the microvasculature of control and HPV groups at different time points after cancer cells inoculation (**Figure 4.13**).

A large number of microvascular network was able to be found around tumor mass on day 21st after CaSki cells inoculation (**Figure 4.13B**). The proliferating neovessels appeared to migrate out to the tumor mass. The results demonstrated markedly increase in neocapillary network in the tumor area.

On day 35th after CaSki cells inoculation, the tumor microvascular ultrastructure has pathological features such as microvascular network with shunt, loop, abrupt changes in the diameters, tortuosity, and hyper-permeability were observed (**Figure 4.13C**).

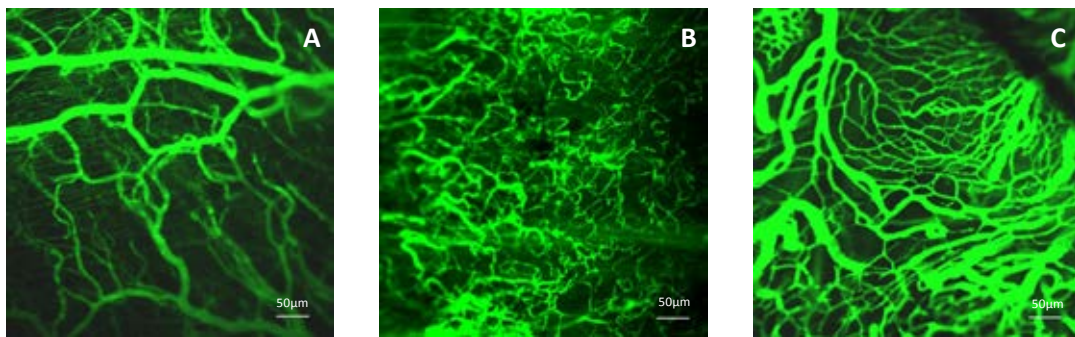


Figure 4.13 Confocal laser microscopic images of dorsal skin microvasculature for control group (A), and HPV groups at day 21st (B), and day 35th (C) after CaSki cells inoculation. The microvascular network was visualized using 5% FITC-dextran fluorescence (MW 200,000), with low magnification $\times 100$, Bar = 50 μm .

Anti-angiogenic Activity of *A. ebracteatus* Vahl. aqueous crude extract in CaSki-implanted nude mice

Figure 4.14 showed the examples of confocal laser scanning micrographs of tumor microvascular affected by AE treatment. The images showed that the appearance of tumor neocapillaries induced by CaSki cells was markedly reduced on 14 and 28 days after treatment of AE in high dose 3,000 mg/kg BW (**Figure 4.14 B and D**). However, this antiangiogenic activity of AE was not observed in low dose treatment (300 mg/kg BW) (**Figure 4.14 A and C**).

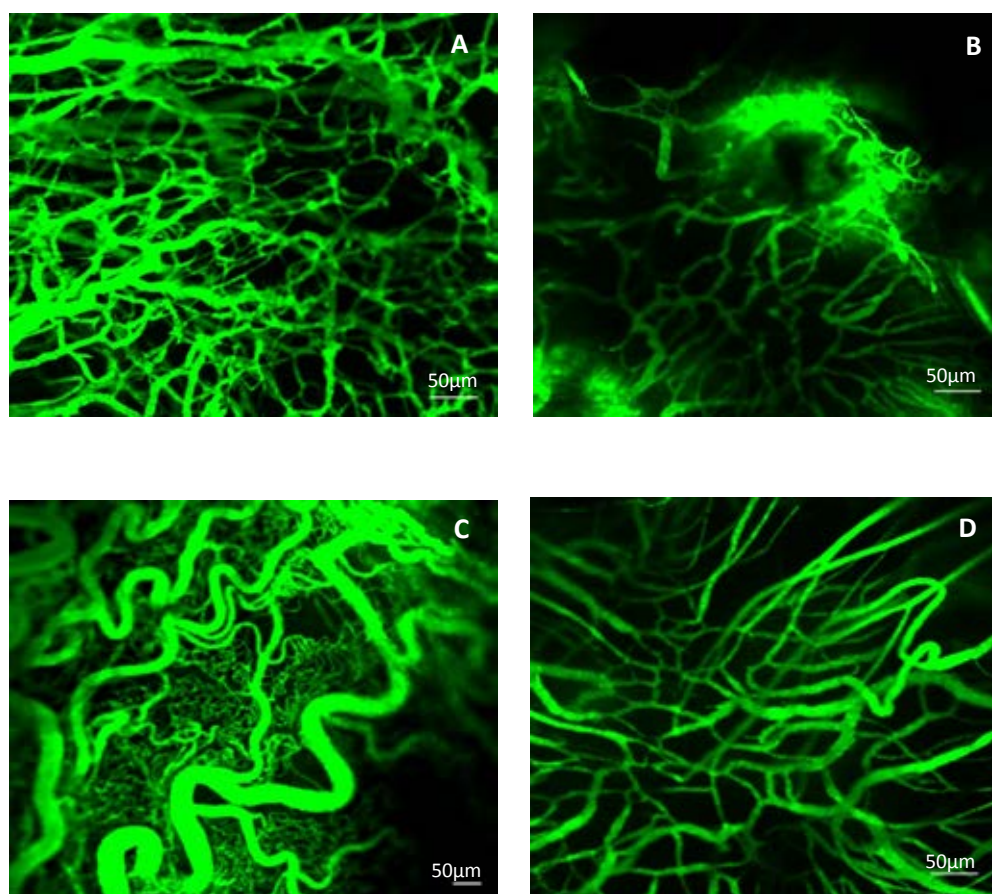


Figure 4.14 Confocal laser microscopic images of tumor microvascular network taken from HPV-300AE (300mg/kg BW) for 14 days (**A**), HPV-3,000AE (3,000mg/kg BW) for 14 days (**B**) HPV-300AE for 28 days (**C**) and HPV-3,000AE for 28 days (**D**). The microvascular network was visualized using 5% FITC-dextran fluorescence (MW 200,000), low magnification $\times 100$, Bar = 50 μm .

Effect of aqueous crude extract of *A. ebracteatus* Vahl. on tumor capillary vascularity in CaSki-implanted nude mice

Based on the confocal laser scanning images, the tumor capillary vascularity (CV) was evaluated using a digital image analysis as previously described. Table 4.7 and Figure 4.15 showed the percentage of capillary vascularity for all groups.

The results demonstrated that in both control groups with and without treatment of AE, the capillary vascularity remained constant (%CV = 21.75 ± 0.87 to 25.16 ± 1.39) during all experimental periods. In HPV-Veh groups, the capillary vascularity (CV) were significant increase both at day 14th (% CV = 63.91 ± 4.34) and day 28th (%CV = 71.80 ± 2.43) after treatment ($P < 0.001$), when compared to the aged-matched control groups with and without AE treatment (**Table 4.7**). Moreover, the capillary vascularity in HPV groups on day 14th of treatment was not significant difference compared with the capillary vascularity value on day 28th of treatment. This result indicated that the cervical carcinoma-induced neovascularization occurred in early stage of cancer development.

The mean capillary vascularity of HPV group with low dose AE (300 mg/kg BW) was significant decrease when treatment for 14 days (%CV = 49.55 ± 3.91) ($P < 0.001$), but not significantly different in 28 days of treatment (%CV = 68.33 ± 2.25) when compared to untreated group. In addition, high dose AE (3,000 mg/kg BW), could significantly decrease mean capillary vascularity compared to HPV-Veh and HPV-300AE at both 14 and 28 days of treatment (%CV = 26.93 ± 3.57 and 37.95 ± 1.64 , respectively) ($P < 0.001$). This result indicated that anti-angiogenic activity of *A.ebracteatus* Vahl. aqueous crude extract on cervical carcinoma was dose-dependent manner, but not depend on the duration of treatment.

It was noteworthy that, although the capillary vascularity was reduced in HPV-3,000AE 28 days of treatment, there were still higher than all control groups ($P < 0.001$). This was meant that the cervical carcinoma-induced neovascularization still in progressed. This result indicated that the induction of capillary vascularity in CaSki cells-implanted

nude mice was attenuated with high dose treatment of *A.ebracteatus* Vahl. aqueous crude extract.

The relationship between capillary vascularity and tumor volume of every HPV groups was demonstrated in Figure 4.16. The results showed a significant correlation with a linear relationship between the mean of capillary vascularity and the mean of tumor volume with a correlation coefficient, $R^2 = 0.52$ ($P < 0.05$). This result suggested that the reduction in tumor capillary vascularity was linearly correlated with the decrease in tumor volume.

Table 4.7 Capillary vascularity (%) of tumor tissue of CaSki cells-implanted nude mice with and without AE treatment.

Groups	Capillary vascularity (%)/ Days after treatment	
	At day 14 th	At day 28 th
Con-Veh	21.75 ± 0.87 (n=4)	21.78 ± 1.34 (n=4)
Con-300AE	25.16 ± 1.39 (n=5)	23.35 ± 2.27 (n=5)
Con-3,000AE	24.50 ± 1.00 (n=4)	24.09 ± 1.50 (n=4)
HPV-Veh	63.91 ± 4.34 [†] (n=5)	71.80 ± 2.43 [†] (n=4)
HPV-300AE	49.55 ± 3.91 ^{†,‡} (n=3)	68.33 ± 2.25 ^{†,‡,NS} (n=4)
HPV-3,000AE	26.93 ± 3.57 ^{‡,€} (n=4)	37.95 ± 1.64 ^{#,€} (n=4)

Notes: Data are expressed as mean ± SEM,

[†] $P < 0.001$ significant difference compared to age matched Con-Veh,

^{*} $P < 0.001$ significant difference compared to age matched HPV-Veh,

[#] $P < 0.005$ significant difference compared to age matched HPV-Veh,

[‡] $P < 0.001$ significant difference compared within HPV-300AE group,

[€] $P < 0.005$ significant difference compared to age matched HPV-300AE,

^{NS}Non-significant difference compared to age matched HPV-Veh.

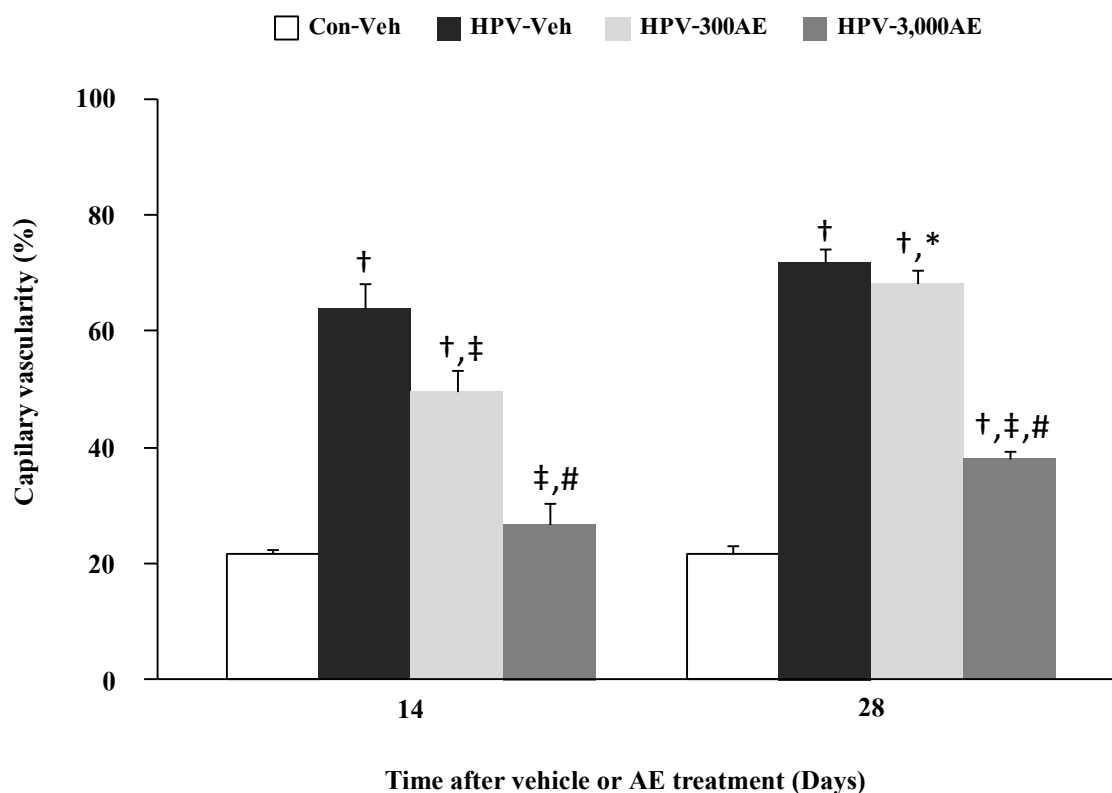


Figure 4.15 The percentage of Capillary vascularity of 14 days and 28 days after vehicle (distilled water), AE (300 and 3,000 mg/kg BW) treatment in control and HPV groups.

Notes: Data are expressed as mean \pm SEM,

[†] $P < 0.001$ significant difference compared to age matched Con-Veh group,

[‡] $P < 0.001$ significant difference compared to age matched HPV-Veh group,

[#] $P < 0.005$ significant difference compared to age matched HPV-300AE group,

^{*} $P < 0.001$ significant difference compared between day 14th and day 28th of treatment.

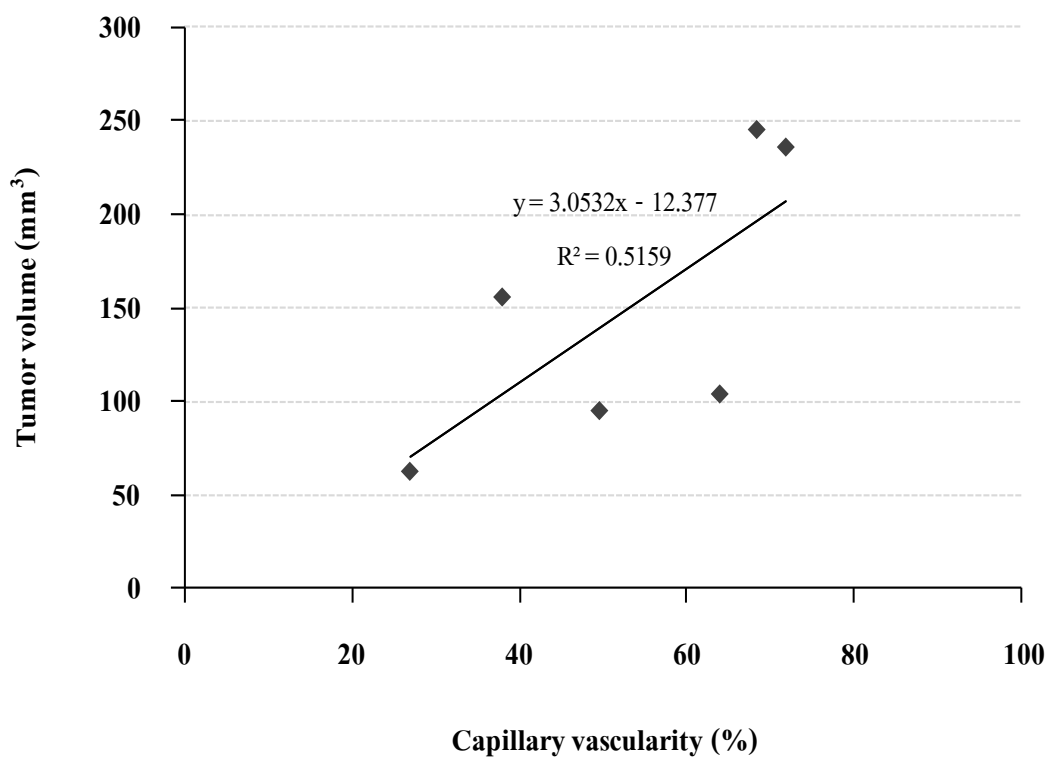


Figure 4.16 Plotting of data of % capillary vascularity (CV, (x-axis)) and tumor volume (y-axis) for three groups (HPV-Veh, HPV-300AE, HPV-3,000AE). The solid line represent correlations between x and y, the correlation is expressed of $y = 3.0532x - 12.377$, $R^2=0.52$, $p=0.108$).

Effect of aqueous crude extract of *A. ebracteatus* Vahl. on tumor angiogenic and apoptotic biomarker : VEGF and P53

Tumor expression of VEGF and P53 was determined by immunohistochemical analysis. Quantification the level of tumor VEGF and P53 expression by using Image-Pro Plus software program.

Tumor tissue VEGF expression

VEGF expression was mainly detected on the cell cytoplasm and the membrane of the tumor cells and the positively stained cells showed a brown-yellow color (**Figure 4.17 and 4.18**).

Figure 4.17 showed VEGF immunoreactivity of mice skin from control groups with and without treatment of AE crude extract, and the weakly stained cells with light brown staining of VEGF positive were found in all layers of skin. VEGF expression were observed in basal cells and glands in epidermis layer, sweat gland and endothelium cell of vessels in dermis layer, and muscular layer.

Quantification of the percentage of area of VEGF staining per ROI (%), the % area of VEGF expression per ROI of vehicle control group (32.89 ± 2.06 to 33.17 ± 1.12) was not significantly different compared with Con-AE groups (29.64 ± 2.22 to 40.40 ± 3.47) (**Table 4.8**). This data demonstrated the physiological level of VEGF expression in normal mice skin, which was the same level in normal mice received AE in the dosage of 300 mg/kg BW and 3,000 mg/kg BW for 14 and 28 day.

In both HPV-Veh 14 and 28 days groups, the strongly intensity of VEGF staining was detected in cytoplasm and cell membrane in almost all tumor cells in the tumor area (**Figure 4.18**). AE treatment in high dose (3,000 mg/kg BW) showed moderate intensity brown staining, while strong intensity brown stained tumor cells were seen in low dose treatment (300 mg/kg BW).

Table 4.8 and Figure 4.19 demonstrated that the percentage of area of VEGF expression in tumor tissue in HPV-3,000AE both groups (14 and 28 days) was significantly less than HPV-Veh and HPV-300AE groups in age-matched compared ($P < 0.001$). This result suggested that high dose treatment of *A. ebracteatus* Vahl. aqueous crude extract could reduce the increasing of level of tumor VEGF expression in cervical carcinoma bearing mice. This inhibitory activity on VEGF expression of *A. ebracteatus* Vahl. aqueous crude extract was dose-dependent, but not depend on the period of treatment.

Figure 4.20 presented the relationship between % area of tumor VEGF expression and tumor volume of all HPV groups, which was not significantly correlated ($y = 1.6686x + 33.686$, $R^2=0.11$, $P=0.518$).

The relationship between % area of tumor VEGF expression and capillary vascularity of every HPV groups was presented in Figure 4.21. The resulted demonstrated a significant correlation fitted with a linear relationship between the mean of % area of tumor VEGF expression and the mean of capillary vascularity with a correlation coefficient, $R^2 = 0.82$, $y = 0.9306x - 11.219$, $P<0.05$. This result indicated that the reduction in tumor VEGF expression was linearly correlated with the decrease in tumor capillary vascularity.

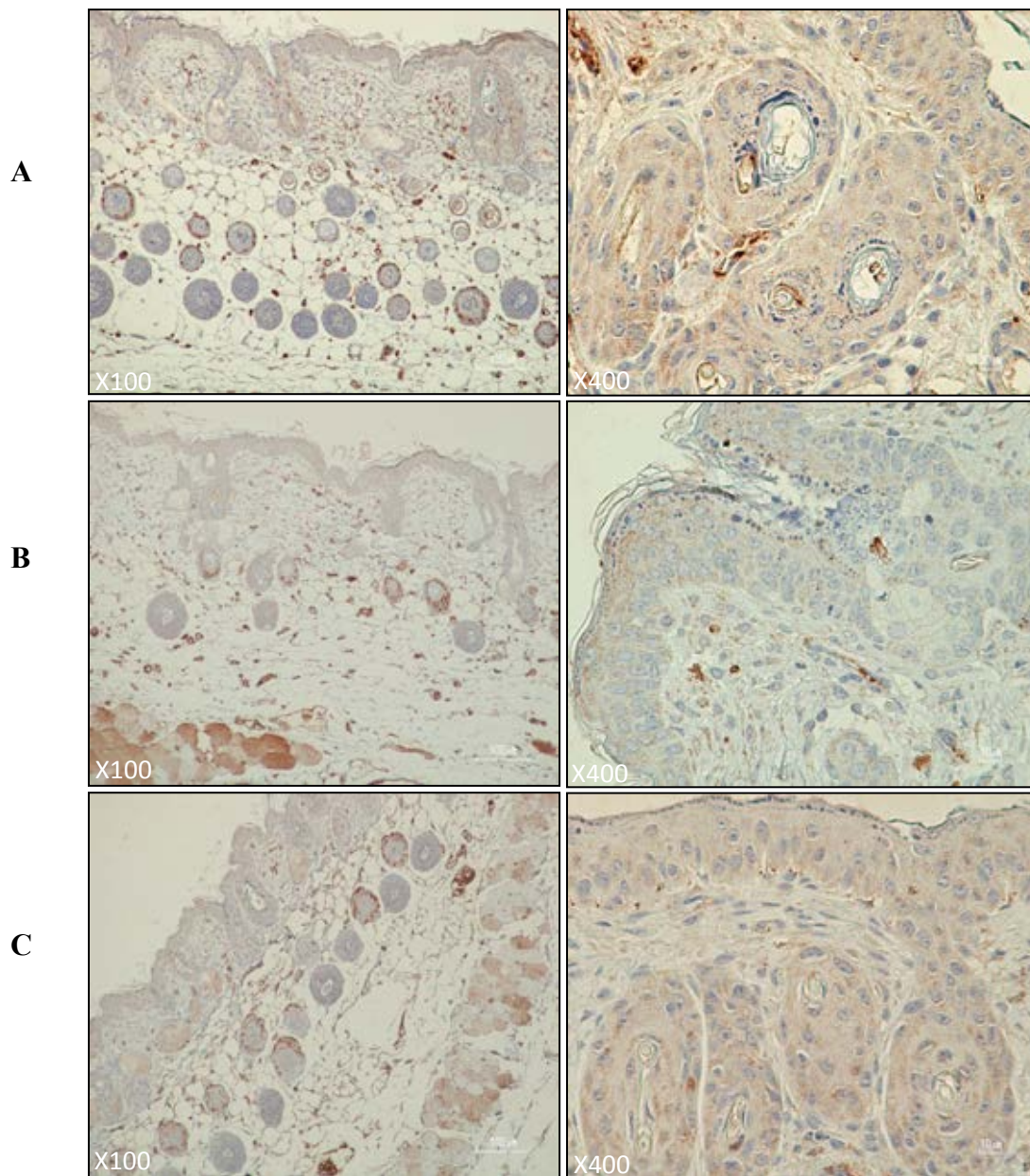


Figure 4.17 The immunoreactivity of VEGF expression in epithelial layer of nude mice normal skin from Con-Veh group (A), Con-300AE group (B), and Con-3,000AE group (C).

Notes: The histological study by H&E, at magnification x100, and x400.

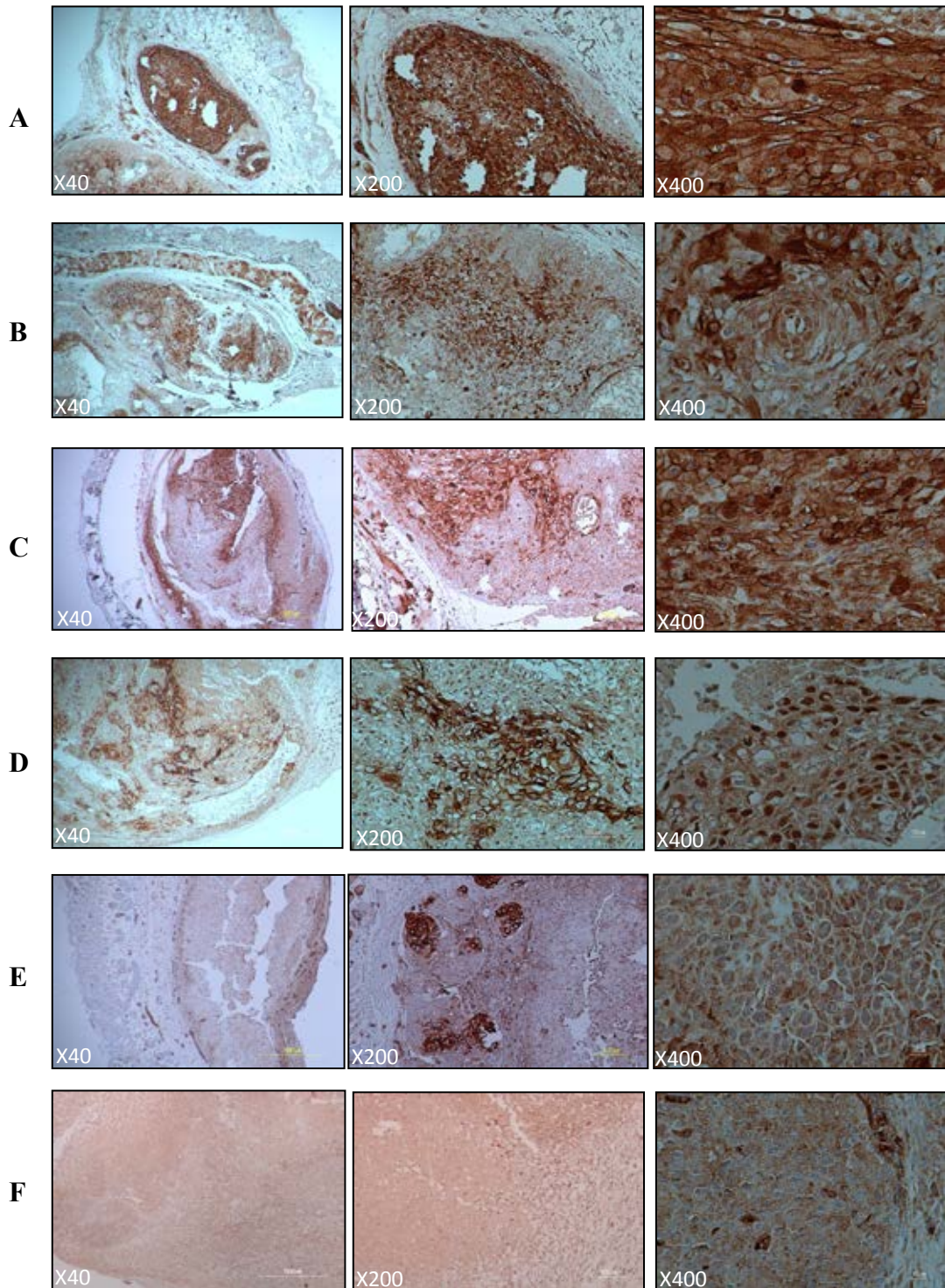


Figure 4.18 The expression of VEGF in subcutaneous tumor nodule excised from CaSki cells-implanted nude mice of HPV-Veh14day (A), HPV-Veh28day (B), HPV-300AE14day (C), HPV-300AE28day (D), HPV-3,000AE14day (E), and HPV-3,000AE28day (F). The histological study by H&E, at magnification x100, and x400.

Table 4.8 Percent of area VEGF expression per ROI (%) in tumor tissue from CaSki cells-implanted nude mice with and without AE treatment.

Groups	Area of VEGF expression per ROI (%)	
	Days after treatment	
	At day 14 th	At day 28 th
Con-Veh	32.89 ± 2.06 (n=4)	33.17 ± 1.12 (n=4)
Con-300AE	29.64 ± 2.22 (n=5)	37.26 ± 1.49 (n=5)
Con-3,000AE	40.40 ± 3.47 (n=4)	35.17 ± 3.05 (n=4)
HPV-Veh	80.96 ± 2.16 (n=5) [†]	80.56 ± 1.09 (n=4) [†]
HPV-300AE	77.33 ± 3.87 (n=3) ^{†,NS}	77.99 ± 2.30 (n=4) ^{†,NS}
HPV-3,000AE	54.64 ± 3.59 (n=5) ^{†,*‡}	45.63 ± 3.47 (n=4) ^{*‡}

Notes: Data are expressed as mean ± SEM,

[†] $P < 0.001$ significant difference compared to age matched Con-Veh group,

^{*} $P < 0.001$ significant difference compared to age matched HPV-Veh group,

[‡] $P < 0.001$ significant difference compared to age matched HPV-300AE group,

^{NS} Non-significant difference compared to age matched HPV-Veh group.

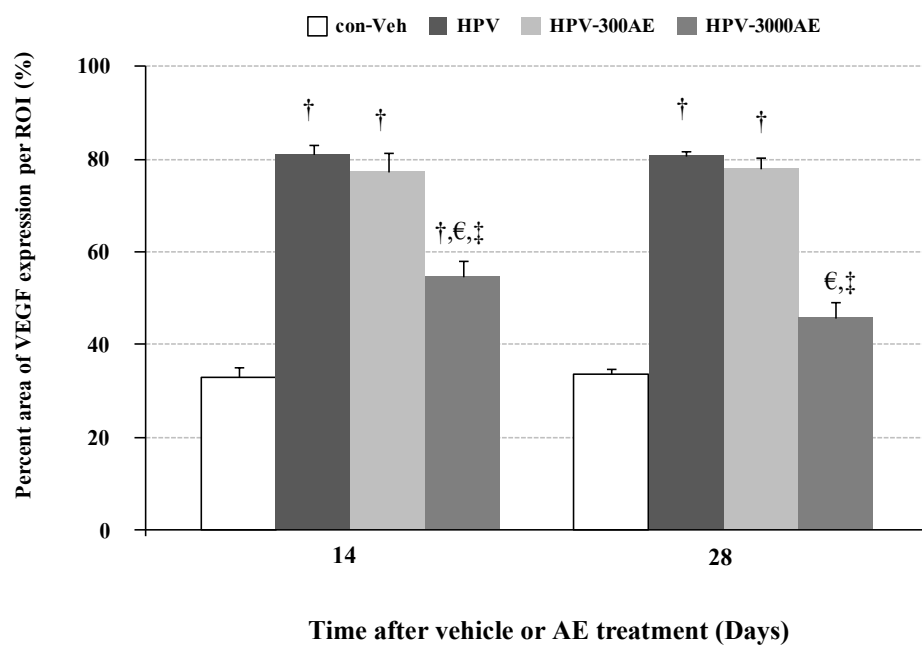


Figure 4.19 The percentage area of VEGF expression per ROI (%) in tumor tissue of 14 days and 28 days after vehicle (distilled water), AE (300 and 3,000 mg/kg BW) treatment in control and HPV groups.

Notes: Data are expressed as mean \pm SEM,

[†] $P < 0.001$ significant difference compared to age matched Con-Veh groups,

[€] $P < 0.001$ significant difference compared to age matched HPV-Veh groups,

[‡] $P < 0.001$ significant difference compared to age matched HPV-300AE groups.

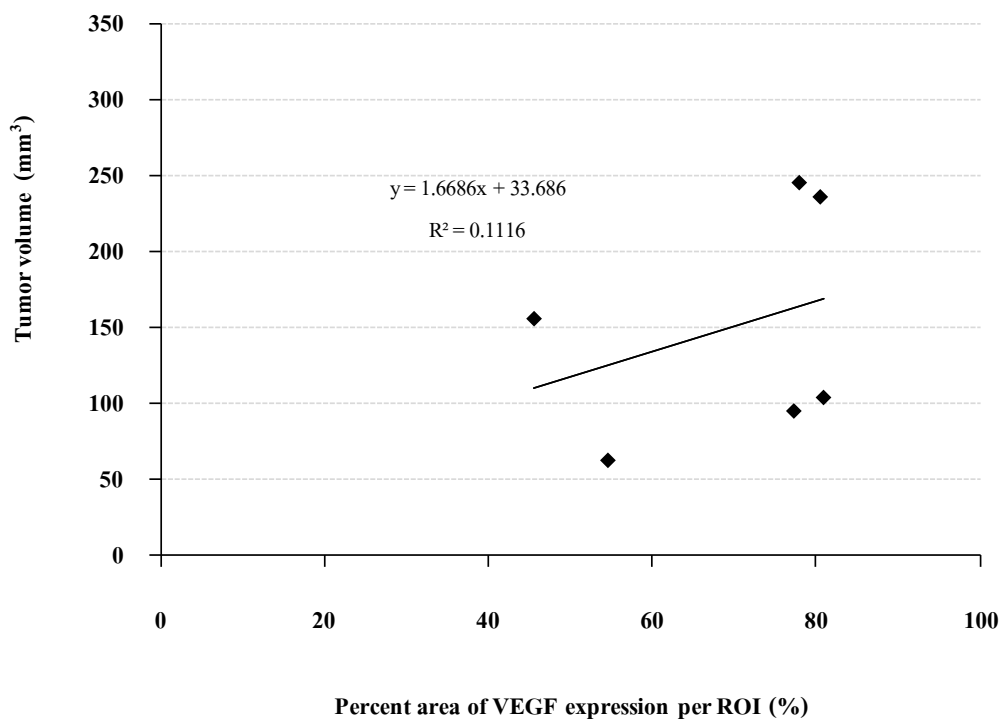


Figure 4.20 Plotting of data of % area of VEGF expression per ROI in tumor tissue (x-axis) and tumor volume (y-axis) for three groups (HPV-Veh, HPV-300AE, HPV-3,000AE). The solid line represent correlations between x and y, the correlation is expressed of $y = 1.6686x + 33.686$, $R^2=0.11$, $P=0.518$.

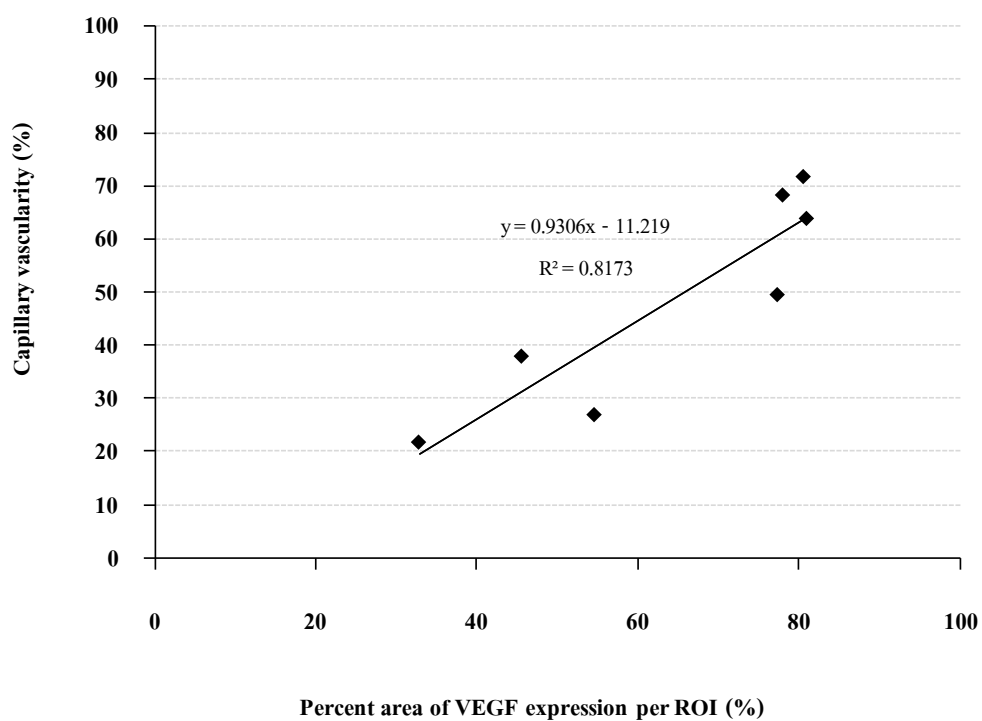


Figure 4.21 Plotting of data of % Area of VEGF expression per ROI in tumor tissue (x-axis) and %capillary vascularity (%CV, (y-axis)) for three groups (HPV-Veh, HPV-300AE, HPV-3,000AE). The solid line represent correlations between x and y, the correlation is expressed of $y = 0.9306x - 11.219$, $R^2=0.82$, $P=0.030$.

Tumor tissue P53 expression

Tumor P53 expression was mainly detected in the cell nuclei and the positively stained cells showed a dark brown color. Staining intensity was generally moderate to strong (**Figure 4.22**).

P53 immunoreactivity of mice skin from every control groups with and without treatment of AE crude extract were not detected the P53 positive cells in all layers of skin.

In both HPV-Veh 14 and 28 days groups, p53 stained tumor cell was found in a very small number or almost none (**Figure 4.2**). Table 4.9 and Figure 4.23 showed proportion of number of P53-positive tumor cells per total tumor cells (%). The results showed that the number of p53-positive tumor cell in HPV group without AE treatment (1.75 ± 0.23 to 2.96 ± 2.96) was lower than age-matched HPV groups with AE treatment ($P < 0.001$).

In HPV-AE groups, the number of p53-positive tumor cells were significantly elevated compared with age-matched HPV-Veh group. Elevations of P53 expression in HPV group with high dose AE (3,000 mg/ kg BW) (32.66 ± 4.18 to 35.48 ± 0.35) were significantly higher than in low dose AE (300 mg/kg BW) in both 14 and 28 days of treatment (16.27 ± 2.43 to 13.51 ± 4.46) ($P < 0.001$). Tumor P53 expression of HPV-AE treated groups were not significantly different between the period of treatment (**Table 4.9 and Figure 4.23**). This result suggested that *A. ebracteatus* Vahl. aqueous crude extract could be restored p53 expression in cervical carcinoma in dose-dependent manner, but the time response was not observed.

Figure 4.24 presented the relationship between % P53-positive tumor cells and tumor volume of all HPV groups, which were very low ($R^2 = 0.14$, $P=0.464$). However, these results demonstrated the trend of reduction in tumor volume was linearly correlated with the increase in tumor p53 expression.

The relationship between % P53-positive tumor cells and % capillary vascularity of every HPV groups was presented in Figure 4.25. The result demonstrated a significant correlation fitted with a linear relationship between the mean of P53-positive tumor cells and the mean of capillary vascularity with a correlation coefficient, $R^2 = 0.82$, $y = -1.1347x + 72.485$, $P < 0.05$. This result indicated that the reduction in tumor capillary vascularity was linearly correlated with the increase in tumor p53 expression.

Figure 4.26 presented the relationship between % P53-positive tumor cells and % area of VEGF expression in tumor tissue of every HPV groups. The result demonstrated a significant correlation fitted with a linear relationship between the mean of P53-positive tumor cells and the mean of % area of tumor VEGF expression with a correlation coefficient, $R^2 = 0.86$, $y = -0.9593x + 85.313$, $P < 0.01$.

This result indicated that the reduction in tumor VEGF expression was linearly correlated with the increase in tumor p53 expression.

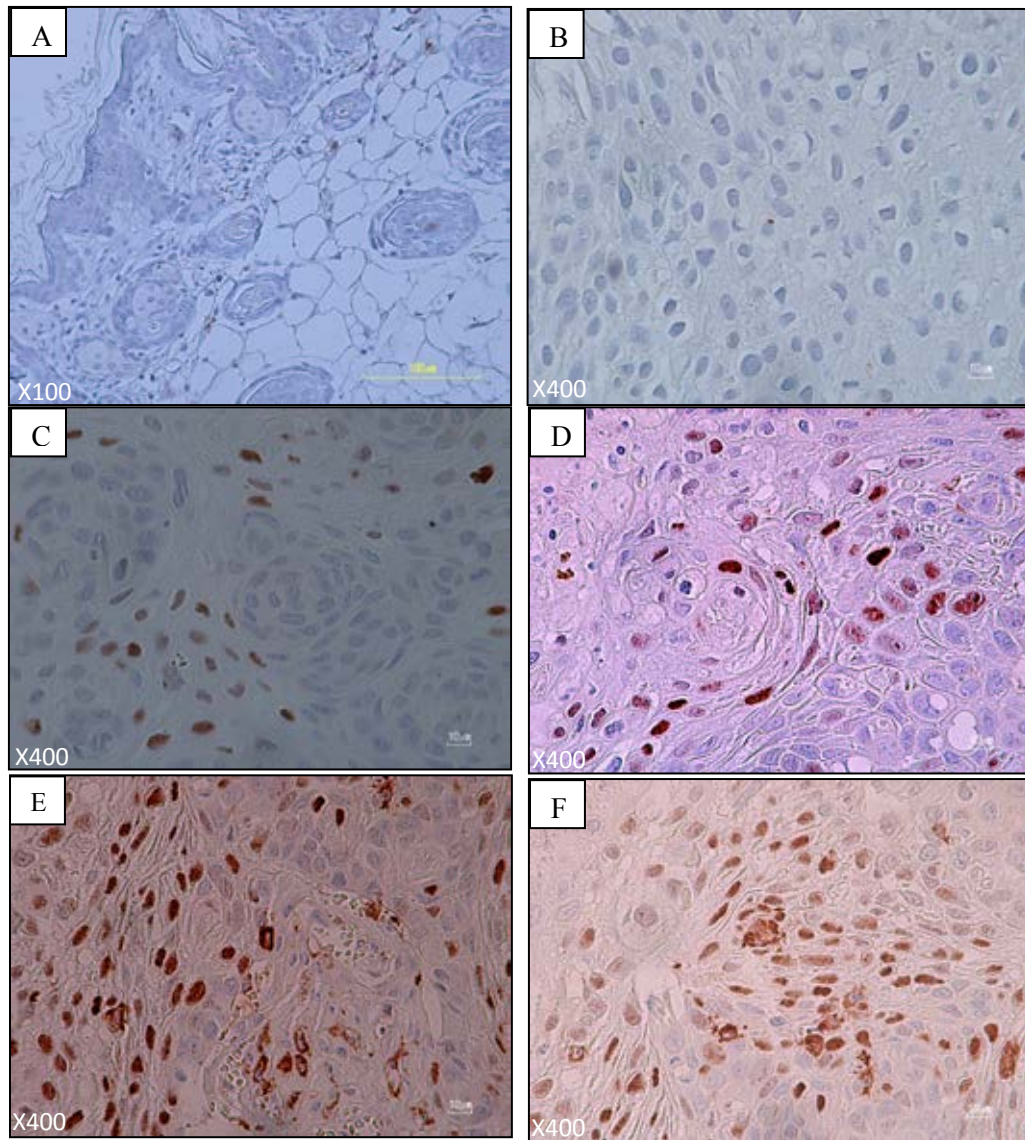


Figure 4.22 Immunohistological study of nuclear staining of p53 in tumor cells of normal skin and tumor tissue excised from CaSki cells-implanted nude mice with and without AE treatment, normal skin (**A**), HPV-Veh (**B**), HPV-300AE14day (**C**), HPV-300AE28day (**D**), HPV-3,000AE14day (**E**), and HPV-3,000AE28day (**F**).

Table 4.9 Proportion of number of P53-positive tumor cells per total tumor cells (%) of tumor tissue from CaSki cells-implanted nude mice with and without AE treatment.

Groups	Number of P53-positive cells (%) /	
	Days after treatment	
	At day 14 th	At day 28 th
HPV-Veh (n=9)	1.75 ± 0.23	2.96 ± 2.96
HPV-300AE (n=7)	16.27 ± 2.43 [*]	13.51 ± 4.46 ^{*,NS}
HPV-3,000AE (n=9)	32.66 ± 4.18 ^{*,†}	35.48 ± 0.35 ^{*,†,NS}

Notes: Data are expressed as mean ± SEM,

^{*}*P*<0.001 significant difference compared to age matched HPV-Veh group,

[†]*P*<0.001 significant difference compared to age matched HPV-300AE group,

^{NS} Non-significant difference within group.

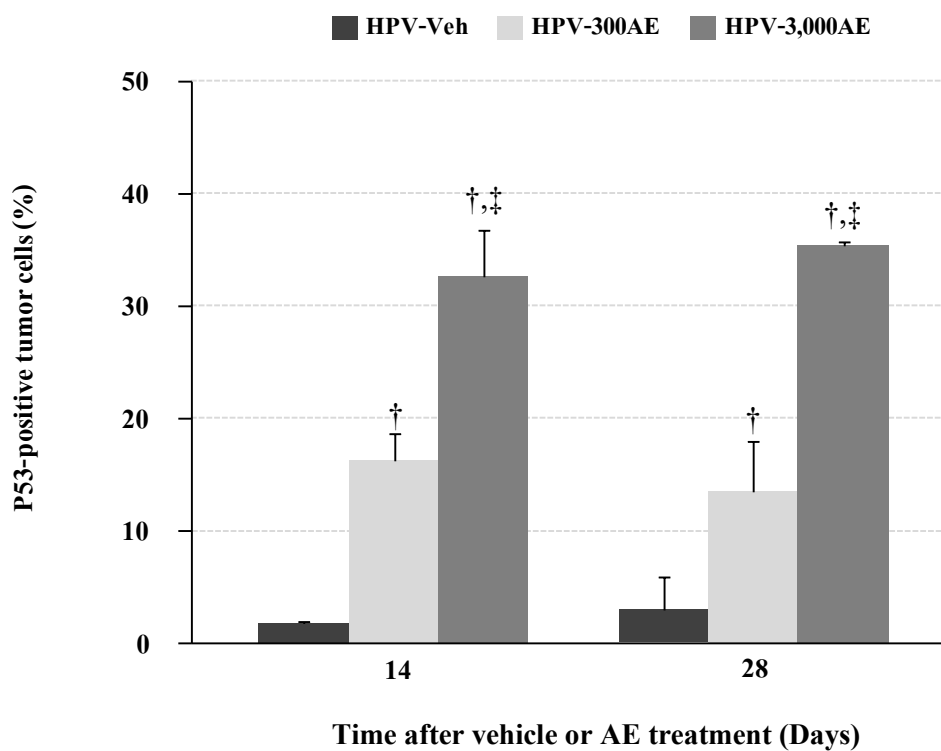


Figure 4.23 The proportion of number of P53-positive tumor cells per total tumor cells of tumor tissue from CaSki cells-implanted nude mice at 14 days and 28 days after vehicle (distilled water), AE (300 and 3,000 mg/kg BW) treatment in HPV groups.

Notes: Data are expressed as mean \pm SEM,

† $P < 0.001$ significant difference compared to age matched HPV-Veh groups,

‡ $P < 0.001$ significant difference compared to age matched HPV-300AE group.

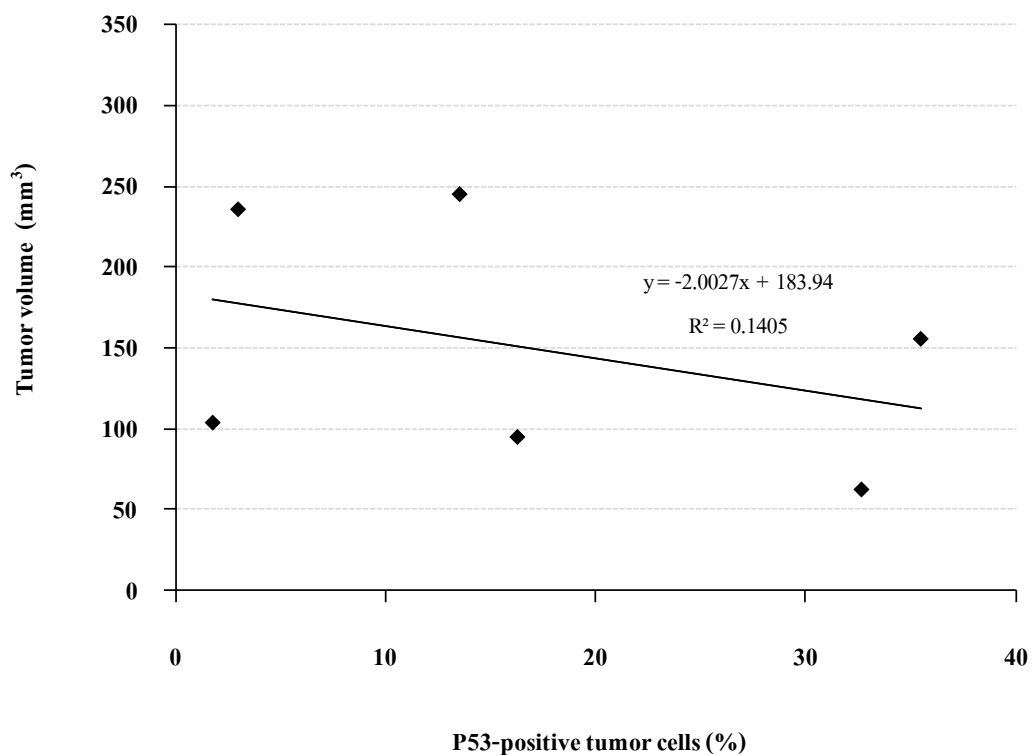


Figure 4.24 Plotting of data of The proportion of number of P53-positive tumor cells in tumor tissue (%) (x-axis) and Tumor volume (y-axis) for three groups (HPV-Veh, HPV-300AE, HPV-3,000AE). The solid line represent correlations between x and y, the correlation is expressed of $y = -2.0027x + 183.94$, $R^2=0.14$, $P=0.464$.

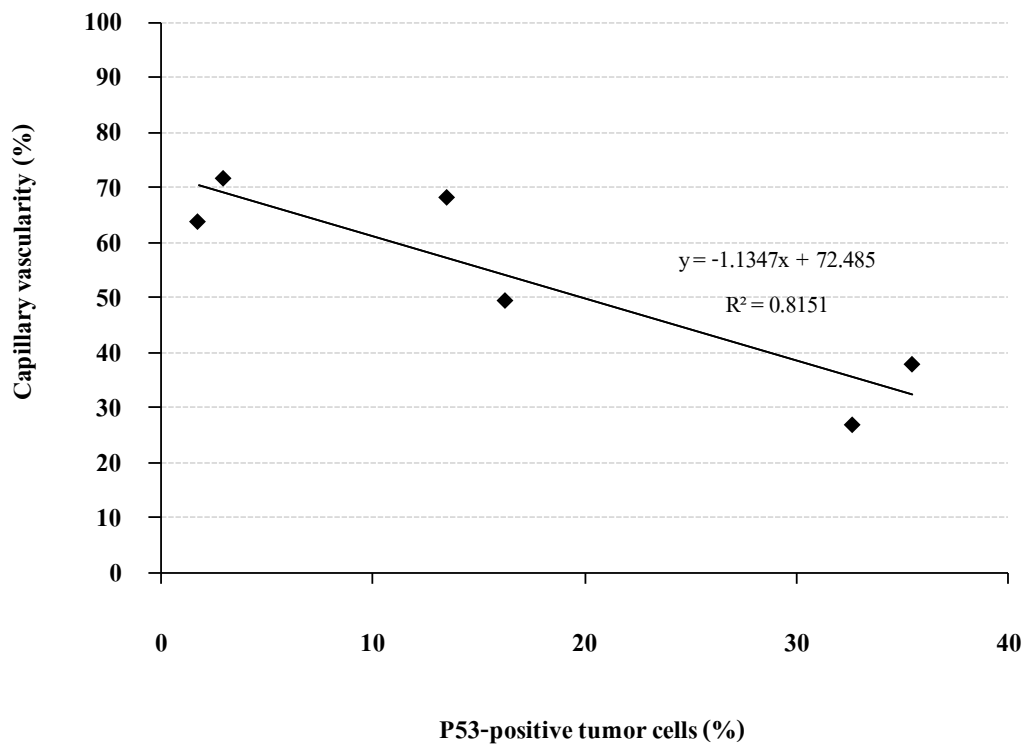


Figure 4.25 Plotting of data of The proportion of number of P53-positive tumor cells in tumor tissue (%) (x-axis) and % Capillary vascularity ((%CV),y-axis) for three groups (HPV-Veh, HPV-300AE, HPV-3,000AE). The solid line represent correlations between x and y, the correlation is expressed of $y = -1.1347x + 72.485$, $R^2=0.82$, $P=0.014$.

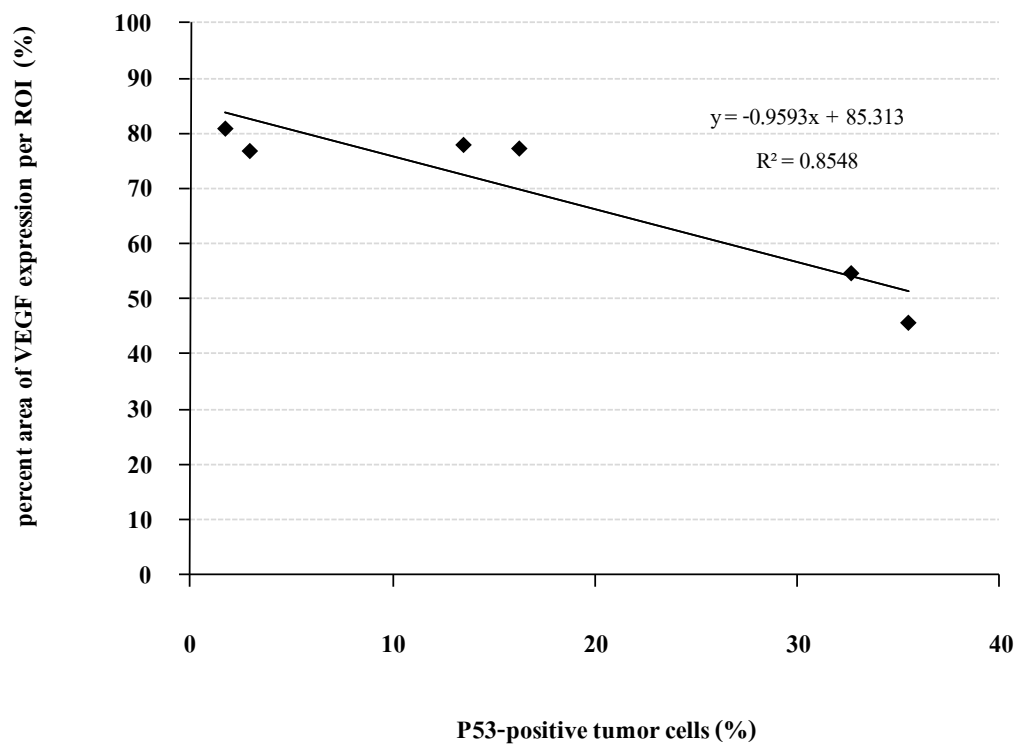


Figure 4.26 Plotting of data of The proportion of number of P53-positive tumor cells in tumor tissue (%) (x-axis) and Tumor area of VEGF expression (%) (y-axis) for three groups (HPV-Veh, HPV-300AE, HPV-3,000AE). The solid line represent correlations between x and y, the correlation is expressed of $y = -0.9593x + 85.313$, $R^2=0.86$, $P=0.005$.

CHAPTER V

DISCUSSION

Cervical cancer is one of the leading cancer causes of death, and the second most common cancers in women worldwide, especially in developing countries [9]. The most important etiological factor of cervical cancer is HPV infection, and more than 99% of all cervical cancer have been found to be positive for HPV [6]. High-risk HPV strain are oncogenic, which are known to be directly associated with cervical cancer. HPV16 is the most type associated with cervical cancer worldwide, and responsible for 50% of HPV-associated cancer, followed by HPV18 is responsible for 20% of HPV-associated cancer [50]. In Thailand, cervical cancer is the most common cancer and the third common cause of death among Thai women [246-252]. The histological type of overall cervical cancer have been reported that 80 percent of cervical cancer are squamous cell carcinomas (SCCs), while adenocarcinomas are found about 20 percent. In addition, HPV16 is the most genotype was detected in all SCCs, followed by HPV18 [34]. Therefore, HPV16 is considered as the one key target for cervical cancer prevention and treatment.

Furthermore, there are also many other factors that important on cervical cancers growth such as tumor angiogenesis, the development of new blood vessels in order to maintain tumor cells growth and differentiation. Several studies have demonstrated the association between the tumor progression and clinical pathological features including microvascular density and the expression of angiogenic factors such as VEGF and PD-ECGF [17, 23, 253]. Therefore, anti-angiogenic agents are considered for cancer therapeutic drugs.

In the present study, all experiments were designed to investigate the effects of aqueous crude extract of *A. ebracteatus* Vahl. on tumor growth and tumor angiogenesis

and level of apoptotic and angiogenic biomarkers, VEGF and P53 by using cervical cancer cells with integrated HPV-16 DNA-implanted nude mice model.

Part I : In vitro study of anti-proliferative effect of *A. ebracteatus* Vahl. aqueous crude extract in cervical cancer

The *in vitro* study was performed by using the short-term 3 hours incubation of AE in 3 different cancer cells and one normal cell lines. The trypan blue exclusion study demonstrated that the solution of AE (10^{-3} - 10^4 $\mu\text{g/ml}$) was nontoxic towards all cancer cells, CaSki, HeLa and HepG2, and normal cell, HDF with the percentage of cell viability was more than 90% (**Table 4.1**). This medicinal herb was extracted with water and could be soluble in the cell culture medium, from this reason the crude extract may be less acute toxic to the cells. With this *in vitro* finding, it implied that AE (10^{-3} - 10^4 $\mu\text{g/ml}$) did not show any acute damages or causing any direct killing effects on both cancer and normal cells. However, in the study of Babu and co-workers (2002) who demonstrated that 3-hour **incubation of alcoholic extract** of *A. ilicifolius* Linn. (10-1,000 $\mu\text{g/ml}$) with two ascites tumor cells, DLA cells and EAC cells did not show any nontoxic results [34]. Both *A. ilicifolius* Linn. and *A. ebracteatus* Vahl belong to the same *Acanthus spp.*, both of them have similar bioactivities and almost bioactive ingredients [91].

From Table 4.2 by using MTT assay, the results showed that *A. ebracteatus* Vahl. aqueous crude extract exhibited growth-inhibitory effect against CaSki, HeLa, HepG2 and HDFs in dose-dependent manner (10^{-3} – 10^4 $\mu\text{g/ml}$) and not depend on the duration time of incubations, 24, 48 and 72 hours. In addition, the results also showed that the growth inhibitory effect of AE against cancer cells seem to lower than those required for normal cells when compared at the same incubation period.

According to the data of dose-response curve with exposure time of 48 hours (**Figure 4.7 - 4.9**), AE inhibited the growth of three cancer cells better than normal cells. Since, AE exhibited anti-proliferative activity against CaSki, HeLa, HepG2 and HDFs cells with IC_{50} values was $4,984.68 \pm 498.72$ $\mu\text{g/ml}$, $6,072.50 \pm 573.29$ $\mu\text{g/ml}$, $6,419.50 \pm 2,282.62$ $\mu\text{g/ml}$, and $7,382.40 \pm 211.05$ $\mu\text{g/ml}$, respectively. In particularly, when the

values of the mean of IC_{50} of AE from each experiment of each cell were calculated, the results showed that the IC_{50} value of CaSki was significantly lower than IC_{50} value of HDFs ($P < 0.001$).

As an overall of the *in vitro* assay findings, the results implied that 48 hours exposure of *A. ebracteatus* Vahl. aqueous crude extract could decrease the number of viable CaSki cancer cells which may associate with its inhibitory effect on cellular proliferation. However, this aqueous extract showed a weak effect of cytotoxicity to CaSki cell, but not for normal cells. Because the concentration of AE that produced ~50% net cell death was relatively high when considered by the criterion of cytotoxic activity for natural crude extract on cancer cells recommended by the American National Cancer Institute (NCI) ($IC_{50} < 100 \mu\text{g/ml}$) [254]. Because of *A. ebracteatus* Vahl. aqueous extract compounds were extracted by boiling with water, which could separate the active ingredients in a small amount comparison with others extraction solutes.

Our results were similar to the study of Phisalaphong and co-workers in 2006, their MTT assay data demonstrated that aqueous extract of *A. ebracteatus* Vahl. showed the cytotoxicity against both cancer cells, KB cells ($IC_{50} = 4,000 \mu\text{g/ml}$) and HeLa cells ($IC_{50} = 3,800 \mu\text{g/ml}$). In addition, when the aqueous extract of *A. ebracteatus* Vahl. was removed the salt by nanofiltration membrane or called *desalted* product, it exhibited better toxicity against both KB and HeLa cancer cells with $IC_{50} = 3,200 \mu\text{g/ml}$ and $IC_{50} = 3,500 \mu\text{g/ml}$, respectively [48]. Moreover, the alcoholic extract of *A. ilicifolius* Linn. (*Acantus spp.*), which were claimed for having similar bioactivity as *A. ebracteatus* Vahl., was found to inhibit murine lung fibrosarcoma cells (L929) with IC_{50} values = $18 \mu\text{g/ml}$ with explosion time was 72 hours [34]. The previous study reported by Siripong and co-workers in 1998 who have isolated active constituents of the *A. ebracteatus* Vahl. with various solvents (such as water, *n*-pentane, ethyl acetate, methanol, and *n*-butanol) by chromatographic methods had found that five isolated constituents, sulphur, stigmasterol, β -sitosterol, lupeol, and polysaccharide showed no cytotoxic activity against P388 lymphocytic leukemia ($IC_{50} > 30 \mu\text{g/ml}$) [41].

Therefore, the results of the present study using in vitro assay seem to confirm that A. ebracteatus Vahl. aqueous crude extract showed non-toxic in short-term

treatment with significant weak inhibitory activity on CaSki cells growth. And it suggests that desalt or modified isolation method may require for enhancing AE potential in the future.

The potential active ingredients in *A. ebracteatus* Vahl. aqueous crude extract that might responsible for this weak growth inhibitory effect on CaSki Cells are described as followings:-

From the results encountered that *A. ebracteatus* Vahl. aqueous crude extract had growth-inhibitory activity on CaSki cells more than other two types of cancer cells, HeLa and HepG2. The type and quantity of certain active compounds found in AE may be exhibited specific growth-inhibitory activity on certain types of cancer cells. This result is related to many previous investigation that found many bioactive compounds from *A. ebracteatus* Vahl. had different anti-tumor activity specific to some kind of cancer cells. According to Siripong and co-workers (1998) have demonstrated that *A. ebracteatus* Vahl. aqueous extract and its bioactive compounds, sulphur, stigmasterol, β -sitosterol, lupeol, and polysaccharide were non-toxic towards P388 lymphocytic leukemia [41]. On the other hand, numerous studies suggested that dietary phytosterol may offer cancer protection [255]. *In vitro* studies using established the cancer cell lines have revealed an inhibitory effect of β -sitosterol, the most common dietary phytosterol. β -sitosterol has been found to have anti-tumor effect on CA755 mouse mammary adenocarcinoma, L1210 mouse lymphocytic leukemia, walkwer 256 carcinosarcoma (WA256), but non-toxic to B16 melanocarcinoma, Lewis lung carcinoma (LE), Sarcoma180 (SA180), KB human nasopharyngeal carcinoma [47]. In addition, supplementation with β -sitosterol (16 mmol/L for 5 days) exhibited growth-inhibitory activity on HT-29 cells, a human colon cancer cell and LNCaP, a human prostate cancer cells [256, 257]. While, Stigmasterol was non-toxic towards P388 lymphatic leukemia, CA755, L1210, SA180, and WA256 cancer cell lines.

Apoptosis or programmed cell death as influenced by β -sitosterol, has been investigated in cancer cell lines, 16 mmol/L β -sitosterol was found to induce apoptosis of MDA-MB-231, breast cancer cells and LNCaP cells by 4-6 fold above control levels after

3–5 d of treatment [255]. The mechanism by which β -sitosterol inhibited cancer cells growth and stimulated apoptosis has been investigated [226, 227, 258]. β -sitosterol-induced-apoptosis through caspases activation in HCT116, human colon cancer and MDA-MB-231 [225, 259]. Similarly, Park and co-workers (2007) have reported that β -sitosterol stimulated apoptosis of human leukemia cells by increased activity of caspase-3 through downregulation of Bcl-2 [227]. Moreover, β -sitosterol induced MCA-102 tumor cells apoptosis via alteration of P53 and P21 resulting decreased anti-apoptotic Bcl-2 protein and IAP family (XIAP, cIAP-1 and cIAP-2) and increased pro-apoptotic Bax [226]. They also suggested that β -sitosterol stimulated apoptosis through the activation of ERK and the blockage of the PI3K/Akt signaling pathway. Moreover, β -sitosterol is non-cytotoxic at physiologic levels on cells (4–70 mmol/L in the blood) [260]. Furthermore, treatment of β -sitosterol in breast cancer cell line at the highest concentration (16 mmol/L) had no effect on membrane integrity, indicated that β -sitosterol was not damaged cancer cells directly. Interestingly, β -sitosterol also has anti-microtubule activity which might contribute to the proliferation inhibition of HPV-associated cervical cancer SiHa cells [261].

Focus on lupeol, the triterpenoids that was found in that *A. ebracteatus* Vahl., which was claimed to has capacity for inhibiting the proliferation of a variety of cancer cells. Lupeol exhibited an anti-tumor activity against WA256, HepG2, H-411E (rat hepatoma), A-431 (human epidermoid carcinoma), but not to LE, SA and KB cancer cell lines [262]. Similarly, Lambertini and co-workers (2005) demonstrated that lupeol inhibited MDA-MB-231 cells proliferation in dose-dependent manner [263]. On the other hand, lupeol presented weak anti-proliferative activity on MCF-7 breast cancer cells [264]. In other investigation, lupeol affected on HeLa cell growth was inhibited by 27.6% [265] with IC_{50} values as higher than 50 μ M [266]. The mechanism in growth inhibition of lupeol depended on the specific cancer cell types, that lupeol may display slightly difference mechanisms of inducing apoptosis [214]. In A431 cancer cells, lupeol was associated with the caspases-dependent-mitochondrial cell apoptosis pathway by activated Bax, caspases, apoptotic protease activating factorv1 (Apaf1), decreased Bcl-2

expression, cleaved poly(ADP)ribose polymerase (PARP) [267]. In hepatocellular carcinoma SMMC7721 cells, lupeol showed the inducing apoptosis by activation of caspase-3 expression, down-regulation of death receptor 3 (DR3) and overexpression of FADD mRNA [268]. Moreover, some studies demonstrated that Lupeol acted as a potent inhibitor of protein kinases and serine proteases, and inhibits the activity of DNA topoisomerase II, a target for anticancer chemotherapy [262, 269-272].

Other triterpene, Ursolic acid (UA), which found in *Acanthus spp.*, *A. ilicifolius* Linn. has been demonstrated to have the effects of anti-inflammatory, antioxidant, and antitumor [273-275]. Numerous studies have demonstrated many pathways of the mechanism of action of UA in cancer cell growth inhibition. UA could inhibit the activities of DNA polymerase and DNA topoisomerase and decrease in cell proliferation [276]. Moreover, UA could induce cancer cell apoptosis by increasing the level of intracellular calcium ion [277], suppressing the expression of FoxM1 [278] and up-regulating of death receptors [279]. Furthermore, UA exhibited growth-inhibitory activity on gastric cancer BGC-803 cells in dose- and time-dependent manner by stimulated apoptosis through activated caspases and down-regulated Bcl-2 [278].

Interestingly, ursolic acid has demonstrated that suppressed the growth of HeLa, CaSki, and SiHa, HPV-positive cervical carcinoma cells in a dose- and time-dependent manner, but was not in the HPV-negative cervical cancer cell line (C33A). Moreover, UA inhibit HPV-associated cervical cancer (Hela) proliferation through stimulating apoptosis via the signal pathway Fas→caspase-8→PARP". Moreover, in UA-treated HeLa cells have also observed the decreasing of HPV-18 E6/E7 gene expression would contribute to growth inhibition, but the levels of p53 and pRb proteins did not change [280]. Thus, ursolic acid may be one of the important active compounds from *A. ebracteatus* Vahl. which might be useful for an effective anticancer drug in treatment of HPV-associated cervical neoplasia.

Moreover, benzoxazolines-2-one were extracted from the roots of *A. ilicifolius* Linn. [46], and ribose derivatives of this compounds were known to be active as anticancer and antiviral agents [33].

Another point is interesting that plant derived extracts containing antioxidant principles exhibited cytotoxicity towards cancer cells [281]. Since, from previous biochemicals composition study of *A. ebracteatus* Vahl. demonstrated that were rich in antioxidant compounds such as alkaloids, flavonoids, lignan glycosides, phenylethanol glycosides, triterpenoids, and polysaccharide [37, 38, 40, 42, 46, 96, 97, 99, 104, 110, 204]. In addition, the antioxidant genes related to reactive oxygen species (ROS) scavenging system have been analyzed from many parts of this plant [282]. Numerous studies have shown that alkaloids, the phenolic compounds, can inhibit carcinogenesis by affecting the molecular events in the initiation, promotion or progression states. In addition, the phenolic compounds have cytotoxic activity towards HeLa cells [283]. Anti-cancer activity of antioxidative phytochemicals may be related with the induction of cancer cells apoptosis [284]. The free radical hypothesis that ROS can act as anticancer by the promotion of cell-cycle stasis, senescence, apoptosis and necrosis, or as pro-cancer by stimulating cell proliferation, causing DNA mutations, and promoting genetic instability [285]. Therefore, the antioxidative activity of *A. ebracteatus* Vahl. aqueous crude extract may be involved in the induction of cancer cells apoptosis that causes of cancer cells growth inhibition.

From the above reviewed evidences for AE active ingredients, it can confirm our idea that AE was not directly kill the cancer cells, but its anti-cancer property appears to inhibit cancer cells growth in associated to *stimulating cell apoptosis*, However, its exact mechanism(s) need to perform further investigation including the *in vivo* model that will be described in the following Part II.

Part II: *In vivo* study: Anti-tumor and anti-angiogenic effects of *A. ebracteatus* Vahl. aqueous crude extract in cervical cancer

In the following session, the results of *in vivo* study will be discussed in two different categories, one is about the cervical cancer mice model and the other one is about effects of *A. ebracteatus* Vahl. aqueous crude extract on tumor growth and tumor-angiogenesis.

Cervical cancer mice model

The innovation on establish a mouse model for CaSki-containing HPV-16 cervical cancer study is successfully attained. We have modified our previous technique for induced HeLa-containing cervical cancer mouse [244] by using subcutaneous injection of 1×10^7 CaSki cells into mouse's dorsal skin. With this technique, a tumor nodule at dorsal skin was established at 1 week after the inoculation as shown in **Figure 4.10 (C)**.

In addition, the successfully establishment of this mouse acquired HPV-associated cervical cancer mice model was confirmed by the histopathological examination as well (**Figure 4.11**). These histological data which was interpreted under the Pathologist's supervise demonstrated that malignant tumor features with particularly morphology of squamous cell carcinomas was appeared since 1 week after CaSki cells inoculation (**Figure 4.11 C and D**). Moreover, the histological examination performed for different specimens from different organs indicated that there was no metastasis observed in the peritoneal cavity, liver and lung.

The number of CaSki cells that were used to create this tumor model was more than previous model of HeLa-containing cervical cancer mouse [244]. Since there are two distinct factors, the first one is type of cancer cell lines, Caski cells contained DNA of HPV-16 type approximately 500-600 copies/cell, presented E6 and E7 oncogenes transcription that expressed in malignant cancer cells [286], while HeLa cells contain with only 20-50 copies of HPV-18 type DNA. In addition, epidemiological report that HPV-16 was mostly detected in squamous cervical carcinoma followed by HPV-18. HPV-18 was commonly found in adenocarcinoma than HPV-16 [287]. This is consistent with our results of the pathological examination of tumor tissue from CaSki cells-implanted mice. The second different factor is method of modeling, CaSki cell were injected into subcutaneous layer of mice dorsal skin directly, while the dorsal skin fold chamber was used in previous model [244]. Inoculated cancer cells were trapped within the exactly area in the chamber and contact the basal epithelium layer of mice skin

directly. While, dorsum subcutaneously injection of CaSki cell which could not limit the cell in specific area and cancer cells spread throughout under mice skin. However, it close to several experiments that CaSki cells were used in amount of $5 \times 10^6 - 2 \times 10^7$ cells/mouse to produce cervical cancer mice model by subcutaneously injection [288-291].

From the results indicated that HPV16-associated cervical carcinoma mice model comprise basic feature of the malignant HPV-associated lesion, squamous cervical carcinoma. In addition, modeling by subcutaneously injection is an easy simply, not cause of stress in mice, do not need anesthesia, and highly reproducible. Therefore, this tumor mice model may provide a valuable of investigation of novel agents and therapeutic treatment for HPV16-associated cervical cancer in the future.

Tumor growth in cervical cancer mice model

When CaSki cells were injected subcutaneously into dorsal skin of nude mice, the cells grew rapidly to form solid tumors in almost all animals within 2-3 weeks after inoculation. The tumor volume were measured by vernier caliper and calculated by the formulas; volume (mm^3) = $\pi/6 \cdot (\text{length}) \cdot (\text{width}) \cdot (\text{height})$ [292]. As shown in **Table 4.5**, the increasing in tumor volume were observed during tumor progression from day 14th - day 28th, and tumor volume at day 28th was more than day 14th ($P < 0.05$). Moreover, tumor bud could be seen within 1 weeks after cells inoculation, and then it rapidly grew up to tumor nodule and tumor mass within 2-3 weeks later (**Figure. 4.10 A-E**).

CaSki is a cervical cancer-derived cell lines, which contained only integrated DNA, and transcripts were presented that could code for the early open reading frame (ORF) E6 and E7 [286]. HPV DNA E6 and E7 are the critical viral oncogenic proteins, which interact and interfere the functions of tumor suppressor proteins p53 and pRb, resulting in initiate pre-cancerous lesions and cancer [293]. P53 and pRb are known as regulators of cell cycle and cell apoptosis. When HPV-E6 oncoproteins bind to host p53 tumor suppressor protein through E6-AP protein, then it will cause p53 to degrade via the ubiquitin proteolytic pathway [57, 58]. After this HPV-E6 induced failure of p53 function, therefore, HPV infected cells turn to proliferate uncontrollably, and may lead to carcinogenesis and formation of malignant tumors. The other side, E7 viral protein binds

to the pRb and interfere their function by interruption of pRb-E2F complex results in the release of E2F, and allows it act as transcriptional activator of necessary proteins for DNA synthesis, and progression into the S phase of cell cycle [9, 62, 64]. Moreover, when HPV infected cancer cells exhibited the overexpression of E6 and E7 proteins that will further enable uncontrolled proliferation through activating cellular cyclin E and A [59, 60], and then allow immortalization and malignancy transformation of cells [9].

This data indicated that CaSki, HPV-16 derived cervical cancer cells proved tumorigenic activity when injected into nude mice subcutaneously at dorsal skin, formed solid tumors. Similarly to other studies that subcutaneously injection with CaSki cells (1.5×10^6 cells) could detect the palpable tumor within about 7 days after cell injection [288, 289, 294]. During tumor progression, the HPV genomes often integrate into the host chromosome, which results in a constant level of E6/E7 proteins via stabilization of the mRNA, accumulation of oncogenes mutation, further loss of cell-growth control, and ultimately cancer [63]. As the results showed that the implanted CaSki cells grew up rapidly to form solid tumors in almost all animals within 2-3 weeks after inoculation, and tumor volume significantly increase continuously after inoculation until 35 days.

In **Table 4.4.**, it showed that the values of body weight between CaSki-cells implanted mice and its aged-match control were no significant difference, even though the tumor growth was observed during this period ($P < 0.05$). Unfortunately, we did not monitor weight of each tumor mass, therefore, the ratio of tumor weight per body weight of each group could not inform in this study.

Tumor p53 expression in cervical carcinoma tissue

By using immunohistochemical technique, the results showed that p53 expression was not found in normal skin from all control nude mice (**Figure 4.22A**). It is well known that in normal, unstressed cells, the level of p53 protein is extremely low, through a consequent continuing degradation of p53 by Mdm2 [295-297].

According to HPVE6/E6AP protein could inactivate and accelerate loss of active p53 protein, however, the expression of p53 was detected very low in tumor tissue from CaSki cells-induced cervical cancer mice (**Figure 4.22B and Table 4.8**). This result is

fully agreement with the previous reports by Butz and co-workers demonstrating that p53 protein is not completely inactivated in cervical cancer cells [298, 299]. This indicated that tumor mice model induce by CaSki cells lacked of active p53 causes by tumorigenic activity of HPVE6 protein. Moreover, founding of the expression of p53 in cervical cancer induced by CaSki cells was to confirm that this model was tumor harboring wild-type p53, which has a functional p53 protein if very low amounts due to extensive degradation [300, 301]. However, study of p53 expression in cervical cancer are also controversial, several studies have suggested that p53 protein accumulation may be an early event in cervical carcinogenesis [302-305]. While, numerous studies have reported that p53 is involved lately in the process of tumor progression with poor prognosis in SCCs [306]. In the other side, it has been reported that p53 expression was not correlated with clinical stage and tumor volume in early stage SCCs with and without invasion to lymphatic vascular space [268], and invasive SCCs [307]. Moreover, Looi and co-workers (2008) have reported that p53 expression was found in 27% of cervical SCC cases, but it had no significant relationship with SCC staging [308], however, the alteration of anti-apoptotic protein, bcl-2 was observed in HGCIN (CIN3) and it correlated with HGCIN staging that involved in the progression of neoplasia in the uterine cervix. As mention above, p53 expression seem to be detected in almost stages of cervical cancer lesion, but the relationship between p53 expression and clinical pathology factor still remain unclear and cannot be conclusive.

By using Pearson Correlation, our present study showed that the p53 expression was not correlated with the increase in CaSki tumor volume during 14-28 days of experiment ($R^2 = 0.14$, $P = 0.464$).

Tumor microvascularature in cervical carcinoma tissue

Base on the confocal microscopic images (**Figure 4.14**), the high density of neocapillaries network around tumor-bearing site were found. These fluorescence labeled microvascular images indicated the particular characteristics for these 21-day tumor newly-formed capillaries which included endothelial cell sprouting, increase permeability, increase capillary-diameter size, and high tortuous. After cells inoculation,

the tumor capillary diameter at day 35th (diameter ~ 10-15 μm) seem larger than at day 21st (diameter ~ <10 μm), that consistent with other studies also reported that the diameter of tumor capillaries increased with time [309, 310]. This phenomenon is commonly recognized as tumor angiogenesis. The earliest histopathological features of tumor angiogenesis such as microvascular dilation, tortuosity, hypermeability, and edema have been reported by Hanahan and Folkman (1996) [311].

As well known that, VEGF and its receptors, play important roles in the formation and growth of normal blood vessels and in tumor angiogenesis [82, 312]. Inhibition of VEGF signaling not only block growth of new tumor vessels, but can also disrupts tumor angiogenesis process, remodel or destroys tumor vessels [313-317]. Such as, VEGF/VEGFR inhibition can decrease the diameter, tortuosity, and permeability of tumor vessels [313, 317], and transform tumor vessels which still alive into a more normal phenotype [318, 319]. Therefore, the increases of tumor capillaries diameters in HPV16-associated cervical cancer mice model might be due to the increment of angiogenic factors, VEGF. Accordingly, the tumor VEGF expression was markedly increased in 21 and 35 days of HPV groups after inoculation.

In the present study, *tumor angiogenic index* were evaluated and described by the capillary vascularity shown in **Table 4.6**. The results indicated that in HPV-Veh groups, capillary vascularity was significantly higher than the aged-matched control group. This result indicated the tumor angiogenesis occurred in Caski cells-implanted mice through the induction process of HPV16 DNA which described above. This result was compatible with recent studies that angiogenesis is an important phenotype in all stage of cervical cancer development [15, 16, 18-22, 80]. However, previous study has suggested that the onset of angiogenesis in cervical cancer occurs very early during premalignant stages [21], a cervical neoplasia [29] and that HPV oncoproteins may involve in this process [29, 320]. In addition, previous studies have described that the inactivation of wild-type p53 by high risk HPV oncoproteins E6 and E7 has the indirect effect on promoting tumor angiogenesis via up-regulation of angiogenic factor, VEGF [27, 29, 86, 321]. Beside this process also results in down-regulation of a potent

angiogenic inhibitor, thrombospondin-1 (TSP-1) [321]. Our results demonstrated the cervical carcinoma-induced neovascularization occurred in early stage of cancer development, and the amount of neocapillaries of Caski cells-implanted mice was significantly increased when compared to its aged-match controls ($P < 0.001$) (**Figure 4.15**).

Moreover, by using Pearson Correlation, the increasing of capillary vascularity of Caski cell-implanted mice was specifically correlation to the increment of tumor VEGF expression ($y = 0.9306x - 11.219$, $R^2=0.82$, $P<0.05$) (**Figure 4.21**). In order to confirm the importance of tumor angiogenesis for tumor growth and tumor progression, the Pearson correlation was used and the result showed that the increase in tumor capillary vascularity positively correlated with means of tumor volume ($y = 3.0532x - 12.377$, $R^2=0.52$, $P = 0.108$) (**Figure 4.16**).

VEGF expression in cervical carcinoma tissue

VEGF exhibits a potent angiogenic effect in cervical cancer [17]. Numerous studies have reported that VEGF expression was found in all stages of cervical cancer lesion correlated with microvascular density. Particularly, this MVD is used as an important prognosis marker in cervical cancer [83, 322, 323].

Our present study showed the VEGF expression with strong intensity in tumor area from CaSki cells-implanted mice skin (**Figure 4.18 A,B**), and percent area of VEGF expression per ROI (%) was significantly increased up to **~2.5 times** of aged-match control value (**Table 4.7**). Moreover, by using Pearson correlation, our results shown in **Figure 4.21** indicated the significant correlation between VEGF expression and capillary vascularity as previously mentioned.

The possible mechanisms of HPV-associated cervical carcinoma induced VEGF expression have been proposed through many pathways including (i) *HIF-1 α up-regulated VEGF expression pathway*, as well recognized as the *hypoxic response mechanism* [324, 325], (ii) *HPV-E6 induced p53-degradation caused up-regulation of VEGF* [14, 25], (iii) *HPV-E6 induced HIF-1 α and up-regulation of VEGF expression*

[28, 79] (iv) **HPV E6- and E7-directly induced VEGF expression** [26, 27], (v) **HPV E7 up-regulates VEGF expression via c-myc pathway** [29].

As mentioned above, inactivation of active P53 protein status by E6 viral oncoprotein not only is an important step in the HPV-associated carcinogenesis, but also directly related in tumor angiogenesis process. In accordance with our results of the relationship between VEGF and p53 expression showed highly negative correlation ($y = 0.9593x - 85.313$, $R^2=0.86$, $P < 0.01$). Moreover, p53 expression was also highly negative correlated with capillary vascularity ($y = 1.1347x - 72.485$, $R^2=0.82$, $P < 0.05$). Therefore, based on our finding, it implied that not only the basic hypoxic response mechanism, but also the degradation of p53 through HPV-E6 oncoprotein might be accounted as the other mechanism caused the increase in VEGF expression, with consequently initiate angiogenesis in CaSki cells-implant nude mice.

Effects of *A. ebracteatus* Vahl. aqueous crude extract on tumor growth and tumor-angiogenesis.

In the present study, we demonstrated for the first time that *A. ebracteatus* Vahl. aqueous crude extract could inhibit tumor angiogenesis and tumor growth in cervical cancer derived HPV16-implanted nude mice model.

High dose of AE (HPV-3,000AE) could inhibit or delay tumor growth, that verified by the reduction of tumor volume (compared with HPV-Veh group, $P < 0.001$) (**Figure 4.12**), when treated for 28 days. This result indicated that AE exhibited the inhibitory effect on tumor growth in dose- and time-dependent manner. Previously report of *in vivo* antitumor studies revealed that crude aqueous extract and their active compounds exhibited a weak antitumor activity against Sarcoma 180 ascites cell-transplanted ICR rats [41]. In addition, *Acanthus spp.*, *Acanthus ilicifolius* Linn. could reduced tumor volume of ascites tumor harboring animals [34].

In present study, the growth-inhibitory activity of AE may produce through its potential on the induction of cancer cells apoptosis. This action of cell apoptosis induction may responsible by its active ingredients like β -sitosterol, lupeol, and ursolic acid, which have been discussed in the previous Part I, the *in vitro* study. Especially, β -

sitosterol could also induce cancer cells apoptosis via alteration of p53 and p21 in murine fibrosarcoma MCA-102 cancer cell lines [226]. Therefore, β -sitosterol from *A. ebracteatus* Vahl. may involve in the restoration of active p53 in CaSki cell-implanted mice. Moreover, the growth-inhibitory effect of *A. ebracteatus* Vahl. may enhance by its antioxidant induced cancer cells apoptosis, as mentioned earlier. However, *A. ebracteatus* Vahl. aqueous crude extract exhibited weak anti-tumor activity against CaSki cells-implanted mice, since AE was not directly caused CaSki cells death when observed under *in vitro* assay. Therefore, others factors that involved in the growth-inhibitory property of *A. ebracteatus* Vahl. aqueous crude extract should be considered, including the inhibition of tumor angiogenesis process.

AE aqueous crude extract affects p53 restoration in cervical carcinoma

Our study demonstrated that the 28-day oral feeding of *A. ebracteatus* Vahl. aqueous crude extract is capable to increase the level of active p53 expression in HPV16-associated cervical cancer in dose-dependent manner (**Table 4.8**) (**4.56-time** for 300mg/kg BW; and **12-time** for 3,000 mg/kg BW). Especially, our results also showed that when AE-potentially-induced increased p53 expression, the apoptosis of cervical cancer cells was also enhanced. From the literature reviews (Chapter II), it suggested that β -sitosterol, AE bioactive compounds, could induce the accumulations of p53 and p21 in MCA-102 cancer cell lines, and result in decreased anti-apoptotic Bcl-2 and increased pro-apoptotic Bax [226]. It is well known that HPV-associated cervical carcinoma containing E6 protein could cause the host-cell abnormalities including p53 inactivation, impairment of inhibitory process of normal cell-cycle, and then allowing HPV-infected cell proliferation. In addition, E6 and E7 viral proteins also express continuously to maintain the transformed phenotype of cancer cells. However, p53 gene was still functional as wide-type p53 in HPV-positive cervical cancer cell lines [64, 65]. However, the correlation test for these p53 expression with tumor growth results after AE treatment did not show any significant correlation ($R^2 = 0.14$, $P = 0.464$) (**Figure 4.24**). This suggested that even though AE could enhance p53 expression and decrease tumor volume, the mechanism of p53 may not affect tumor growth directly but it may involve in

many other mechanisms such as anti-angiogenesis as well. Therefore, the correlation between our obtained data of both factors may be not fit by the simple linear relationship.

Many previous studies have reported the mechanism of restoration of p53 expression in HPV-associated cervical carcinoma, that one of the key factors is the down-regulation of HPV E6 protein expression or disruption of E6 activity [67, 68, 71, 326]. Likewise, an anti-sense could be down-regulate E6-AP expression, catalytically inactive of E6-AP mutant, or RNA interference results in the accumulation of p53 in HPV-positive cells [69, 70, 327]. Nevertheless, p53 activity does not need to depend on its quantity [328], but the active portion gradually develops by posttranslational modifications [329, 330]. Additionally, Deng and co-workers (2006) have provided evidence showing that a traditional Chinese herb medicine (TCM), Yigan Kang (YGK) could restore a normal p53 protein in HeLa cervical cancer cells, that correlated with repression of transcription of E6 oncoprotein [71]. They also demonstrated that this herb could reverse the tumorigenic phenotype to less aggressive tumor growth in YGK-treated HeLa cells implanted SCID mice [72]. This indicated that, the down-regulation of viral E6/E7 genes might be direct effect to inhibition of invasive cervical cancer. Therefore, *A. ebracteatus* Vahl. aqueous crude extract delayed tumor growth in HPV16-positive cervical cancer-implanted mice model with wild-type p53, might be act via restoration of cellular p53 and transformed cells to undergo growth arrest or apoptosis.

AE aqueous crude extract affects VEGF expression in cervical carcinoma

This study has demonstrated the anti-angiogenic activity of *A. ebracteatus* Vahl. aqueous crude extract in HPV16-associated cervical cancer. Low dose of AE (300 mg/kg BW) could inhibit tumor neovascularization when treated for 14 days, but was not 28 days. AE exhibited higher potent of anti-angiogenic effects when treated with high dose 3,000 mg/kg BW of AE, which could inhibit tumor neovascularization at 14 and 28 days of treatment. This result indicated that the inhibition of tumor angiogenesis by *A. ebracteatus* Vahl. aqueous crude extract is a dose-dependent manner as well.

Importantly, this anti-angiogenic effect of AE as the reduction of tumor capillary vascularity was highly correlated with angiogenic biomarker, VEGF expression during the HPV16-associated cervical carcinoma progression. Therefore, the inhibitory effect of *A. ebracteatus* Vahl. aqueous crude extract on anti-angiogenesis should be related to its possible mechanism of anti-VEGF expression. As mentioned earlier, the inhibition of VEGF expression in HPV-associated cervical carcinoma might be involved in many factors such as inactivation of HIF1- α , down-regulation of E6 protein or disruption of E6-AP activity resulting the accumulation of p53, blockade E6 induced p53, or down-regulation of E7 protein or inhibition of E7 activates c-myc/eIF4E signaling pathway [14, 25-29, 79, 324, 325].

According to the expression of VEGF in HPV-associated cervical carcinoma was closely correlated with E6 and E7 viral proteins, and level of active p53. Focus on the relationship between the expression of VEGF and p53 after AE treatment in HPV-associated cervical carcinoma, the results showed that AE inhibited tumor VEGF expression was well correlated with the increasing of tumor p53 expression ($y = -0.9593x + 85.313$, $R^2=0.86$, $P < 0.01$) (**Figure 4.16**). Moreover, the increment of p53 expression after AE treatment was also well correlated with the inhibition of tumor angiogenesis ($y = -1.1347x + 72.485$, $R^2=0.82$, $P < 0.05$) (**Figure 4.15**). This data suggested that *A. ebracteatus* Vahl. aqueous crude extract exhibited the down-regulation of tumor VEGF expression in HPV16-associated cervical carcinoma might be relate to the accumulation of tumor active p53 protein and involve with E6, E6-AP, or E7 viral proteins.

Up to our knowledge, *A. ebracteatus* Vahl. has not been reported for its potential mechanisms on the anti-angiogenic effect yet, even though, its bioactive compositions have been reported and some of them also associated with anti-angiogenic property. For example, *A. ebracteatus* Vahl. has polysaccharides as one of its bioactive ingredients. Plant polysaccharides are considered to be bioactive constituents involved in anti-tumor and anti-inflammatory effects [233, 331, 332], in particularly, its anti-tumor angiogenesis and tumor growth [234, 235, 333, 334].

Besides, the other bioactive compounds in *A. ebracteatus* Vahl. seem to have potential roles in anti-angiogenesis. Those are triterpenoids, triterpenes, Lupeol, ursolic acid and oleanolic acid. Among the known angiogenic inhibitors triterpenoids, synthetic dihydrobenzofuran lignans plays a prominent role [335]. In addition previous study has reported that plant triterpenoidal saponins, which isolated from *Polygala senega* has an anti-angiogenic effect, which by inhibition of VEGF-induced *in vitro* tubular formation of HUVECs and basic fibroblast growth factor (bFGF)-induced *in vivo* neovascularization in mouse Matrigel plug assay [191]. Other triterpenes, Lupeol, which exhibited the inhibition of tube formation of HUVEC cells under *in vitro* condition [215]. Moreover, the Anti-angiogenic activity of triterpene acid, Ursolic acid (UA) and oleanolic acid (OA), which were showed the inhibition of angiogenesis in chick embryo chorioallantoic membrane (CAM) assay, and bovine aortic endothelial cell proliferation, in concentration-dependent manner [201]. The plant flavonoids, Quercetin has been reported for its anti-angiogenic potential, which was found to inhibit several steps of angiogenesis including proliferation, migration, and tube formation of human microvascular dermal endothelial cells *in vitro*, and decreased the expression and activity of MMP-2 in CAM *in vivo* assay [140].

The phytosterol, β -sitosterol may involve in the inhibition of tumor angiogenesis through the activation of p53 in HPV-associated cervical cancer. Since, β -sitosterol has been reported that it could increase the level of p53 protein in MCA-102 cells with dose-dependent manner [226]. Our cervical cancer mice model, the dysregulation of p53 by HPV E6 resulting the up-regulation of VEGF, due to HPV E6 blocked p53 induction or increased p53 degradation [14, 25]. Therefore, β -sitosterol in AE may inhibit the tumor angiogenesis by the down-regulation of VEGF via the restoration of p53 in HPV-associated cervical cancer. However, Moon and co-workers (1999) have reported that β -sitosterol from aloe vera possesses angiogenic property and use for management of chronic wounds [228]. In ischemia/reperfusion-damaged brain using Mongolian gerbils model, β -sitosterol was showed for its effectively angiogenic property [229]. Therefore,

more study is required to clarify whether the finding effect of AE on anti-angiogenesis was accounted by β -sitosterol or not.

Since cancer development, metastasis and progression are critically processes which depend on vasculogenesis and angiogenesis. Therefore, we hypothesize that the effects of AE on anti-angiogenesis and anti-tumor particularly, in early stage cervical carcinogenesis should be influence for innovation of treatment and improve patient outcome. In addition, *A. ebracteatus* Vahl. also has been reported that has the anti-inflammatory [32, 118] and anti-oxidative activity [32], that may be toxic toward tumor cell directly through induction of apoptosis [336] or inhibition of tumor angiogenesis [337]. Moreover, the antioxidant genes related to reactive oxygen species (ROS) scavenging system have been analyzed from many parts of this plant [282]. Tumor-mediated inflammatory response could generate an intensive local accumulation of reactive oxygen species (ROS). ROS play a role as the mediator of tumor induced expression of angiogenic factor, VEGF and angiopoietin-1 [338, 339]. However, we need to confirm and explore whether these AE pharmacological properties, including anti-oxidant and anti-inflammation will be possible to explain our findings or not.

In summary, we would like to make the proposed mechanisms for *A. ebracteatus* Vahl. aqueous crude extract in order to describe its potential effects on tumor angiogenesis and on tumor growth in associated to the results of this present study **(Figure 5.1)**.

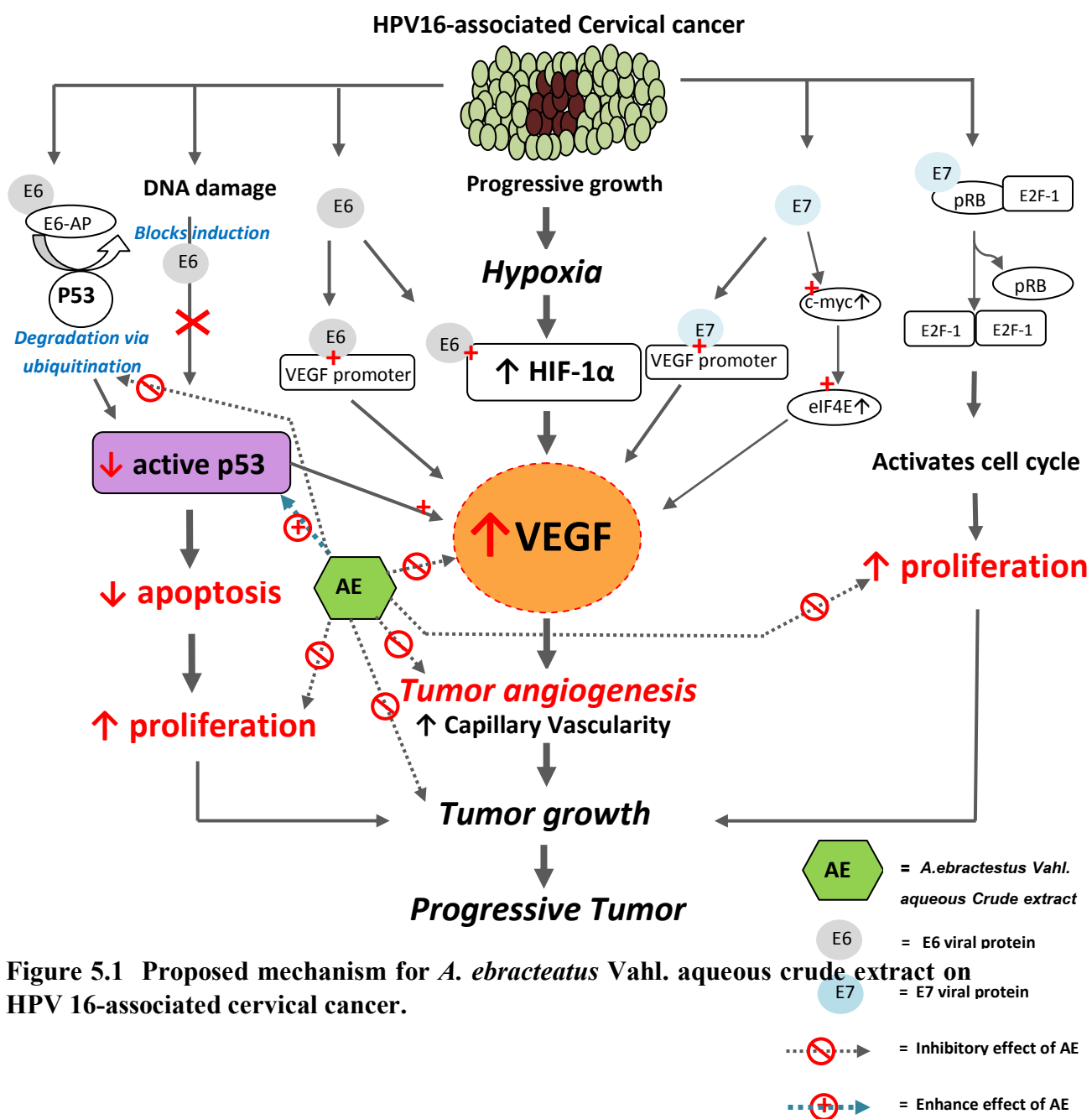


Figure 5.1 Proposed mechanism for *A. ebracteatus* Vahl. aqueous crude extract on HPV 16-associated cervical cancer.

Figure 5.1 illustrates the event that occurs in HPV-16 associated cervical cancer mice model receiving aqueous crude extract of *A. ebracteatus* Vahl. After subcutaneously injection of CaSki cells, the human cervical cancer cells contained integrated HPV-16 DNA, and the oncogenic HPV genomes E6 and E7 which caused cellular p53 degradation and resulted in dysregulation of cell apoptosis and cell cycle control. Consequently, cancer cells increased cell proliferation and growth without angiogenesis until remain small ($< 1\text{-}2\text{ mm}^3$). The lack of oxygen and nutrients supply to cancerous condition, results in cell hypoxia and leading to apoptosis and necrosis [10]. Under hypoxic state, the binding of HIF-1 α to VEGF promoter is a mainly signaling pathway resulting in the induction of VEGF expression [11]. Moreover, HPV E6 and E7 oncogenes also involve in the up-regulation of VEGF expression [14, 26-29, 79]. All of these factors result in highly increased of tumor VEGF expression more than normal mice. Therefore, this model of HPV16-associated cervical cancer has shown that low expression of p53 proteins with high expression of VEGF, which similar to the pathology of human cervical cancer [5,8, 14-24]. AE exhibited inhibitory effect on cervical cancer growth by inhibiting tumor angiogenesis through down-regulation of tumor VEGF expression. In addition, AE could restore active p53 protein in cancer cell and transformed cells to undergo growth arrest or apoptosis that caused tumor growth suppression. Furthermore, increasing of p53 protein in cancer cell might be involved in decreasing of tumor angiogenesis through the down-regulation of VEGF expression [14,25] Others possible mechanism of anti-tumor activity of AE might be involved in dysregulation of E6, E6-AP, and E7 [67, 68, 71, 326] that resulted in accumulation of p53 protein and down-regulation VEGF expression via inactivation of HIF-1 α or VEGF promoter or *c-myc* pathway [26-29, 79].

CHAPTER VI

CONCLUSIONS

In the present study, using the intravital fluorescent confocal laser scanning microscopic techniques, the effects of *Acanthus ebracteatus* Vahl. aqueous crude extract on tumor growth and tumor angiogenesis in HPV16-associated cervical cancer nude mice model and biomarkers, p53 and VEGF expression were investigated. The experimental data including anti-proliferative activity, tumor volume, capillary vascularity, VEGF and p53 expression were determined for each group: Con-Veh, Con-300AE, Con-3,000AE, HPV-Veh, HPV-300AE, HPV-3,000AE in difference of the duration of AE aqueous crude extract treatment.

The significant findings could be summarized as follows;

1. Under the Trypan blue exclusion study of 3 hours incubation *in vitro* condition, AE (10^{-3} - 10^4 $\mu\text{g/ml}$) was nontoxic towards all cancer cells, CaSki, HeLa and HepG2, and HDFs, with the values of the percentage cell viability were more than 90% of all cells.
2. Under *in vitro* MTT assay observation, AE inhibited the growth of CaSki, HeLa and HepG2, and HDFs cells in a dose-dependent manner with exposure time at 48 hours, but a time-dependence was not observed.
3. AE (48 hr) had an anti-proliferative effect on CaSki cells, the only one types of investigated cancer cell that was significantly different from normal cells, HDFs.
4. However, the anti-proliferative effect of 48 hours exposure of AE was not significantly different between CaSki, HeLa, and HepG2.
5. CaSki, a human cervical cancer-derived cell lines with integrated HPV-16 DNA (1×10^7 cells/200 μl /each mouse), could induce cervical cancer bearing mice model by directly injection into subcutaneous layer at middle dorsum skin. Thus, HPV16-associated

cervical cancer mice model could be established, and also exhibited the malignant tumor feature of squamous cell carcinomas (SCCs).

6. The expression of p53 was detected very low in tumor tissue from CaSki cells-induced cervical cancer mice, suggested that this model is HPV16-associated cervical carcinoma with wild-type p53.
7. Tumor angiogenesis was observed after CaSki cells inoculation, indicating the Caski cells-induced angiogenesis, and also correlated with tumor growth. Therefore, the HPV16-associated cervical carcinoma mice provided the tumor angiogenesis mice model.
8. The up-regulation of VEGF was found in Caski cells-implanted mice model, and also exhibited the correlation with the tumor angiogenesis and p53 protein expression.
9. *A.ebracteatus* Vahl. aqueous crude extract exhibited the anti-angiogenic and anti-tumor activities of on HPV16-associated cervical carcinoma was dose-dependent manner, but not depend on the duration of treatment.
10. Possible mechanism of *A. ebracteatus* Vahl. aqueous crude extract on anti-angiogenesis is proposed to be anti-VEGF expression.
11. *A.ebracteatus* Vahl. aqueous crude extract exhibited the down-regulation of tumor VEGF expression in HPV16-associated cervical carcinoma that related to the accumulation of tumor active p53 protein.

REFERENCES

- [1] Ferlay, J., Shin, H.R., Bray, F., Forman, D., Mathers, C.,and Parkin, D.M. GLOBOCAN 2008 v1.2. Available from URL: <http://globocan.iarc.fr>.
- [2] WHO/ICO, H.I.C. Human Papillomavirus and Related Cancers in Thailand. Summary Report 2010 : WHO/ICO, 2010.
- [3] Kjaer, S.K., Tran, T.N., Sparen, P., et al. The burden of genital warts: a study of nearly 70,000 women from the general female population in the 4 Nordic countries. J Infect Dis 196 (Nov 2007): 1447-1454.
- [4] Schiffman, M., Castle, P.E., Jeronimo, J., Rodriguez, A.C.,and Wacholder, S. Human papillomavirus and cervical cancer. Lancet 370 (Sep 2007): 890-907.
- [5] Doorbar, J. Molecular biology of human papillomavirus infection and cervical cancer. Clin Sci (Lond) 110 (May 2006): 525-541.
- [6] Munoz, N., Castellsague, X., de Gonzalez, A.B.,and Gissmann, L. Chapter 1: HPV in the etiology of human cancer. Vaccine 24 Suppl 3 (Aug 31 2006): S3/1-10.
- [7] Prendiville, W.,and Davies, P. The Health Professional's HPV Handbook 1: Human Papillomavirus and cervical cancer. The United kingdom: Taylor&Francis groups, 2004.
- [8] Gonzalez, S.L., Stremlau, M., He, X., Basile, J.R.,and Munger, K. Degradation of the retinoblastoma tumor suppressor by the human papillomavirus type 16 E7 oncoprotein is important for functional inactivation and is separable from proteasomal degradation of E7. J Virol 75 (Aug 2001): 7583-7591.
- [9] Munger, K., Baldwin, A., Edwards, K.M., et al. Mechanisms of human papillomavirus-induced oncogenesis. J Virol 78 (Nov 2004): 11451-11460.
- [10] Folkman, J. What is the evidence that tumors are angiogenesis dependent? J Natl Cancer Inst 82 (Jan 1990): 4-6.

- [11] Roskoski, R., Jr. Vascular endothelial growth factor (VEGF) signaling in tumor progression. Crit Rev Oncol Hematol 62 (Jun 2007): 179-213.
- [12] Folkman, J., and Shing, Y. Angiogenesis. J Biol Chem 267 (Jun 1992): 10931-10934.
- [13] Kerbel, R.S. Tumor angiogenesis. N Engl J Med 358 (May 2008): 2039-2049.
- [14] Monk, B.J., Willmott, L.J., and Sumner, D.A. Anti-angiogenesis agents in metastatic or recurrent cervical cancer. Gynecol Oncol 116 (Feb 2010): 181-186.
- [15] Van Trappen, P.O., Steele, D., Lowe, D.G., et al. Expression of vascular endothelial growth factor (VEGF)-C and VEGF-D, and their receptor VEGFR-3, during different stages of cervical carcinogenesis. J Pathol 201 (Dec 2003): 544-554.
- [16] No, J.H., Jo, H., Kim, S.H., et al. Expression of vascular endothelial growth factor and hypoxia inducible factor-1alpha in cervical neoplasia. Ann N Y Acad Sci 1171 (Aug 2009): 105-110.
- [17] Tokumo, K., Kodama, J., Seki, N., et al. Different angiogenic pathways in human cervical cancers. Gynecol Oncol 68 (Jan 1998): 38-44.
- [18] Obermair, A., Bancher-Todesca, D., Bilgi, S., et al. Correlation of vascular endothelial growth factor expression and microvessel density in cervical intraepithelial neoplasia. J Natl Cancer Inst 89 (Aug 1997): 1212-1217.
- [19] Guidi, A.J., Abu-Jawdeh, G., Berse, B., et al. Vascular permeability factor (vascular endothelial growth factor) expression and angiogenesis in cervical neoplasia. J Natl Cancer Inst 87 (Aug 1995): 1237-1245.
- [20] Dobbs, S.P., Hewett, P.W., Johnson, I.R., Carmichael, J., and Murray, J.C. Angiogenesis is associated with vascular endothelial growth factor expression in cervical intraepithelial neoplasia. Br J Cancer 76 (1997): 1410-1415.
- [21] Smith-McCune, K., Zhu, Y.H., Hanahan, D., and Arbeit, J. Cross-species comparison of angiogenesis during the premalignant stages of squamous carcinogenesis in the human cervix and K14-HPV16 transgenic mice. Cancer Res 57 (Apr 1997): 1294-1300.

- [22] Hammes, L.S., Tekmal, R.R., Naud, P., et al. Up-regulation of VEGF, c-fms and COX-2 expression correlates with severity of cervical cancer precursor (CIN) lesions and invasive disease. Gynecol Oncol 110 (Sep 2008): 445-451.
- [23] Kodama, J., Seki, N., Tokumo, K., et al. Vascular endothelial growth factor is implicated in early invasion in cervical cancer. Eur J Cancer 35 (Mar 1999): 485-489.
- [24] Yu, H., Zhang, S., Zhang, R., and Zhang, L. The role of VEGF-C/D and Flt-4 in the lymphatic metastasis of early-stage invasive cervical carcinoma. J Exp Clin Cancer Res 28 (2009): 98.
- [25] Willmott, L.J., and Monk, B.J. Cervical cancer therapy: current, future and anti-angiogenesis targeted treatment. Expert Rev Anticancer Ther 9 (Jul 2009): 895-903.
- [26] Bequet-Romero, M., and Lopez-Ocejo, O. Angiogenesis modulators expression in culture cell lines positives for HPV-16 oncoproteins. Biochem Biophys Res Commun 277 (Oct 2000): 55-61.
- [27] Lopez-Ocejo, O., Vilorio-Petit, A., Bequet-Romero, M., Mukhopadhyay, D., Rak, J., and Kerbel, R.S. Oncogenes and tumor angiogenesis: the HPV-16 E6 oncoprotein activates the vascular endothelial growth factor (VEGF) gene promoter in a p53 independent manner. Oncogene 19 (Sep 2000): 4611-4620.
- [28] Tang, X., Zhang, Q., Nishitani, J., Brown, J., Shi, S., and Le, A.D. Overexpression of human papillomavirus type 16 oncoproteins enhances hypoxia-inducible factor 1 alpha protein accumulation and vascular endothelial growth factor expression in human cervical carcinoma cells. Clin Cancer Res 13 (May 2007): 2568-2576.
- [29] Matthews-Greer, J., DeBenedetti, A., Tucker, A., Dempsey, S., and Black, D. A model for Angiogenesis in HPV-mediated Cervical neoplasia. J Applied Res 2 (2002): 11.
- [30] Monk, B.J., Sill, M.W., Burger, R.A., Gray, H.J., Buekers, T.E., and Roman, L.D. Phase II trial of bevacizumab in the treatment of persistent or recurrent squamous cell carcinoma of the cervix: a gynecologic oncology group study. J Clin Oncol 27 (Mar 2009): 1069-1074.

- [31] Masathien, C., and Siripong, P. In vitro Immunopotentiating Effect(s) of *Acanthus ebracteatus* Vahl. Roots on Human Lymphocytes. Journal of the Medical Technologist Association of Thailand 15 (1991): 97-103.
- [32] Babu, B.H., Shylesh, B.S., and Padikkala, J. Antioxidant and hepatoprotective effect of *Acanthus ilicifolius*. Fitoterapia 72 (Mar 2001): 272-277.
- [33] Advani, S.B., and Sam, J. Potential anticancer and antiviral agents. Substituted 3-[1'(2',3',4'-tri-O-benzoyl- β -d-ribofuranosyl)]-2-benzoxazinones. Journal of Heterocyclic Chemistry 5 (1968): 119-122.
- [34] Babu, B.H., Shylesh, B.S., and Padikkala, J. Tumour reducing and anticarcinogenic activity of *Acanthus ilicifolius* in mice. J Ethnopharmacol 79 (Jan 2002): 27-33.
- [35] Wu, J., Zhang, S., Xiao, Q., et al. Megastigmane and flavone glycosides from *Acanthus ilicifolius*. Pharmazie 58 (May 2003): 363-364.
- [36] Laupattarakasem, P., Houghton, P.J., Hoult, J.R., and Itharat, A. An evaluation of the activity related to inflammation of four plants used in Thailand to treat arthritis. J Ethnopharmacol 85 (Apr 2003): 207-215.
- [37] Tiwari, K.P., Minicha, P.K., and Masood, M. Acanthifoline-A new alkaloid from *Acanthus ilicifolius*. Polish Journal of Chemistry 54 (1980): 857-858.
- [38] Minocha, P.K., and Tiwari, K.P. A triterpenoidal saponin from roots of *Acanthus ilicifolius*. Phytochemistry 20 (1981): 135-137.
- [39] Jensen, H.F.W., Jensen, S.R., and Nielsen, B.J. Chemotaxonomy of the acanthaceae. Iridoids and quaternary amines. Phytochemistry 27 (1988): 2581-2589.
- [40] Hokputsa, S., Harding, S.E., Inngjerdigen, K., et al. Bioactive polysaccharides from the stems of the Thai medicinal plant *Acanthus ebracteatus*: their chemical and physical features. Carbohydr Res 339 (Mar 2004): 753-762.
- [41] Siripong, P., Kongkathip, B., Kanokmedhakul, K., Hitosuyanagi, Y., Takeya, K., and Itokawa, H. Study on Antitumor Potential of *Acanthus ebracteatus* Vahl. Roots. Thai Cancer Journal 24 (1998): 29.

- [42] Kanchanapoom, T., Kasai, R., Picheansoonthon, C., and Yamasaki, K. Megastigmane, aliphatic alcohol and benzoxazinoid glycosides from *Acanthus ebracteatus*. Phytochemistry 58 (Nov 2001): 811-817.
- [43] P., S., and L., N. Effect of *Acanthus ilicifolius* Linn. in Treatment of Leukemic Mice. Thai Cancer Journal 7 (1981): 89-93.
- [44] Yanapirut, P., and Sriwatanakul, K. Prospective study of adverse reactions of anticancer drugs in Thai patients. J Med Assoc Thai 70 (Aug 1987): 448-454.
- [45] Tiwawech, D., Siripong, P., and Kupradinun, P. Inhibition of Diethylnitrosamine (DEN)-induced Hepatic Foci by Pre and Post Treatment with *Acanthus ebracteatus* Vahl. in Rats. Thai Cancer Journal 1-2 (1993): 7-13.
- [46] Kokpol, U., Chittawong, V., and Miles, D.H. Chemical Constituents of the Roots of *Acanthus ilicifolius*. J Nat Prod 49 (Mar 1986): 355-356.
- [47] Hartwell, J.L. Types of anticancer agents isolated from plants. Cancer Treat Rep 60 (1976): 1031-1067.
- [48] Phisalaphong, M., Thu Ha, N., and Siripong, P. Desalting of Aqueous Extract of *Acanthus ebracteatus* Vahl. by Nanofiltration. Separation Science and Technology 41 (2006): 455-470.
- [49] Ferlay, J., Barry, F., Pisani, P., and Parkin, D.M. GLOBOCAN 2002 : Cancer incidence, mortality and prevalence worldwide. IARC Cancer Base. IARC, Press, Lyon, 2004.
- [50] Parkin, D.M., Bray, F., Ferlay, J., and Pisani, P. Global cancer statistics, 2002. CA Cancer J Clin 55 (Mar-Apr 2005): 74-108.
- [51] Boulet, G., Horvath, C., Vanden Broeck, D., Sahebali, S., and Bogers, J. Human papillomavirus: E6 and E7 oncogenes. Int J Biochem Cell Biol 39 (2007): 2006-2011.
- [52] Lowy, D.R., and Schiller, J.T. Papillomaviruses and cervical cancer: pathogenesis and vaccine development. J Natl Cancer Inst Monogr (1998): 27-30.
- [53] Woodman, C.B., Collins, S.I., and Young, L.S. The natural history of cervical HPV infection: unresolved issues. Nat Rev Cancer 7 (Jan 2007): 11-22.

- [54] Jeon, S., and Lambert, P.F. Integration of human papillomavirus type 16 DNA into the human genome leads to increased stability of E6 and E7 mRNAs: implications for cervical carcinogenesis. Proc Natl Acad Sci U S A 92 (Feb 1995): 1654-1658.
- [55] Corden, S.A., Sant-Cassia, L.J., Easton, A.J., and Morris, A.G. The integration of HPV-18 DNA in cervical carcinoma. Mol Pathol 52 (Oct 1999): 275-282.
- [56] Steger, G., and Corbach, S. Dose-dependent regulation of the early promoter of human papillomavirus type 18 by the viral E2 protein. J Virol 71 (Jan 1997): 50-58.
- [57] Thomas, M., Pim, D., and Banks, L. The role of the E6-p53 interaction in the molecular pathogenesis of HPV. Oncogene 18 (Dec 1999): 7690-7700.
- [58] Scheffner, M. Ubiquitin, E6-AP, and their role in p53 inactivation. Pharmacol Ther 78 (Jun 1998): 129-139.
- [59] Malanchi, I., Caldeira, S., Krutzfeldt, M., Giarre, M., Alunni-Fabbroni, M., and Tommasino, M. Identification of a novel activity of human papillomavirus type 16 E6 protein in deregulating the G1/S transition. Oncogene 21 (Aug 2002): 5665-5672.
- [60] Caldeira, S., de Villiers, E.M., and Tommasino, M. Human papillomavirus E7 proteins stimulate proliferation independently of their ability to associate with retinoblastoma protein. Oncogene 19 (Feb 2000): 821-826.
- [61] Munger, K., and Howley, P.M. Human papillomavirus immortalization and transformation functions. Virus Res 89 (Nov 2002): 213-228.
- [62] Ying, H., and Xiao, Z.X. Targeting retinoblastoma protein for degradation by proteasomes. Cell Cycle 5 (Mar 2006): 506-508.
- [63] Bernard, H.U. Gene expression of genital human papillomaviruses and considerations on potential antiviral approaches. Antivir Ther 7 (Dec 2002): 219-237.
- [64] zur Hausen, H. Papillomaviruses and cancer: from basic studies to clinical application. Nat Rev Cancer 2 (May 2002): 342-350.

- [65] Stanbridge, C.M., Mather, J., Curry, A., and Butler, E.B. Demonstration of papilloma virus particles in cervical and vaginal scrape material: a report of 10 cases. J Clin Pathol 34 (May 1981): 524-531.
- [66] Pan, H., and Griep, A.E. Temporally distinct patterns of p53-dependent and p53-independent apoptosis during mouse lens development. Genes Dev 9 (Sep 1995): 2157-2169.
- [67] Butz, K., Denk, C., Ullmann, A., Scheffner, M., and Hoppe-Seyler, F. Induction of apoptosis in human papillomavirus-positive cancer cells by peptide aptamers targeting the viral E6 oncoprotein. Proc Natl Acad Sci U S A 97 (Jun 6 2000): 6693-6697.
- [68] Butz, K., Ristriani, T., Hengstermann, A., Denk, C., Scheffner, M., and Hoppe-Seyler, F. siRNA targeting of the viral E6 oncogene efficiently kills human papillomavirus-positive cancer cells. Oncogene 22 (Sep 2003): 5938-5945.
- [69] Beer-Romero, P., Glass, S., and Rolfe, M. Antisense targeting of E6AP elevates p53 in HPV-infected cells but not in normal cells. Oncogene 14 (Feb 1997): 595-602.
- [70] Talis, A.L., Huibregtse, J.M., and Howley, P.M. The role of E6AP in the regulation of p53 protein levels in human papillomavirus (HPV)-positive and HPV-negative cells. J Biol Chem 273 (Mar 1998): 6439-6445.
- [71] Deng, W.P., Chao, M.W., Lai, W.F., et al. Correction of malignant behavior of tumor cells by traditional Chinese herb medicine through a restoration of p53. Cancer Lett 233 (Feb 2006): 315-327.
- [72] Gartel, A.L., Radhakrishnan, S.K., Serfas, M.S., Kwon, Y.H., and Tyner, A.L. A novel p21WAF1/CIP1 transcript is highly dependent on p53 for its basal expression in mouse tissues. Oncogene 23 (Oct 2004): 8154-8157.
- [73] Liao, D., and Johnson, R.S. Hypoxia: a key regulator of angiogenesis in cancer. Cancer Metastasis Rev 26 (Jun 2007): 281-290.
- [74] Semenza, G.L. Hypoxia-inducible factor 1: control of oxygen homeostasis in health and disease. Pediatr Res 49 (May 2001): 614-617.

- [75] Forsythe, J.A., Jiang, B.H., Iyer, N.V., et al. Activation of vascular endothelial growth factor gene transcription by hypoxia-inducible factor 1. Mol Cell Biol 16 (Sep 1996): 4604-4613.
- [76] Ikeda, E., Achen, M.G., Breier, G., and Risau, W. Hypoxia-induced transcriptional activation and increased mRNA stability of vascular endothelial growth factor in C6 glioma cells. J Biol Chem 270 (Aug 1995): 19761-19766.
- [77] Felmeden, D.C., Blann, A.D., and Lip, G.Y. Angiogenesis: basic pathophysiology and implications for disease. Eur Heart J 24 (Apr 2003): 586-603.
- [78] Klagsbrun, M. Angiogenesis and cancer: AACR special conference in cancer research. American Association for Cancer Research. Cancer Res 59 (Jan 1999): 487-490.
- [79] Nakamura, M., Bodily, J.M., Beglin, M., Kyo, S., Inoue, M., and Laimins, L.A. Hypoxia-specific stabilization of HIF-1 α by human papillomaviruses. Virology 387 (May 2009): 442-448.
- [80] Triratanachat, S., Niruthisard, S., Trivijitsilp, P., Tresukosol, D., and Jarurak, N. Angiogenesis in cervical intraepithelial neoplasia and early-staged uterine cervical squamous cell carcinoma: clinical significance. Int J Gynecol Cancer 16 (Mar-Apr 2006): 575-580.
- [81] Carmeliet, P. VEGF as a key mediator of angiogenesis in cancer. Oncology 69 Suppl 3 (2005): 4-10.
- [82] Ferrara, N., Gerber, H.P., and LeCouter, J. The biology of VEGF and its receptors. Nat Med 9 (Jun 2003): 669-676.
- [83] Rasila, K.K., Burger, R.A., Smith, H., Lee, F.C., and Verschraegen, C. Angiogenesis in gynecological oncology-mechanism of tumor progression and therapeutic targets. Int J Gynecol Cancer 15 (Sep-Oct 2005): 710-726.
- [84] Kim, S.H., Juhn, Y.S., Kang, S., et al. Human papillomavirus 16 E5 up-regulates the expression of vascular endothelial growth factor through the activation of epidermal growth factor receptor, MEK/ ERK1,2 and PI3K/Akt. Cell Mol Life Sci 63 (Apr 2006): 930-938.
- [85] Song, S.H., Lee, J.K., Hur, J.Y., Kim, I., Saw, H.S., and Park, Y.K. The expression of epidermal growth factor receptor, vascular endothelial growth factor,

matrix metalloproteinase-2, and cyclooxygenase-2 in relation to human papilloma viral load and persistence of human papillomavirus after conization with negative margins. Int J Gynecol Cancer 16 (Nov-Dec 2006): 2009-2017.

- [86] Lee, J.S., Kim, H.S., Park, J.T., Lee, M.C., and Park, C.S. Expression of vascular endothelial growth factor in the progression of cervical neoplasia and its relation to angiogenesis and p53 status. Anal Quant Cytol Histol 25 (Dec 2003): 303-311.
- [87] Li, M.Y., Xiao, Q., Pan, J.Y., and Wu, J. Natural products from semi-mangrove flora: source, chemistry and bioactivities. Nat Prod Rep 26 (Feb 2009): 281-298.
- [88] Ridley, H.N. The flora of the Malay Peninsula UK: L. Reeves and Co, 1923.
- [89] Burkill, I. Dictionary of the Economic Products of the Malay Peninsula. Malaysia, Kuala Lumpur: Ministry of Agriculture and Cooperatives, Malaysia, Kuala Lumpur, 1966:27.
- [90] Lemmens, R.H.M.J., and Bunyaphatsara, N. Plant Resources of South-East Asia. Bogor, Indonesia: Prosea Foundation, 2003.
- [91] Patarakorn Manasomboon. Pharmacognostic properties of acanthus ebracteatus vahl. Master's Thesis, Faculty of Pharmaceutical Sciences. Chulalongkorn University, 2004.
- [92] Subudhi, H.N., Choudhury, B.P., and Acharya, B.C. Some potential medicinal plants of Mahanadi delta in the state of Orissa. Journal of Economic and Taxonomic Botany 16 (1992): 9.
- [93] Perry, L.M. Medicinal Plants of East and Southeast Asia Attributed Properties and Use. Cambridge, London: The Massachusetts Institute of Technology Press, 1980:2.
- [94] Duke, J.A., and Ayensu, E.S. Medicinal plants of China. Reference Publications (Algonac, Mich.) 1985.
- [95] Pongboonrod, S. Medicinal plants of Thailand. Bangkok, Thailand: Kasem Bunnakit Publishing Co., 1971.

- [96] Kanchanapoom, T., Kamel, M.S., Kasai, R., Yamasaki, K., Picheansoonthon, C., and Hiraga, Y. Lignan glucosides from *Acanthus ilicifolius*. Phytochemistry 56 (Feb 2001): 369-372.
- [97] Murthy, M.S.R., Wahidulla, S., and Kamat, S.Y. Isolation of 2-benzoxazolinone from *Acanthus ilicifolius*. Indian Journal of Pharmaceutical Science 46 (1984): 2.
- [98] Kapil, A., Sharma, S., and Wahidulla, S. Leishmanicidal Activity of 2-Benzoxazolinone from *Acanthus ilicifolius* in vitro. Planta Med 60 (1994): 187,188.
- [99] Huo, C.H., Wang, B., Liang, H., Zhao, Y.Y., and Lin, W.H. [Study on chemical constituents of mangrove *Acanthus ilicifolius*]. Zhongguo Zhong Yao Za Zhi 31 (Dec 2006): 2052-2054.
- [100] Ghosh, A., Misra, S., Dutta, A.K., and Choudhury, A. Pentacyclic triterpenoids and sterols from seven species of mangrove. Phytochemistry 24 (1985): 1725-1727.
- [101] Misra, S., K. Datta, A., Chattopadhyay A. Choudhury, S., and Ghosh, A. Hydrocarbons and wax esters from seven species of mangrove leaves. Phytochemistry 26 (1987): 3265-3268.
- [102] Wu, J., Zhang, S., Xiao, Q., et al. Phenylethanoid and aliphatic alcohol glycosides from *Acanthus ilicifolius*. Phytochemistry 63 (Jun 2003): 491-495.
- [103] Minocha, A.A. Medical pluralism and health services in India. Soc Sci Med Med Anthropol 14B (Nov 1980): 217-223.
- [104] Kanchanapoom, T., Kamel, M.S., Kasai, R., Picheansoonthon, C., Hiraga, Y., and Yamasaki, K. Benzoxazinoid glucosides from *Acanthus ilicifolius*. Phytochemistry 58 (Oct 2001): 637-640.
- [105] Wu, J., Huang, J., Xiao, Q., et al. Complete assignments of ¹H and ¹³C NMR data for 10 phenylethanoid glycosides. Magn Reson Chem 42 (Jul 2004): 659-662.
- [106] Kapil, A., Sharma, S., and Wahidulla, S. Leishmanicidal activity of 2-benzoxazolinone from *Acanthus ilicifolius* in vitro. Planta medica 60 (Apr 1994): 187-188.

- [107] D'Souza, L., Wahidulla, S., and Mishra, P.D. Bisoxazolinone from the mangrove *Acanthus iliifolius*. Indian J Chem 36B (1997): 3.
- [108] Huo, C., An, D., Wang, B., Zhao, Y., and Lin, W. Structure elucidation and complete NMR spectral assignments of a new benzoxazolinone glucoside from *Acanthus ilicifolius*. Magn Reson Chem 43 (Apr 2005): 343-345.
- [109] Shi Y, Huo C, Yao H, Gao R, Zhao Y, and B., X. Enantioseparation of 2-O-beta-D-glucopyranosyl-2H-1,4-benzoxazin-3(4H)-one and its 7-chloro-derivative by capillary zone electrophoresis using native and substituted beta-cyclodextrins as chiral additives. J Chromatogr A 29 (2005): 4.
- [110] Nair, A.G.R., and Pouchaname, V. Methylapigenin 7-O-Beta-D-Glucuronate a New Flavone Glycoside from *Acanthus-Ilicifolius*. Journal of the Indian Chemical Society 64 (1987): 2.
- [111] Wu, J., Zhang, S., Huang, J., et al. New aliphatic alcohol and (Z)-4-coumaric acid glycosides from *Acanthus ilicifolius*. Chem Pharm Bull (Tokyo) 51 (Oct 2003): 1201-1203.
- [112] Wu, J., Zhang, S., Li, Q., Huang, J., Xiao, Z., and Long, L. Two New Cycloolignan Glycosides from *Acanthus ilicifolius*. Z. Naturforsch. 59b (2004): 4.
- [113] Chungsamarnyart, N.S., Jiwajinda, W., Jansawan, U., and Buranasilpin, K.P. Effective plant crude-extracts on the ticks (*Boophilus microplus*). I. Larvicidal action. Kasetsart J Nat Sci Suppl 22: (1988): 37.
- [114] Sittiwet, C., Niamsa, N., and Puangpronpitag, D. Antimicrobial Activity of *Acanthus ebracteatus* Vahl. Aqueous Extract: The Potential for Skin Infection Treatment. International Journal of Biological Chemistry 3 (2009): 95-98.
- [115] Cheeptham, N., and Towers, G.H. Light-mediated activities of some Thai medicinal plant teas. Fitoterapia 73 (Dec 2002): 651-662.
- [116] Juthamard Somchaichan. Effect of acanthus ebracteatus vahl. extract in combination with collagen scaffold on angiogenesis and wound closure in mice skin model. Master's Thesis, Graduate School. Chulalongkorn University, 2004.

- [117] Rojanapo, W., Tepsuwan, A., and Siripong, P. Mutagenicity and antimutagenicity of Thai medicinal plants. Basic Life Sci 52 (1990): 447-452.
- [118] Agshikar, N.V., Naik, V.R., Abraham, G.J., Reddy, C.V., Naqvo, S.W., and Mittal, P.K. Analgesic anti-inflammatory activity of *Acanthus illicifolius* Linn. Indian J Exp Biol 17 (Nov 1979): 1257-1258.
- [119] Beckstrom-Sternberg, and Duke, J.A. Searches for plants containing trigonelline and biological activities of trigonelline. Phytochemeco Database produced. MD, USA: USDA Agricultural Research Service., 1997.
- [120] Agarwal, J.S., and Rastogi, R.P. Chemical Examination of Water-soluble fraction of *Mappia foetida* Miers. Indian Journal of Chemistry 7 (1975).
- [121] Anthoni, U., Christophersen, C., Hougaard, L., and Nielsen., P.H. Review: Quaternary ammonium compounds in the biosphere-an example of a versatile adaptive strategy. Comp. Biochem. Physiol. 99B (1991): 18.
- [122] Chopra, S., Ahmad, F.J., Khar, R.K., et al. Validated high-performance thin-layer chromatography method for determination of trigonelline in herbal extract and pharmaceutical dosage form. Anal Chim Acta 577 (Sep 1 2006): 46-51.
- [123] Czok, G. Biopharmacological effects of coffee substances other than caffeine. B. Arch. Sci. Med. 131 (1974): 3.
- [124] Der Marderosian, A.H. Pharmacognosy: Medicinal teas-boon or bane? Drug Ther. 7 (1977): 9.
- [125] Abe, S.a.T.K. Effect of betaines and taurine and its derivatives on plasma cholesterol levels in rats. Eiyo To Shokuryo 28 (1975): 4.
- [126] Shani (Mishkinsky), J., Goldschmied, A., Joseph, B., Ahronson, Z., and Sulman, F.G. Hypoglycaemic effect of *Trigonella Foenum Graecum* [sic] and *Lupinus Termis* (Leguminosae) seeds and their major alkaloids in alloxan-diabetic and normal rats. Arch. Int. Pharmacodyn. 210 (1974): 11.
- [127] Li, C.P. Chinese Herbal Medicine. Washington, D.C., U.S, NIH Pub. , 1974.
- [128] Wolf, R.B., Spencer, G., and Plattner, R.D. Benzoxazolinone, 2,4-dihydroxy-1,4-benzoxazin-3-one, and its glucoside from *Acanthus mollis* seeds inhibit velvetleaf germination and growth. J Nat Prod 48 (1985): 5.

- [129] Otsuka, H., Hirai, Y., Nagao, T., and Yamasaki, K. Anti-inflammatory activity of benzoxazinoids from roots of *Coix lachryma-jobivar. ma-yuen*. J Nat Prod 51 (Jan-Feb 1988): 6.
- [130] Bravo, H.R., and Copaja, S.V. Contents and morphological distribution of 2,4-dihydroxy-1,4-benzoxazin-3-one and 2-benzoxazolinone in *Acanthus mollis* in relation to protection from larvae of *Pseudaletia impuncta*. Annals of Applied Biology 140 (2002): 129-132.
- [131] Sanchez-Moreiras, A.M., de la Pena, T.C., and Reigosa, M.J. The natural compound benzoxazolin-2(3H)-one selectively retards cell cycle in lettuce root meristems. Phytochemistry 69 (Aug 2008): 2172-2179.
- [132] Barnes, J.P., Putnam, A.R., Burke, B.A., and Aasen, A.J. Isolation and characterization of allelochemicals in rye herbage. Phytochemistry 26 (1987): 1385-1390.
- [133] Roberts, K.P., Iyer, R.A., Prasad, G., Liu, L.T., Lind, R.E., and Hanna, P.E. Cyclic hydroxamic acid inhibitors of prostate cancer cell growth: selectivity and structure activity relationships. Prostate 34 (Feb 1 1998): 92-99.
- [134] Niemeyer, H.M. Hydroxamic acids (4-hydroxy-1,4-benzoxazin-3-ones), defence chemicals in the gramineae. Phytochemistry 27 (1988): 3349-3358.
- [135] Simmonds, M.S.J. Importance of flavonoids in insect-plant interactions: feeding and oviposition. Phytochemistry 56 (2001): 245-252.
- [136] Nagaprashantha, L.D., Vatsyayan, R., Singhal, J., et al. Anti-cancer effects of novel flavonoid vicenin-2 as a single agent and in synergistic combination with docetaxel in prostate cancer. Biochem Pharmacol 82 (2011): 1100-1109.
- [137] Levy, J., Teuerstein, I., Marbach, M., Radian, S., and Sharoni, Y. Tyrosine protein kinase activity in the DMBA-induced rat mammary tumor: inhibition by quercetin. Biochem Biophys Res Commun 123 (Sep 28 1984): 1227-1233.
- [138] Havsteen, B. Flavonoids, a class of natural products of high pharmacological potency. Biochem Pharmacol 32 (1983): 1141-1148.

- [139] Corvazier, E., and Maclouf, J. Interference of some flavonoids and non-steroidal anti-inflammatory drugs with oxidative metabolism of arachidonic acid by human platelets and neutrophils. Biochim Biophys Acta 835 (Jul 9 1985): 315-321.
- [140] Tan, W.-f., Lin, L.-p., Li, M.-h., et al. Quercetin, a dietary-derived flavonoid, possesses antiangiogenic potential. Eur J Pharmacol 459 (2003): 255-262.
- [141] Yoshida, M., Sakai, T., Hosokawa, N., et al. The effect of quercetin on cell cycle progression and growth of human gastric cancer cells. FEBS Lett 260 (Jan 15 1990): 10-13.
- [142] Xiao, D., Zhu, S.P., and Gu, Z.L. Quercetin induced apoptosis in human leukemia HL-60 cell. Acta. Pharmacol. Sin. 18 (1998): 4.
- [143] Bucar, F., and Kartnig, T. Flavone glucuronides of *Lycopus virginicus*. Planta Med 61 (Aug 1995): 378-380.
- [144] Gumbinger, H.G., Winterhoff, H., Wylde, R., and Sosa, A. On the influence of the sugar moiety on the antigonadotropic activity of luteoline glycosides. Planta Med 58 (Feb 1992): 49-50.
- [145] Shimizu, M., Ito, T., Terashima, S., et al. Inhibition of lens aldose reductase by flavonoids. Phytochemistry 23 (1984): 1885-1888.
- [146] Zhang, L., Kong, Y., Wu, D., et al. Three flavonoids targeting the β -hydroxyacyl-acyl carrier protein dehydratase from *Helicobacter pylori*: Crystal structure characterization with enzymatic inhibition assay. Protein Science 17 (2008): 1971-1978.
- [147] Du, Q., Xu, Y., Li, L., Zhao, Y., Jerz, G., and Winterhalter, P. Antioxidant constituents in the fruits of *Luffa cylindrica* (L.) Roem. J Agric Food Chem 54 (Jun 14 2006): 4186-4190.
- [148] Tang, R., Chen, K., Cosentino, M., and Lee, K.-H. Apigenin-7-O- β -D-glucopyranoside, an anti-HIV principle from *Kummerowia striata*. Bioorganic & Medicinal Chemistry Letters 4 (1994): 455-458.
- [149] Lee, K.H., Yoon, W.H., and Cho, C.H. Anti-Ulcer Effect of Apigenin-7-O- β -D-Glucuronide Isolated from *Chrysanthemum morifolium* Ramataelle. Korean Journal of Pharmacognosy (2005).

- [150] Wang, P., Kang, J., Zheng, R., et al. Scavenging effects of phenylpropanoid glycosides from *Pedicularis* on superoxide anion and hydroxyl radical by the spin trapping method(95)02255-4. Biochem Pharmacol 51 (Mar1 996): 687-691.
- [151] Heilmann, J., Çalis, I., Kirmizibekmez, H., Schühly, W., Harput, S.,and Sticher, O. Radical Scavenger Activity of Phenylethanoid Glycosides in FMLP Stimulated Human Polymorphonuclear Leukocytes: Structure-Activity Relationships. Planta Med 66 (Dec 2000): 746-748.
- [152] Liao, F., Zheng, R.L., Gao, J.J.,and Jia, Z.J. Retardation of skeletal muscle fatigue by the two phenylpropanoid glycosides: Verbascoside and Martynoside from *Pedicularis plicata* Maxim. Phytotherapy Research 13 (1999): 621-623.
- [153] Miao, J., Wang, W., Yao, S., Navaratnam, S.,and Parson, B.J. Antioxidative properties of Martynoside: pulse radiolysis and laser photolysis study. Free Radic Res 37 (Aug 2003): 829-833.
- [154] Miyase, T., Ishino, M., Akahori, C., Ueno, A., Ohkawa, Y.,and Tanizawa, H. Phenylethanoid glycosides from *Plantago asiatica*. Phytochemistry 30 (1991): 2015-2018.
- [155] Abe, F., Nagao, T.,and Okabe, H. Antiproliferative constituents in plants 9. Aerial parts of *Lippia dulcis* and *Lippia canescens*. Biol Pharm Bull 25 (Jul 2002): 920-922.
- [156] Korkina, L.G. Phenylpropanoids as naturally occurring antioxidants: from plant defense to human health. Cell Mol Biol (Noisy-le-grand) 53 (2007): 15-25.
- [157] Zhou, B.-N., Bahler, B.D., Hofmann, G.A., Mattern, M.R., Johnson, R.K.,and Kingston, D.G.I. Phenylethanoid Glycosides from *Digitalis purpurea* and *Penstemon linarioides* with PKC α -Inhibitory Activity. J Nat Prod 61 (No 1998): 1410-1412.
- [158] Tasdemir, D., Scapozza, L., Zerbe, O., Linden, A., Çalis, I.,and Sticher, O. Iridoid Glycosides of *Leonurus persicus*. J Nat Prod 62 (June 1999): 811-816.
- [159] Nakamura, T., Okuyama, E., Tsukada, A., et al. Acteoside as the analgesic principle of Cedron (*Lippia triphylla*), a Peruvian medicinal plant. Chem Pharm Bull (Tokyo) 45 (1997): 6.

- [160] Li, J., Ge, R.C., Zheng, R.L., Liu, Z.M., and Jia, Z.J. Antioxidative and chelating activities of phenylpropanoid glycosides from *Pedicularis striata*. Zhongguo Yao Li Xue Bao 18 (Jan 1997): 77-80.
- [161] Xiong, Q., Tezuka, Y., Kaneko, T., et al. Inhibition of nitric oxide by phenylethanoids in activated macrophages. Eur J Pharmacol 400 (Jul 2000): 137-144.
- [162] Seidel, V., Verholle, M., Malard, Y., et al. Phenylpropanoids from *Ballota nigra* L. inhibit in vitro LDL peroxidation. Phytother Res 14 (Mar 2000): 93-98.
- [163] Salvi, A., Brühlmann, C., Migliavacca, E., Carrupt, P.-A., Hostettmann, K., and Testa, B. Protein Protection by Antioxidants: Development of a Convenient Assay and Structure-Activity Relationships of Natural Polyphenols. Helvetica Chimica Acta 85 (2002): 867-881.
- [164] Liu, M.J., Li, J.X., Guo, H.Z., Lee, K.M., Qin, L., and Chan, K.M. The effects of verbascoside on plasma lipid peroxidation level and erythrocyte membrane fluidity during immobilization in rabbits: a time course study. Life Sci 73 (Jul 2003): 883-892.
- [165] Lee, K.J., Woo, E.R., Choi, C.Y., et al. Protective effect of acteoside on carbon tetrachloride-induced hepatotoxicity. Life Sci 74 (Jan 9 2004): 1051-1064.
- [166] Akbay, P., Calis, I., Undeger, U., Basaran, N., and Basaran, A.A. In vitro immunomodulatory activity of verbascoside from *Nepeta ucrainica* L. Phytother Res 16 (Sep 2002): 593-595.
- [167] Saleem, M., Kim, H.J., Ali, M.S., and Lee, Y.S. An update on bioactive plant lignans. Nat Prod Rep 22 (Dec 2005): 696-716.
- [168] He, Z.D., But, P.P.H., Chan, T.W., et al. Antioxidative glucosides from the fruits of *Ligustrum lucidum*. Chem Pharm Bull (Tokyo) 49 (Jun 2001): 780-784.
- [169] Ohno, T., Inoue, M., Ogihara, Y., and Saracoglu, I. Antimetastatic Activity of Acteoside, a Phenylethanoid Glycoside. Biological and Pharmaceutical Bulletin 25 (2002): 666-668.
- [170] Herbert, J.M., Maffrand, J.P., Taoubi, K., Augereau, J.M., Fouraste, I., and Gleye, J. Verbascoside isolated from *Lantana camara*, an inhibitor of protein kinase C. J Nat Prod 54 (Nov-Dec 1991): 1595-1600.

- [171] Hayashi, K., Nagamatsu, T., Ito, M., Yagita, H., and Suzuki, Y. Acteoside, a component of *Stachys sieboldii* MIQ, may be a promising antinephritic agent (3): effect of acteoside on expression of intercellular adhesion molecule-1 in experimental nephritic glomeruli in rats and cultured endothelial cells. Jpn J Pharmacol 70 (Feb 1996): 157-168.
- [172] Zhang, F., Jia, Z., Deng, Z., Wei, Y., Zheng, R., and Yu, L. In vitro modulation of telomerase activity, telomere length and cell cycle in MKN45 cells by verbascoside. Planta Med 68 (Feb 2002): 115-118.
- [173] Avila, J.G., de Liverant, J.G., Martinez, A., et al. Mode of action of *Buddleja cordata* verbascoside against *Staphylococcus aureus*. J Ethnopharmacol 66 (Jul 1999): 75-78.
- [174] Didry, N., Seidel, V., Dubreuil, L., Tillequin, F., and Bailleul, F. Isolation and antibacterial activity of phenylpropanoid derivatives from *Ballota nigra*. J Ethnopharmacol 67 (Nov 1999): 197-202.
- [175] Molnar, J., Gunics, G., Mucsi, I., et al. Antimicrobial and immunomodulating effects of some phenolic glycosides. Acta Microbiol Hung 36 (1989): 425-432.
- [176] Kernan, M.R., Amarquaye, A., Chen, J.L., et al. Antiviral phenylpropanoid glycosides from the medicinal plant *Markhamia lutea*. J Nat Prod 61 (May 1998): 564-570.
- [177] Kim, H.J., Woo, E.R., Shin, C.G., Hwang, D.J., Park, H., and Lee, Y.S. HIV-1 integrase inhibitory phenylpropanoid glycosides from *Clerodendron trichotomum*. Arch Pharm Res 24 (Aug 2001): 286-291.
- [178] Bermejo, P., Abad, M.J., Diaz, A.M., et al. Antiviral activity of seven iridoids, three saikosaponins and one phenylpropanoid glycoside extracted from *Bupleurum rigidum* and *Scrophularia scorodonia*. Planta Med 68 (Feb 2002): 106-110.
- [179] Kimura, Y., Okuda, H., Nishibe, S., and Arichi, S. Effects of caffeoylglycosides on arachidonate metabolism in leukocytes. Planta Med 53 (Apr 1987): 148-153.
- [180] Murai, M., Tamayama, Y., and Nishibe, S. Phenylethanoids in the herb of *Plantago lanceolata* and inhibitory effect on arachidonic acid-induced mouse ear edema. Planta Med 61 (Oct 1995): 479-480.

- [181] Sahpaz, S., Garbacki, N., Tits, M., and Bailleul, F. Isolation and pharmacological activity of phenylpropanoid esters from *Marrubium vulgare*. J Ethnopharmacol 79 (Mar 2002): 389-392.
- [182] Lee, J.Y., Woo, E.R., and Kang, K.W. Inhibition of lipopolysaccharide-inducible nitric oxide synthase expression by acteoside through blocking of AP-1 activation. J Ethnopharmacol 97 (Mar 2005): 561-566.
- [183] Houghton, P.J., and Hikino, H. Anti-Hepatotoxic Activity of Extracts and Constituents of *Buddleja* Species. Planta Med 55 (1989): 123,126.
- [184] Xiong, Q., Hase, K., Tezuka, Y., Tani, T., Namba, T., and Kadota, S. Hepatoprotective Activity of Phenylethanoids from *Cistanche deserticola*. Planta Med 64 (1998): 120,125.
- [185] Xiong, Q., Hase, K., Tezuka, Y., Namba, T., and Kadota, S. Acteoside inhibits apoptosis in D-Galactosamine and lipopolysaccharide-induced liver injury. Life Sci 65 (1999): 421-430.
- [186] Zheng, R.L., Wang, P.F., Li, J., Liu, Z.M., and Jia, Z.J. Inhibition of the autoxidation of linoleic acid by phenylpropanoid glycosides from *Pedicularis* in micelles. Chem Phys Lipids 65 (Jun 1993): 151-154.
- [187] Pettit, G.R., Numata, A., Takemura, T., et al. Antineoplastic agents, 107. Isolation of acteoside and isoacteoside from *Castilleja linariaefolia*. J Nat Prod 53 (Mar-Apr 1990): 456-458.
- [188] Sasaki, H., Nishimura, H., Morota, T., et al. Immunosuppressive principles of *Rehmannia glutinosa* var. *hueichingensis*. Planta Med. 55 (1989): 6.
- [189] Karim, A., Noor, A.T., Malik, A., Qadir, M.I., and Choudhary, M.I. Barlerisides A and B, new potent superoxide scavenging phenolic glycosides from *Barleria acanthoides*. J Enzyme Inhib Med Chem 24 (Dec 2009): 1332-1335.
- [190] Jiménez, C., and Riguera, R. Phenylethanoid glycosides in plants: structure and biological activity. Nat Prod Rep. 11 (1994): 16.
- [191] Arai, M., Hayashi, A., Sobou, M., et al. Anti-angiogenic effect of triterpenoidal saponins from *Polygala senega*. J Nat Med 65 (2011): 8.

- [192] Tian, F., Zhang, X., Tong, Y., et al. PE, a New Sulfated Saponin from Sea Cucumber, Exhibits Anti-Angiogenic and Anti-Tumor Activities In Vitro and In Vivo. Cancer Biology & Therapy 4 (2005): 9.
- [193] Foubert, K., Cuyckens, F., Matheeußen, A., et al. Antiprotozoal and antiangiogenic saponins from *Apodytes dimidiata*. Phytochemistry 72 (2011): 1414-1423.
- [194] Recio MC, Giner RM, Mañez S, and JL, R.o. Structural requirements for the anti-inflammatory activity of natural triterpenoids. Planta Med 61 (1995): 181.
- [195] Akihisa, T., Yasukawa, K., Kimura, Y., Yamanouchi, S., and Tamura, T. Sasanquol, A 3,4-seco-triterpene alcohol from sasanqua oil, and its anti-inflammatory effect. Phytochemistry 48 (1998): 301-305.
- [196] Loggia, R.D., Tubaro, A., Sosa, S., Becker, H., Saar, S., and Isaac, O. The Role of Triterpenoids in the Topical Anti-Inflammatory Activity of *Calendula officinalis* Flowers. Planta Med 60 (05.01.2007 1994): 516,520.
- [197] Navarrete, A., Trejo-Miranda, J.L., and Reyes-Trejo, L. Principles of root bark of *Hippocratea excelsa* (Hippocrataceae) with gastroprotective activity. J Ethnopharmacol 79 (Mar 2002): 383-388.
- [198] Xiu-Zhen, Y., Yao-Haur, K., Tsong-Jyh, L., et al. Cytotoxic components of *Diospyros morrisiana*. Phytochemistry 28 (1989): 1541-1543.
- [199] Hsu, H.Y., Yang, J.J., and Lin, C.C. Effects of oleanolic acid and ursolic acid on inhibiting tumor growth and enhancing the recovery of hematopoietic system postirradiation in mice. Cancer Lett 111 (Jan 1 1997): 7-13.
- [200] Tanaka, R., Minami, T., Ishikawa, Y., Matsunaga, S., Tokuda, H., and Nishino, H. Cancer chemopreventive activity of serratane-type triterpenoids on two-stage mouse skin carcinogenesis. Cancer Lett 196 (Jul 2003): 121-126.
- [201] Sohn, K.H., Lee, H.Y., Chung, H.Y., Young, H.S., Yi, S.Y., and Kim, K.W. Anti-angiogenic activity of triterpene acids. Cancer Lett 94 (Aug 1995): 213-218.
- [202] Kim, Y.-K., Yoon, S.K., and Ryu, S.Y. Cytotoxic Triterpenes from Stem Bark of *Physocarpus intermedius*. Planta Med 66 (Dec 2000): 485,486.

- [203] Fernandes, J., Castilho, R.O., da Costa, M.R., Wagner-Souza, K., Coelho Kaplan, M.A., and Gattass, C.R. Pentacyclic triterpenes from Chrysobalanaceae species: cytotoxicity on multidrug resistant and sensitive leukemia cell lines. Cancer Lett 190 (Feb 2003): 165-169.
- [204] Kapil, A., and Sharma, S. Effect of oleanolic acid on complement in adjuvant- and carrageenan-induced inflammation in rats. J Pharm Pharmacol 47 (Jul 1995): 585-587.
- [205] Liu, Y., Hartley, D.P., and Liu, J. Protection against carbon tetrachloride hepatotoxicity by oleanolic acid is not mediated through metallothionein. Toxicol Lett 95 (Mar 1998): 77-85.
- [206] Alvarez, M.E., Rotelli, A.E., Pelzer, L.E., Saad, J.R., and Giordano, O. Phytochemical study and anti-inflammatory properties of *Lampaya hieronymi* Schum. ex Moldenke. Farmaco 55 (Jun-Jul 2000): 502-505.
- [207] Yen, G.C., Duh, P.D., and Hung, Y.L. Contributions of major components to the antimutagenic effect of Hsian-tsao (*Mesona procumbens* Hemsl.). J Agric Food Chem 49 (Oct 2001): 5000-5004.
- [208] Jeong, H.G. Inhibition of cytochrome P450 2E1 expression by oleanolic acid: hepatoprotective effects against carbon tetrachloride-induced hepatic injury. Toxicol Lett 105 (Apr 1999): 215-222.
- [209] Rodriguez, J.A., Astudillo, L., and Schmeda-Hirschmann, G. Oleanolic acid promotes healing of acetic acid-induced chronic gastric lesions in rats. Pharmacol Res 48 (Sep 2003): 291-294.
- [210] Liu, J. Pharmacology of oleanolic acid and ursolic acid. J Ethnopharmacol 49 (Dec 1995): 57-68.
- [211] Ying, Q.L., Rinehart, A.R., Simon, S.R., and Cheronis, J.C. Inhibition of human leucocyte elastase by ursolic acid. Evidence for a binding site for pentacyclic triterpenes. Biochem J 277 (Pt 2) (Jul 1991): 521-526.
- [212] Somova, L.I., Shode, F.O., Ramnanan, P., and Nadar, A. Antihypertensive, antiatherosclerotic and antioxidant activity of triterpenoids isolated from *Olea europaea*, subspecies *africana* leaves. J Ethnopharmacol 84 (Feb 2003): 299-305.

- [213] Murtaza, I., Saleem, M., Adhami, V.M., Hafeez, B.B.,and Mukhtar, H. Suppression of cFLIP by Lupeol, a Dietary Triterpene, Is Sufficient to Overcome Resistance to TRAIL-Mediated Apoptosis in Chemoresistant Human Pancreatic Cancer Cells. Cancer Res 69 (February 2009): 1156-1165.
- [214] Gallo, M.B.C.,and M.J., S. Biological Activities of Lupeol. International Journal of Biomedical and Pharmaceutical Sciences 3 (2009): 21.
- [215] You, Y.J., Nam, N.H., Kim, Y., Bae, K.H.,and Ahn, B.Z. Antiangiogenic activity of lupeol from *Bombax ceiba*. Phytother Res 17 (Apr 2003): 341-344.
- [216] Dzubak, P., Hajduch, M., Vydra, D., et al. Pharmacological activities of natural triterpenoids and their therapeutic implications. Nat Prod Rep 23 (Jun 2006): 394-411.
- [217] Chaturvedi, P.K., Bhui, K.,and Shukla, Y. Lupeol: Connotations for chemoprevention. Cancer Lett 263 (2008): 1-13.
- [218] Lee, T.K., Poon, R.T., Wo, J.Y., et al. Lupeol suppresses cisplatin-induced nuclear factor-kappaB activation in head and neck squamous cell carcinoma and inhibits local invasion and nodal metastasis in an orthotopic nude mouse model. Cancer Res 67 (Sep 2007): 8800-8809.
- [219] Nigam, N., Prasad, S.,and Shukla, Y. Preventive effects of lupeol on DMBA induced DNA alkylation damage in mouse skin. Food Chem Toxicol 45 (Nov 2007): 2331-2335.
- [220] Dzubak, P., Hajduch, M., Vydra, D., et al. Pharmacological activities of natural triterpenoids and their therapeutic implications. Natural Product Reports 23 (2006): 394-411.
- [221] Geetha, T.,and Varalakshmi, P. Anti-inflammatory activity of lupeol and lupeol linoleate in rats. J Ethnopharmacol 76 (Jun 2001): 77-80.
- [222] Abid Ali Khan, M.M., Jain, D.C., Bhakuni, R.S., Zaim, M.,and Thakur, R.S. Occurrence of some antiviral sterols in *Artemisia annua*. Plant Science 75 (1991): 161-165.

- [223] Sharma, M., Sasvari, Z., and Nagy, P.D. Inhibition of sterol biosynthesis reduces tombusvirus replication in yeast and plants. J Virol 84 (Mar 2010): 2270-2281.
- [224] Semwal, S., and Sharma, R.K. Antibacterial sesquiterpene lactone glucoside from seed pods of *Bauhinia retusa*. J Asian Nat Prod Res 13 (Jan 2011): 75-79.
- [225] Awad, A.B., Roy, R., and Fink, C.S. Beta-sitosterol, a plant sterol, induces apoptosis and activates key caspases in MDA-MB-231 human breast cancer cells. Oncol Rep 10 (Mar-Apr 2003): 497-500.
- [226] Moon, D.O., Lee, K.J., Choi, Y.H., and Kim, G.Y. Beta-sitosterol-induced-apoptosis is mediated by the activation of ERK and the downregulation of Akt in MCA-102 murine fibrosarcoma cells. Int Immunopharmacol 7 (Aug 2007): 1044-1053.
- [227] Park, C., Moon, D.O., Rhu, C.H., et al. Beta-sitosterol induces anti-proliferation and apoptosis in human leukemic U937 cells through activation of caspase-3 and induction of Bax/Bcl-2 ratio. Biol Pharm Bull 30 (Jul 2007): 1317-1323.
- [228] Moon, E.J., Lee, Y.M., Lee, O.H., et al. A novel angiogenic factor derived from Aloe vera gel: beta-sitosterol, a plant sterol. Angiogenesis 3 (1999): 117-123.
- [229] Choi, S., Kim, K.W., Choi, J.S., et al. Angiogenic activity of beta-sitosterol in the ischaemia/reperfusion-damaged brain of Mongolian gerbil. Planta Med 68 (Apr 2002): 330-335.
- [230] Yamada, S., Sakamoto, K., Tsuda, H., Yoshida, K., Sugiura, M., and Sugahara, K. Structural studies of octasaccharides derived from the low-sulfated repeating disaccharide region and octasaccharide serines derived from the protein linkage region of porcine intestinal heparin. Biochemistry 38 (Jan 12 1999): 838-847.
- [231] Alban, S., Classen, B., Brunner, G., and Blaschek, W. Differentiation between the complement modulating effects of an arabinogalactan-protein from *Echinacea purpurea* and heparin. Planta Med 68 (Dec 2002): 1118-1124.

- [232] Michaelsen, T.E., Gilje, A., Samuelsen, A.B., Hogasen, K., and Paulsen, B.S. Interaction between human complement and a pectin type polysaccharide fraction, PMII, from the leaves of *Plantago major* L. Scand J Immunol 52 (Nov 2000): 483-490.
- [233] Wang, J.Z., Tsumura, H., Shimura, K., and Ito, H. Antitumor activity of polysaccharide from a Chinese medicinal herb, *Acanthopanax giraldii* Harms. Cancer Lett 65 (Jul 1992): 79-84.
- [234] Chen, S.C., Lu, M.K., Cheng, J.J., and Wang, D.L. Antiangiogenic activities of polysaccharides isolated from medicinal fungi. FEMS Microbiol Lett 249 (Aug 2005): 247-254.
- [235] Cheng, J.J., Huang, N.K., Chang, T.T., Wang, D.L., and Lu, M.K. Study for anti-angiogenic activities of polysaccharides isolated from *Antrodia cinnamomea* in endothelial cells. Life Sci 76 (May 2005): 3029-3042.
- [236] Sandoval, M., Okuhama, N.N., Zhang, X.J., et al. Anti-inflammatory and antioxidant activities of cat's claw (*Uncaria tomentosa* and *Uncaria guianensis*) are independent of their alkaloid content. Phytomedicine 9 (May 2002): 325-337.
- [237] Na Songkla, B. Thai medicinal plants. Bangkok, Thailand: Newthamada Publishing, 1976.
- [238] Srivatanakul, P., and Naka, L. Effect of *Acanthus ilicifolius* Linn. in Treatment of Leukemic Mice. Thai Cancer Journal 7 (1981): 89-93.
- [239] Siripong, P., Kupradinun, P., and Piyaviriyagul, S. Chronic toxicity of *Acanthus ebracteatus* Vahl. in rats. Bull. Dept. Med. Sci. Th. 43 (2001): 15.
- [240] Kuttan, R., Bhanumathy, P., Nirmala, K., and George, M.C. Potential anticancer activity of turmeric (*Curcuma longa*). Cancer Lett 29 (Nov 1985): 197-202.
- [241] Babu, T.D., Kuttan, G., and Padikkala, J. Cytotoxic and anti-tumour properties of certain taxa of Umbelliferae with special reference to *Centella asiatica* (L.) Urban. J Ethnopharmacol 48 (Aug 1995): 53-57.

- [242] Uthaisang, W., and Khawsak, P. Cytotoxicity of crude extracts from *Allamanda cathartica*, *Guaiacum officinale* and *Artabotrys siamensis* to some cancer cells. Journal of Medicine and Health Sciences 12 (2005): 11.
- [243] Saetung, A., Itharat, A., Dechsukum, C., Keawpradub, K., and Wattanapiromsakul, C., and Ratanasuwan, P. Cytotoxic activity of Thai medicinal plants for cancer treatment. Songklanakar J. Sci. Technol. 27 (2005): 10.
- [244] Lertworapreecha, M., Patumraj, S., Niruthisard, S., Hansasuta, P., and Bhattarakosol, P. Mouse acquired HPV tumor using dorsal skin-fold window chamber. Indian J Exp Biol 47 (May 2009): 327-332.
- [245] Fok, T.C.O., Jan, A., Peel, S.A.F., Evans, A.W., Clokie, C.M.L., and Sándor, G.K.B. Hyperbaric oxygen results in increased vascular endothelial growth factor (VEGF) protein expression in rabbit calvarial critical-sized defects. Oral Surgery, Oral Medicine, Oral Pathology, Oral Radiology, and Endodontology 105 (2008): 417-422.
- [246] Bhattarakosol, P., Poonnanti, A., and Niruthisard, S. Detection and typing of human papillomavirus in cervical cancer in the Thai. J Med Assoc Thai 79 Suppl 1 (Dec 1996): S56-64.
- [247] Siritantikorn, S., Laiwejpithaya, S., Siripanyaphinyo, U., et al. Detection and typing of human papilloma virus DNAs in normal cervix, intraepithelial neoplasia and cervical cancer in Bangkok. Southeast Asian J Trop Med Public Health 28 (Dec 1997): 707-710.
- [248] Chichareon, S., Herrero, R., Munoz, N., et al. Risk factors for cervical cancer in Thailand: a case-control study. J Natl Cancer Inst 90 (Jan 7 1998): 50-57.
- [249] Clifford, G.M., Gallus, S., Herrero, R., et al. Worldwide distribution of human papillomavirus types in cytologically normal women in the International Agency for Research on Cancer HPV prevalence surveys: a pooled analysis. Lancet 366 (Sep 17-23 2005): 991-998.
- [250] Thomas, D.B., Ray, R.M., Kuypers, J., et al. Human papillomaviruses and cervical cancer in Bangkok. III. The role of husbands and commercial sex workers. Am J Epidemiol 153 (Apr 15 2001): 740-748.
- [251] Thomas, D.B., Qin, Q., Kuypers, J., et al. Human papillomaviruses and cervical cancer in Bangkok. II. Risk factors for in situ and invasive squamous cell cervical carcinomas. Am J Epidemiol 153 (Apr 15 2001): 732-739.

- [252] Thomas, D.B., Ray, R.M., Koetsawang, A., et al. Human papillomaviruses and cervical cancer in Bangkok. I. Risk factors for invasive cervical carcinomas with human papillomavirus types 16 and 18 DNA. Am J Epidemiol 153 (Apr 2001): 723-731.
- [253] Goncharuk, I.V., Vorobjova, L.I., Lukyanova, N.Y., and Chekhun, V.F. Vascular endothelial growth factor expression in uterine cervical cancer: correlation with clinicopathologic characteristics and survival. Exp Oncol 31 (Sep 2009): 179-181.
- [254] Boyd, M.R. Anticancer drug development guide; preclinical screening, clinical trails and approval. Human Press Inc., Totowa, NJ., 1997.
- [255] Awad, A.B., and Fink, C.S. Phytosterols as Anticancer Dietary Components: Evidence and Mechanism of Action. J Nutr 130 (September 2000): 2127-2130.
- [256] Awad, A.B., Chen, Y.C., Fink, C.S., and Hennessey, T. beta-Sitosterol inhibits HT-29 human colon cancer cell growth and alters membrane lipids. Anticancer Res 16 (Sep-Oct 1996): 2797-2804.
- [257] von Holtz, R.L., Fink, C.S., and Awad, A.B. beta-Sitosterol activates the sphingomyelin cycle and induces apoptosis in LNCaP human prostate cancer cells. Nutr Cancer 32 (1998): 8-12.
- [258] Awad, A.B., Chinnam, M., Fink, C.S., and Bradford, P.G. beta-Sitosterol activates Fas signaling in human breast cancer cells. Phytomedicine 14 (Nov 2007): 747-754.
- [259] Choi, Y.H., Kong, K.R., Kim, Y.A., et al. Induction of Bax and activation of caspases during beta-sitosterol-mediated apoptosis in human colon cancer cells. Int J Oncol 23 (Dec 2003): 1657-1662.
- [260] Awad, A.B., von Holtz, R.L., Cone, J.P., Fink, C.S., and Chen, Y.C. beta-Sitosterol inhibits growth of HT-29 human colon cancer cells by activating the sphingomyelin cycle. Anticancer Res 18 (Jan-Feb 1998): 471-473.
- [261] Wang, L., Yang, Y.J., Chen, S.H., Ge, X.R., Xu, C.J., and Gui, S.Q. [Effects of beta-sitosterol on microtubular systems in cervical cancer cells]. Zhonghua Yi Xue Za Zhi 86 (Oct 2006): 2771-2775.

- [262] Moriarty, D.M., Huang, J., Yancey, C.A., et al. Lupeol is the Cytotoxic Principle in the Leaf Extract of *Dendropanax cf. querceti*. Planta Med 64 (1998): 370,372.
- [263] Lambertini, E., Lampronti, I., Penolazzi, L., et al. Expression of estrogen receptor alpha gene in breast cancer cells treated with transcription factor decoy is modulated by Bangladeshi natural plant extracts. Oncol Res 15 (2005): 69-79.
- [264] Mellanen, P., Petanen, T., Lehtimaki, J., et al. Wood-derived estrogens: studies in vitro with breast cancer cell lines and in vivo in trout. Toxicol Appl Pharmacol 136 (Feb 1996): 381-388.
- [265] Hata, K., Hori, K., Murata, J., and Takahashi, S. Remodeling of actin cytoskeleton in lupeol-induced B16 2F2 cell differentiation. J Biochem 138 (Oct 2005): 467-472.
- [266] Ding, Y., Nguyen, H.T., Kim, S.I., Kim, H.W., and Kim, Y.H. The regulation of inflammatory cytokine secretion in macrophage cell line by the chemical constituents of *Rhus sylvestris*. Bioorg Med Chem Lett 19 (Jul 2009): 3607-3610.
- [267] Prasad, S., Madan, E., Nigam, N., Roy, P., George, J., and Shukla, Y. Induction of apoptosis by lupeol in human epidermoid carcinoma A431 cells through regulation of mitochondrial, Akt/PKB and NFkappaB signaling pathways. Cancer Biol Ther 8 (Sep 2009): 1632-1639.
- [268] Zhang, R., Song, Y., Gao, W.J., et al. [Expression of P53, COX2 and CD44V6 in early-stage squamous carcinoma of cervix with lymph vascular space invasion positive and negative and its relationship with prognosis]. Zhonghua Yi Xue Za Zhi 89 (Dec 2009): 3341-3345.
- [269] Hasmeda, M., Kweifio-Okai, G., Macrides, T., and Polya, G.M. Selective inhibition of eukaryote protein kinases by anti-inflammatory triterpenoids. Planta Med 65 (Feb 1999): 14-18.
- [270] Rajic, A., Kweifio-Okai, G., Macrides, T., Sandeman, R.M., Chandler, D.S., and Polya, G.M. Inhibition of serine proteases by anti-inflammatory triterpenoids. Planta Med 66 (Apr 2000): 206-210.
- [271] Hodges, L.D., Kweifio-Okai, G., and Macrides, T.A. Antiprotease effect of anti-inflammatory lupeol esters. Mol Cell Biochem 252 (Oct 2003): 97-101.

- [272] Wada, S., Iida, A., and Tanaka, R. Screening of triterpenoids isolated from *Phyllanthus flexuosus* for DNA topoisomerase inhibitory activity. J Nat Prod 64 (Dec 2001): 1545-1547.
- [273] Banno, N., Akihisa, T., Tokuda, H., et al. Triterpene acids from the leaves of *Perilla frutescens* and their anti-inflammatory and antitumor-promoting effects. Biosci Biotechnol Biochem 68 (Jan 2004): 85-90.
- [274] De Angel, R.E., Smith, S.M., Glickman, R.D., Perkins, S.N., and Hursting, S.D. Antitumor effects of ursolic acid in a mouse model of postmenopausal breast cancer. Nutr Cancer 62 (2010): 1074-1086.
- [275] Ramos, A.A., Pereira-Wilson, C., and Collins, A.R. Protective effects of ursolic acid and luteolin against oxidative DNA damage include enhancement of DNA repair in Caco-2 cells. Mutat Res 692 (Oct 2010): 6-11.
- [276] Mizushina, Y., Iida, A., Ohta, K., Sugawara, F., and Sakaguchi, K. Novel triterpenoids inhibit both DNA polymerase and DNA topoisomerase. Biochem J 350 Pt 3 (Sep 2000): 757-763.
- [277] Lauthier, F., Taillet, L., Trouillas, P., Delage, C., and Simon, A. Ursolic acid triggers calcium-dependent apoptosis in human Daudi cells. Anticancer Drugs 11 (Oct 2000): 737-745.
- [278] Wang, M., and Gartel, A.L. Micelle-encapsulated thiostrepton as an effective nanomedicine for inhibiting tumor growth and for suppressing FOXM1 in human xenografts. Mol Cancer Ther 10 (Dec 2011): 2287-2297.
- [279] Prasad, S., Yadav, V.R., Kannappan, R., and Aggarwal, B.B. Ursolic acid, a pentacyclin triterpene, potentiates TRAIL-induced apoptosis through p53-independent up-regulation of death receptors: evidence for the role of reactive oxygen species and JNK. J Biol Chem 286 (Feb 2011): 5546-5557.
- [280] Yim, E.K., Lee, M.J., Lee, K.H., Um, S.J., and Park, J.S. Antiproliferative and antiviral mechanisms of ursolic acid and dexamethasone in cervical carcinoma cell lines. Int J Gynecol Cancer 16 (Nov-Dec 2006): 2023-2031.

- [281] Li, J.-J., and Oberley, L.W. Overexpression of Manganese-containing Superoxide Dismutase Confers Resistance to the Cytotoxicity of Tumor Necrosis Factor α and/or Hyperthermia. Cancer Res 57 (May 1997): 1991-1998.
- [282] Nguyen, P., Ho, C.-L., Teo, S.-S., Harikrishna, J., and Rahim, R. Sequence and transcript analyses of antioxidant genes from *Acanthus ebracteatus* Vahl. Tree Genetics & Genomes 4 (2008): 705-713.
- [283] Custodio, L., Escapa, A.L., Fernandes, E., et al. Phytochemical profile, antioxidant and cytotoxic activities of the carob tree (*Ceratonia siliqua* L.) germ flour extracts. Plant Foods Hum Nutr 66 (Mar 2011): 78-84.
- [284] Zimmermann, K.C., Bonzon, C., and Green, D.R. The machinery of programmed cell death. Pharmacol Ther 92 (Oct 2001): 57-70.
- [285] Halliwell, B. Oxidative stress and cancer: have we moved forward? Biochem J 401 (Jan 2007): 1-11.
- [286] Smotkin, D., and Wettstein, F.O. Transcription of human papillomavirus type 16 early genes in a cervical cancer and a cancer-derived cell line and identification of the E7 protein. Proc Natl Acad Sci U S A 83 (Jul 1986): 4680-4684.
- [287] Clifford, G.M., Smith, J.S., Plummer, M., Munoz, N., and Franceschi, S. Human papillomavirus types in invasive cervical cancer worldwide: a meta-analysis. Br J Cancer 88 (Jan 2003): 63-73.
- [288] Ahn, W.S., Bae, S.M., Lee, K.H., et al. Recombinant adenovirus-p53 gene transfer and cell-specific growth suppression of human cervical cancer cells in vitro and in vivo. Gynecol Oncol 92 (Feb 2004): 611-621.
- [289] Jonson, A.L., Rogers, L.M., Ramakrishnan, S., and Downs, L.S., Jr. Gene silencing with siRNA targeting E6/E7 as a therapeutic intervention in a mouse model of cervical cancer. Gynecol Oncol 111 (Nov 2008): 356-364.
- [290] Choo, C.K., Ling, M.T., Suen, C.K., Chan, K.W., and Kwong, Y.L. Retrovirus-mediated delivery of HPV16 E7 antisense RNA inhibited tumorigenicity of CaSki cells. Gynecol Oncol 78 (Sep 2000): 293-301.

- [291] Yabushita, H., Yoshikawa, K., Hirata, M., et al. Effects of electrochemotherapy on CaSki cells derived from a cervical squamous cell carcinoma. Gynecol Oncol 65 (May 1997): 297-303.
- [292] Tomayko, M.M., and Reynolds, C.P. Determination of subcutaneous tumor size in athymic (nude) mice. Cancer Chemother Pharmacol 24 (1989): 148-154.
- [293] Steger, G., Rehtanz, M., and Schnabel, C. Identification of a promoter in position 56 within the long control region of human papillomavirus type 18. Arch Virol 146 (2001): 2069-2084.
- [294] Bagnato, A., Cirilli, A., Salani, D., et al. Growth inhibition of cervix carcinoma cells in vivo by endothelin A receptor blockade. Cancer Res 62 (Nov 2002): 6381-6384.
- [295] Kubbutat, M.H., Jones, S.N., and Vousden, K.H. Regulation of p53 stability by Mdm2. Nature 387 (May 1997): 299-303.
- [296] Kubbutat, M.H., and Vousden, K.H. Proteolytic cleavage of human p53 by calpain: a potential regulator of protein stability. Mol Cell Biol 17 (Jan 1997): 460-468.
- [297] Vousden, K.H. Functions of p53 in metabolism and invasion. Biochem Soc Trans 37 (Jun 2009): 511-517.
- [298] Butz, K., Shahabeddin, L., Geisen, C., Spitkovsky, D., Ullmann, A., and Hoppe-Seyler, F. Functional p53 protein in human papillomavirus-positive cancer cells. Oncogene 10 (Mar 1995): 927-936.
- [299] Butz, K., Whitaker, N., Denk, C., Ullmann, A., Geisen, C., and Hoppe-Seyler, F. Induction of the p53-target gene GADD45 in HPV-positive cancer cells. Oncogene 18 (Apr 1999): 2381-2386.
- [300] Zhao, C.Y., Szekeley, L., Bao, W., and Selivanova, G. Rescue of p53 function by small-molecule RITA in cervical carcinoma by blocking E6-mediated degradation. Cancer Res 70 (Apr 2010): 3372-3381.
- [301] Scheffner, M., Huibregtse, J.M., Vierstra, R.D., and Howley, P.M. The HPV-16 E6 and E6-AP complex functions as a ubiquitin-protein ligase in the ubiquitination of p53. Cell 75 (Nov 1993): 495-505.

- [302] Scheffner, M., Munger, K., Byrne, J.C., and Howley, P.M. The state of the p53 and retinoblastoma genes in human cervical carcinoma cell lines. Proc Natl Acad Sci U S A 88 (Jul 1991): 5523-5527.
- [303] Crook, T., Wrede, D., Tidy, J.A., Mason, W.P., Evans, D.J., and Vousden, K.H. Clonal p53 mutation in primary cervical cancer: association with human-papillomavirus-negative tumours. Lancet 339 (May 1992): 1070-1073.
- [304] Kim, M.S., Li, S.L., Bertolami, C.N., Cherrick, H.M., and Park, N.H. State of p53, Rb and DCC tumor suppressor genes in human oral cancer cell lines. Anticancer Res 13 (Sep-Oct 1993): 1405-1413.
- [305] Miwa, K., Miyamoto, S., Kato, H., et al. The role of p53 inactivation in human cervical cell carcinoma development. Br J Cancer 71 (Feb 1995): 219-226.
- [306] Moon, A., Won, K.Y., Lee, J.Y., Kang, I., Lee, S.K., and Lee, J. Expression of BDNF, TrkB, and p53 in early-stage squamous cell carcinoma of the uterine cervix. Pathology 43 (Aug 2011): 453-458.
- [307] Lenczewski, A., Terlikowski, S., Sulkowska, M., Musiatowicz, B., and Kulikowski, M. [Immunohistochemically expression of the protein p53 evaluated in invasive squamous cell carcinoma of the cervix]. Ginekol Pol 70 (Jul 1999): 478-483.
- [308] Looi, M.L., Dali, A.Z., Ali, S.A., Ngah, W.Z., and Yusof, Y.A. Expression of p53, bcl-2 and Ki-67 in cervical intraepithelial neoplasia and invasive squamous cell carcinoma of the uterine cervix. Anal Quant Cytol Histol 30 (Apr 2008): 63-70.
- [309] Liotta, L.A., Kleinerman, J., and Saidel, G.M. Quantitative relationships of intravascular tumor cells, tumor vessels, and pulmonary metastases following tumor implantation. Cancer Res 34 (May 1974): 997-1004.
- [310] Leunig, M., Yuan, F., Menger, M.D., et al. Angiogenesis, microvascular architecture, microhemodynamics, and interstitial fluid pressure during early growth of human adenocarcinoma LS174T in SCID mice. Cancer Res 52 (Dec 1992): 6553-6560.
- [311] Hanahan, D., and Folkman, J. Patterns and emerging mechanisms of the angiogenic switch during tumorigenesis. Cell 86 (Aug 1996): 353-364.

- [312] Ellis, L.M., Takahashi, Y., Liu, W., and Shaheen, R.M. Vascular endothelial growth factor in human colon cancer: biology and therapeutic implications. Oncologist 5 Suppl 1 (2000): 11-15.
- [313] Yuan, F., Chen, Y., Dellian, M., Safabakhsh, N., Ferrara, N., and Jain, R.K. Time-dependent vascular regression and permeability changes in established human tumor xenografts induced by an anti-vascular endothelial growth factor/vascular permeability factor antibody. Proc Natl Acad Sci U S A 93 (Dec 1996): 14765-14770.
- [314] Shaheen, R.M., Davis, D.W., Liu, W., et al. Antiangiogenic therapy targeting the tyrosine kinase receptor for vascular endothelial growth factor receptor inhibits the growth of colon cancer liver metastasis and induces tumor and endothelial cell apoptosis. Cancer Res 59 (Nov 1999): 5412-5416.
- [315] Bruns, C.J., Liu, W., Davis, D.W., et al. Vascular endothelial growth factor is an in vivo survival factor for tumor endothelium in a murine model of colorectal carcinoma liver metastases. Cancer 89 (Aug 2000): 488-499.
- [316] Huang, J., Frischer, J.S., Serur, A., et al. Regression of established tumors and metastases by potent vascular endothelial growth factor blockade. Proc Natl Acad Sci U S A 100 (Jun 2003): 7785-7790.
- [317] Inai, T., Mancuso, M., Hashizume, H., et al. Inhibition of vascular endothelial growth factor (VEGF) signaling in cancer causes loss of endothelial fenestrations, regression of tumor vessels, and appearance of basement membrane ghosts. Am J Pathol 165 (Jul 2004): 35-52.
- [318] Jain, R.K., and Carmeliet, P.F. Vessels of death or life. Sci Am 285 (Dec 2001): 38-45.
- [319] Erber, R., Thurnher, A., Katsen, A.D., et al. Combined inhibition of VEGF and PDGF signaling enforces tumor vessel regression by interfering with pericyte-mediated endothelial cell survival mechanisms. FASEB J 18 (Feb 2004): 338-340.
- [320] Dellas, A., Schultheiss, E., Leivas, M.R., Moch, H., and Torhorst, J. Association of p27Kip1, cyclin E and c-myc expression with progression and prognosis in HPV-positive cervical neoplasms. Anticancer Res 18 (Nov-Dec 1998): 3991-3998.

- [321] Toussaint-Smith, E., Donner, D.B., and Roman, A. Expression of human papillomavirus type 16 E6 and E7 oncoproteins in primary foreskin keratinocytes is sufficient to alter the expression of angiogenic factors. Oncogene 23 (Apr 2004): 2988-2995.
- [322] Fujiwaki, R., Hata, K., Iida, K., Maede, Y., and Miyazaki, K. Vascular endothelial growth factor expression in progression of cervical cancer: correlation with thymidine phosphorylase expression, angiogenesis, tumor cell proliferation, and apoptosis. Anticancer Res 20 (Mar-Apr 2000): 1317-1322.
- [323] Rak, J., Mitsuhashi, Y., Bayko, L., et al. Mutant ras oncogenes upregulate VEGF/VPF expression: implications for induction and inhibition of tumor angiogenesis. Cancer Res 55 (Oct 1995): 4575-4580.
- [324] Hopfl, G., Ogunshola, O., and Gassmann, M. HIFs and tumors--causes and consequences. Am J Physiol Regul Integr Comp Physiol 286 (Apr 2004): R608-623.
- [325] Brown, L.M., Cowen, R.L., Debray, C., et al. Reversing hypoxic cell chemoresistance in vitro using genetic and small molecule approaches targeting hypoxia inducible factor-1. Mol Pharmacol 69 (Feb 2006): 411-418.
- [326] Hietanen, S., Lain, S., Krausz, E., Blattner, C., and Lane, D.P. Activation of p53 in cervical carcinoma cells by small molecules. Proc Natl Acad Sci U S A 97 (Jul 2000): 8501-8506.
- [327] Hengstermann, A., Whitaker, N.J., Zimmer, D., Zentgraf, H., and Scheffner, M. Characterization of sequence elements involved in p53 stability regulation reveals cell type dependence for p53 degradation. Oncogene 17 (Dec 3 1998): 2933-2941.
- [328] Weinberg, W.C., Azzoli, C.G., Chapman, K., Levine, A.J., and Yuspa, S.H. p53-mediated transcriptional activity increases in differentiating epidermal keratinocytes in association with decreased p53 protein. Oncogene 10 (Jun 1995): 2271-2279.
- [329] Meek, D.W. Mechanisms of switching on p53: a role for covalent modification? Oncogene 18 (Dec 1999): 7666-7675.

- [330] Kudo, Y., Takata, T., Ogawa, I., Sato, S., and Nikai, H. Expression of p53 and p21CIP1/WAF1 proteins in oral epithelial dysplasias and squamous cell carcinomas. Oncol Rep 6 (May-Jun 1999): 539-545.
- [331] Muller, A., Rice, P.J., Ensley, H.E., et al. Receptor binding and internalization of a water-soluble (1-->3)-beta-D-glucan biologic response modifier in two monocyte/macrophage cell lines. J Immunol 156 (May 1996): 3418-3425.
- [332] Vetvicka, V., Thornton, B.P., and Ross, G.D. Soluble beta-glucan polysaccharide binding to the lectin site of neutrophil or natural killer cell complement receptor type 3 (CD11b/CD18) generates a primed state of the receptor capable of mediating cytotoxicity of iC3b-opsonized target cells. J Clin Invest 98 (Jul 1996): 50-61.
- [333] Ho, J.C., Konerding, M.A., Gaumann, A., Groth, M., and Liu, W.K. Fungal polysaccharopeptide inhibits tumor angiogenesis and tumor growth in mice. Life Sci 75 (Jul 2004): 1343-1356.
- [334] Zhang, C., Yang, F., Zhang, X.W., et al. Grateloupia longifolia polysaccharide inhibits angiogenesis by downregulating tissue factor expression in HMEC-1 endothelial cells. Br J Pharmacol 148 (Jul 2006): 741-751.
- [335] Apers, S., Paper, D., Burgermeister, J., et al. Antiangiogenic activity of synthetic dihydrobenzofuran lignans. J Nat Prod 65 (May 2002): 718-720.
- [336] Ming, L., Jill, C.P., Jingfang, J., Edward, C., and Brash, E. Antioxidant action via p53 mediated apoptosis. Cancer Res 58 (1998): 7.
- [337] Putul, M., Sunit, C., and Pritha, B. Neovascularisation offers a new perspective to glutamine related therapy. Indian Journal of Experimental Biology 38 (2000): 3.
- [338] Harfouche, R., Malak, N.A., Brandes, R.P., Karsan, A., Irani, K., and Hussain, S.N. Roles of reactive oxygen species in angiopoietin-1/tie-2 receptor signaling. FASEB J 19 (Oct 2005): 1728-1730.
- [339] Ikeda, S., Ushio-Fukai, M., Zuo, L., et al. Novel role of ARF6 in vascular endothelial growth factor-induced signaling and angiogenesis. Circ Res 96 (Mar 2005): 467-475.